

https://dspace.org/

Investigation of the impact of recharge water with respect to quality into the Khutala Colliery Rehabilitated block I opencast operation

Repinga, Mandla Ralph

2012-01-19
http://hdl.handle.net/10539/11110

Downloaded from a DSpace repository. https://dspace.org/

INVESTIGATION OF THE IMPACT OF RECHARGE WATER WITH RESPECT TO QUALITY INTO THE KHUTALA COLLIERY REHABILITATED BLOCK I OPENCAST OPERATION

Name and Surname: Mandla Ralph Repinga

Student Number: 9108658V

Degree of Masters in Environmental Science

A research report submitted to the Faculty of Science, University of the Witwatersrand, Johannesburg, in partial fulfilment of the requirements for the degree of Master of Science

Johannesburg, 2010

DECLARATION

I declare that this research report is my own, unaided work. It is being submitted for the Degree of Masters of Science in the University of Witwatersrand, Johannesburg. It has not been submitted before for any degree or examination in any University.

Mandla Ralph Repinga

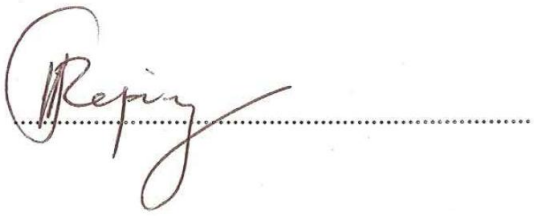

(Signature)

10th day of August 2011

ABSTRACT

This study was an investigation of the impact of recharge water with respect to quality and quantity into the Rehabilitated Block I opencast operation, a former opencast coal mine in Mpumalanga, Witbank Coalfields western complex. The rehabilitated areas consisted of three mined mini-pit areas known as Block I, Block I Extension A and B. The area has been rehabilitated by backfilling and leveling of spoil material, subsoil material, placement of approximately 400-mm topsoil layer and grassing. As part of the vegetation maintenance lime is added per annum, in an effort to neutralize the soil cover and further assist in neutralizing the potential acid mine drainage. Additional monitoring boreholes were drilled to increase the monitoring of the water quantity and qualities. Ground and surface water samples were taken, analysed for pH, conductivity, redox potential, sulphates, carbonates and trace metals. The pH of the ground and surface water ranged from moderately acidic to alkaline. One of the monitoring boreholes located on the lowest elevation of the Block I area was observed to be filled up to the collar level of the borehole with water samples showing elevated Fe and Mn concentrations of 216 and 46.2 mg l^{-1} respectively. The water classification revealed the following facies: Ca-Mg sulphate type for the borehole water and Ca-Mg sulphate-bicarbonate type for the surface waters. Acid base accounting studies on the soil samples showed a negative net neutralising potential of up to -9.8 kg t^{-1} $CaCO_3$ which indicated the potential of acid mine drainage in the area. The total metal analyses showed that the area was contaminated with heavy metals such as Fe, Cr, Mn, Ni and Zn and the metalloid As was also detected. The highest recorded concentrations of total metals were 78 252; 2 402; 1 959; 1 360 and 15 109 mg kg^{-1} respectively. The highest concentration of Arsenic was detected at 824 mg kg^{-1} respectively. The transmissivity of the boreholes in the spoil material was highly variable and ranges from 100 to 5 000 m^2 day^{-1}. Pump testing suggests that borehole yields of between 23 and 4 l s^{-1} can be expected in the spoil areas. The specific yield or the drainage porosity of the spoil material was in the range of 25 to 30 %.

DEDICATION

In memory of my father Lazarus Lashi Repinga

(1941 – 1999)

and my mother Tondisali Eselina Repinga

(1940 – 2006).

To my wife Cebelihle Sandra Repinga

ACKNOWLEDGEMENTS

I would like to give my thanks to my supervisor, Dr Hlanganani Tutu for the support and opportunity he gave me whilst conducting this research. Furthermore, I would like to thank my colleagues Fulufhelo Mabuduga, Patience Nchabeleng and Kubashni Mari who gave me a word of encouragement and input into the planning of this research project. I also thank the contribution made by Lebohang Maku in ensuring that this research project is a success.

TABLE OF CONTENTS

Contents

DECLARATION .....**Error! Bookmark not defined.**

ABSTRACT iii

DEDICATION iv

ACKNOWLEDGEMENTS v

LIST OF TABLES ix

LIST OF FIGURES x

1. INTRODUCTION 1

1.1 General Introduction 1

1.2 Study Area 4

1.2.1 Application of top soil on the old mining area 8

1.2.2 Planting of grass on the added top soil 8

1.2.3 Neutralising acidity on the area by applying lime annually 8

2 AIMS OF THE PROJECT AND STUDY AREA 9

2.1 Aims of the Project 9

3 LITERATURE REVIEW 10

3.1 Acid Mine Drainage (AMD) 10

3.2 Phase in the Development of AMD 12

3.3 Acid-Base Accounting 13

3.4 Basic Chemistry of AMD Generation and acid generating reactions 16

3.5 Basic Chemistry of AMD Generation and Acid Generating Reactions 22

3.6 Sampling and analysis methodologies 23

3.6.1 Field methods 23

3.6.2 Static tests 24

3.6.3 Kinetic tests 25

3.6.4 Modelling 26

4. METHODOLOGY 28

4.1 Drilling 28

4.2 Pump testing 29

4.3 Sampling procedure 29

4.4 Field measurements 30

4.5 Sample preparation 30

5. RESULTS AND DISCUSSION 35

5.1 Pump Testing Results 35

5.2 Volume calculation 38

5.3 Water Chemistry 39

5.3.1 pH 40

5.3.2 Electrical Conductivity 40

5.3.3 Oxidation Reduction Potential (Eh) 42

5.3.4 Sulphates 43

5.3.5 Carbonates 44

5.3.6 Trace Metal Concentration 46

5.3.7 Water Classification 50
5.4 Soil Chemistry 51
5.4.1 Total metal analysis 51
5.4.2 Leaching tests 58
5.4.3 Acid Base Accounting 65
6. CONCLUSION AND FUTURE WORK 69
6.1 Conclusion 69
6.2 Future Studies and Recommendations 71
7. REFERENCES 76
8. APPENDIX 87

LIST OF TABLES

Table 4.1: Positions of newly drilled boreholes 28

Table 5.1: Pump testing results 35

Table 5.2: Summary of pump test parameters (transmissivity) 38

Table 5.3: Summary of volumes of water in rehabilitated areas 39

LIST OF FIGURES

Figure 1.1: Location map of the opencast Blocks reflecting monitoring boreholes, dams and streams 5

Figure 1.2: Location map of the opencast Blocks reflecting monitoring boreholes 6

Figure 1.3: Location map of the opencast Blocks reflecting surface water monitoring points 7

Figure 5.1: The log EC-pH relationship of the borehole and surface waters at the detailed site 42

Figure 5.2: The Eh-pH relationship of the water in the lower discharge and above the discharge point. 43

Figure 5.3: Trace metal concentrations of Cu, Mg, Fe Mn, Ca and Zn on the borehole and surface water at Block I 49

Figure 5.4: Distribution of % ($Na^+ + K^+$), % Mg^{2+}, and % Ca^{2+} and % Cl^-, % SO_4^{2-}, % ($HCO_3^- + CO_3^{2-}$) depicting the classification of borehole and surface waters at Block I 51

Figure 5.5: Plot of total concentrations of selected metal ions such as Cu, Fe, Cr, Ni, Mn and Cd 55

Figure 5.6: A correlation of concentration of sulphur with Fe, Mn, Cu and Ni. 57

Figure 5.7: Pourbaix diagrams of (a) Mn, (b) Fe, (c) Cr and (d) Cd 61

Figure 5.8: Extractions of various metal ions with solutions of 0.1 M EDTA, 0.01 M $CaCl_2$, 0.1 M Na_2CO_3 and artificial rainwater 64

Figure 5.9: The initial and final pH of soil samples before and after complete pyrite oxidation 66

Figure 5.10: The acid potential and neutralising potential of soil samples from Block I 67

Figure 5.11: Variation in the net neutralising potential of soil samples at Block I 68

1. INTRODUCTION

1.1 General Introduction

Coal is found in South Africa in 19 coalfields, located mainly in KwaZulu-Natal, Mpumalanga, Limpopo, and the Free State, with lesser amounts in Gauteng, the North West Province and the Eastern Cape (Jeffrey, 2005). The main coal mining areas are presently in the Witbank-Middelburg, Ermelo and Standerton-Secunda areas of Mpumalanga, around Sasolburg-Vereeniging in the Free State/Gauteng and in northwestern KwaZulu-Natal where smaller operations are found (Jeffrey, 2005).

Estimates for South Africa's coal recoverable reserves made in 1999 range from nine to 59 billion tons; latest estimates by the Minerals Bureau suggest that 33 billion tons is a more likely figure (Prevost, 2004). As much as 70% of that coal is located in the Waterberg, Witbank, and Highveld coalfields, as well as lesser amounts in the Ermelo, Free State and Springbok Flats coalfields.

However, the Witbank and Highveld coalfields are approaching exhaustion (estimated 9 billion tons of recoverable coal remaining in each), while the coal quality or mining conditions in the Waterberg, Free State and Springbok Flats coalfields are significant barriers to immediate, conventional exploitation.

The latest Minerals Bureau estimate sets the reserves at 33.8 billion tons, considered to last until around 2050 (Prevost, 2004). Bredell, 1987 defined coal reserves as referring 'only to that portion of the total coal resources of which the nature and distribution have been fairly well established and which is at present economically recoverable or borders on economic recoverability'.

Coal mining has been ongoing in the Mpumalanga Witbank Coalfields for more than 100 years. The Witbank Coalfield is nearing depletion and additional sources for coal supply must soon be identified if the coal industry is to continue into the 21st century.

The Colliery started mining early in 1980 with underground bord and pillar mining and supplying to Kendal Power Station. The operation started site preparation to mine and produce 13.2 Million tonnes of Run-of-Mine coal per annum in 1984. The first coal was mined in August 1986 and supplied to the Kendal Power Station. The mine is mining the number 2 and 4 seams using bord and pillar mining with continuous miners supplemented by a contractor truck and shovel opencast operation mining the number 2, 4 and 5 coal seams.

In 2000 an opencast operation was opened at the Block I section with three mini-pits mined, that is Block I, Block I Extension A and B. Mining ceased in 2003 and the opencast pits were rehabilitated and vegetated in 2005. When mining ceased all recharge water and water that accumulated before rehabilitation started filling up the pit. Coal and coal spoils contains pyrite which is permeable to water and causes the pyrite to leach. During and post mining, the presence of geological fissures and rainfall falling on the rehabilitated areas results in recharge of water into the back-filled opencast workings.

Coal occurs in thick seams and is fairly shallow (De Jager, 1992). 40 % of South Africa's coal is produced from opencast mining (Krantz, 1993). Acid mine drainage (AMD) is a widespread phenomenon affecting the quality of water at many South African collieries. Techniques to determine the likely leachate quality are numerous and have, thus far, been applied without uniformity. Coal occurs in the Karoo System (De Jager, 1992) and no coal will be found underneath the Dwyka series (Plumstead, 1957). A variety of minerals can be found in South African coalfields: silica, feldspar, clay and pyrite. The first three are in a non-reactive state due to their bonding with silica. Through weathering some of the elements can be released. Pyrite and the carbonates, however, are the most reactive (Hodgson, 1992).

As an illustration, in the Witbank Dam Catchment, a total sulphate production of 45 – 90 t d^{-1} (average 70 tons per day) is produced by opencast mines, largely due to AMD (Hodgson and Krantz, 1995). Hodgson and Krantz further found that, extrapolation of this data to include future open casting at existing mines, the sulphate contribution can escalate to an anticipated value of 120 t d^{-1}. The latter translates into a sulphate concentration in the Witbank Dam of 450 mg l^{-1}.

Acid mine drainage occurs when sulphide minerals in rock are oxidised, usually as a result of exposure to moisture and oxygen. This results in the generation of sulphates, metals and acidity that can have manifold environmental consequences. It is therefore of utmost importance to the mining industry to know the characteristics/capacity of waste rock, overburden, pit walls, pit floor and tailings to produce acid mine drainage.

1.2 Study Area

The Colliery is an opencast coal mining area which is situated 55 km west of Witbank in Mpumalanga. The Main office buildings of the colliery area located on the farm Cologne 34-IS and it is part of the Witbank Coalfields. The project study area is located on the farm Leeuwfontein 219-IR and Schoongezicht 218_IR. Site preparation was initiated in March 1984 and the first coal was mined in August 1986 with the delivery to Kendal Power Station in November 1986.

The mining area investigated were Block I, Block I Extension A and B of the Colliery, which are located on the farms Schoongezicht 218_IR and Leeuwfontein 219-IR. These blocks have been rehabilitated since mining ceased in 2005. Figure 1.1 provides a location map of the localities of the sampling sites as well as the streams and the dam in the area.

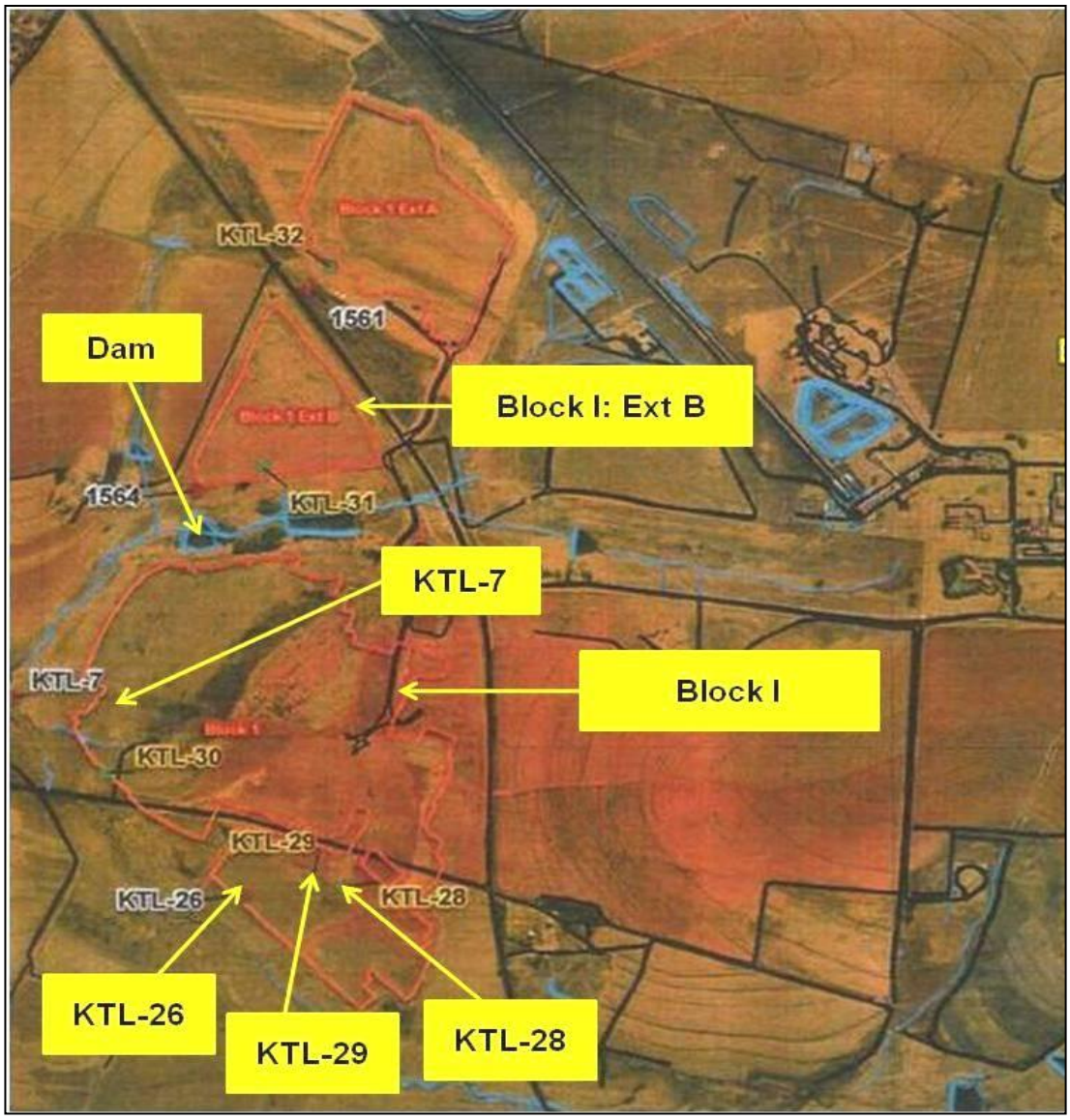

Figure 1.1: Location map of the opencast Blocks reflecting monitoring boreholes, dams and streams



Figure 1.2: Location map of the opencast Blocks reflecting monitoring boreholes

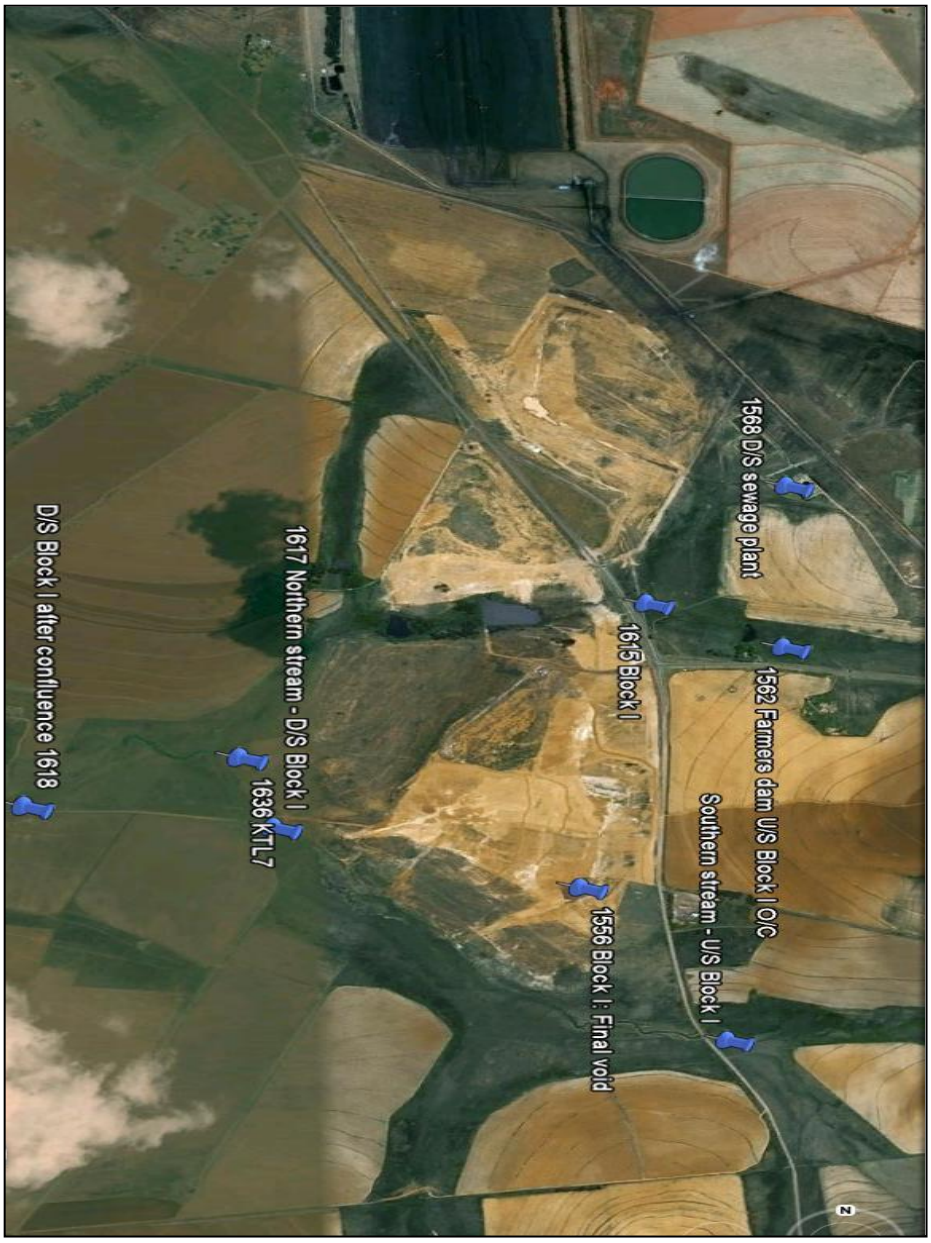

Figure 1.3: Location map of the opencast Blocks reflecting surface water monitoring points

A dam in Block I, next to sampling site KTL-31 is located at elevation 1 593 m. The water flow is downwards from a dam towards borehole KTL-7 at elevation 1 571 m. At borehole KTL-7, the groundwater from the borehole decants to the surface and

joins the stream along the boundary of the Block I mining area. The area is being rehabilitated in an effort to reduce the effect of acid mine drainage.

1.2.1 Application of top soil on the old mining area

The former mining area in Block I has had top soil added to the overburden in an effort to restore the area to its natural state. The top soil applied was originally from the same mining area before mining started. Topsoil layer of about 400-mm was placed on top of the leveled overburden spoil material.

1.2.2 Planting of grass on the added top soil

Vegetation has been restored in the area by planting grass on the top soil. The vegetation is used as a cover to minimise soil erosion, infiltration of surface run-off and to some extent prevent the spreading of pollution plume.

1.2.3 Neutralising acidity on the area by applying lime annually

Every year in January, lime is applied in Block I and Block I Extensions A and B at a dose of 700 kg of lime per hectare. The lime helps with, not only neutralising the acidity associated with acid mine drainage but also with immobilising heavy metals by precipitation to prevent them from leaching from the soil as a result of the acidic water.

2 AIMS OF THE PROJECT AND STUDY AREA

2.1 Aims of the Project

- To perform geochemical analyses of different variables occurring as part of the recharge water and the mine affected water within the colliery Block I, Block I Extension A and B rehabilitated opencast area and determine the potential of these samples to cause acid mine drainage.
- To assess the groundwater recharge and borehole yield capacities.
- To further investigate the groundwater and surface water quality at the Block I, Block I Extension A and B area
- Assess the potential of both surface and groundwater pollution on the downstream water resource.
- To investigate the extraction efficiencies of metal ions from the soil with various extractants as a way of assessing the potential risk of pollution to receiving water systems.
- To draw conclusions that can be useful for current and future remediation strategies to minimise and/or prevent the potential of acid mine drainage in rehabilitated and future areas to be rehabilitated.

3 LITERATURE REVIEW

3.1 Acid Mine Drainage (AMD)

Acid mine drainage (AMD) and heavy metals pollution can poison groundwater and drinking water and destroy aquatic life and habitat. The acid dissolves heavy metals such as lead, zinc, copper, arsenic, selenium, mercury and cadmium into ground- and surface water (Hadley and Snow, 1974). Heavy metals kill, because they prevent the energy that is essential for life from being produced, by binding with –SH (mercaptan) functional groups in enzymes and other proteins (Stevenson, 1997).

Certain bacteria, naturally present, can significantly increase the oxidation rate. The contaminated water is often reddish-brown in colour, indicating high levels of oxidised iron (Hadley and Snow, 1974). Bright orange coloured water and stained rocks are usually telltale signs of acid mine drainage. The orange colour is due to ferric hydroxide ($Fe(OH)_3$) (yellow boy) precipitating from the water. The precipitate forms as acid mine drainage becomes neutralised. At low pH-values the metal ions remain soluble. When the pH rises, the iron oxidises and precipitates out. Depending on the conditions, the orange coloured precipitates may form inside the mine, or several distance downstream. The precipitates can be harmful to aquatic life in several ways. The clumps reduce the amount of light that can penetrate the water, which affects photosynthesis and the vision of animals. When the precipitate settles, it blankets the streambed, smothering the bottom-dwellers and their food resources

AMD can develop at several points throughout the mining process in underground workings, open pit mine faces, waste rock dumps, tailings deposits and ore stockpiles. Acid generation can last for decades, centuries, or longer and its impacts can travel

many distance downstream. Roman mine sites in Great Britain continue to generate acid drainage, 2000 years after mining ceased (BC Mining Watch, 1996). Acid drainage from mining operations has a long history, dating back thousands of years to Phoenician times when the Iberian Pyritic Belt in Spain, from where the Rio Tinto (Red River) flows, was first exploited (Miller, 1998).

Industry, labour, government and environmentalists agree on one issue: that AMD is the number one environmental problem facing the mining industry (BC Mining Watch (1996), Domvile *et al.* (1994), Lawrence and Wang (1997) and Schafer Laboratory (1997)). Waste rock and tailings are the most important sources of AMD. There is no dispute that AMD:

- devastates fish and aquatic habitat,
- is virtually impossible to reverse with existing technology,
- once started, costs millions annually to treat and can continue for centuries (BC Mining Watch, 1996) and
- is very complex to control and treat (Lawrence and Day (1997), Evangelou (1995)).

AMD is a severe environmental pollution problem associated with coal and other sulphide-containing ore mining operations, and results mainly from the oxidation of pyrite. It is estimated that each year in the US, the wet cleaning of coal alone leaves behind aqueous slurries of refuse containing at least 10 million tons of pyrite (Evangelou and Zhang, 1995).

3.2 Phase in the Development of AMD

It is only relatively recently that the full implications of its impact have been acknowledged in mine planning. Nordstom *et al*. (1999) report on the famous Iron Mountain site, at Richmond California. This mine has drainage with a negative pH (as low as –3.6), metals around 200 g l^{-1} and sulphate as high as 760 g l^{-1}. This contamination is a result of AMD resulting from of pyrite oxidation.

The Equity Silver Mine in Northern BC, for example, received permits in 1979 to operate without proper consideration for the potential of AMD. Within months it became an infamous site of contamination due to the generation of metal-contaminated and acidic drainage from waste rock, tailings and many structures around the mine site, which had been constructed from acid-generating rock (Lawrence and Day, 1997). Phases in the development of AMD:

The development of AMD involves a complex combination of organic and inorganic processes and reactions. To produce severe acid drainage, where the pH of the system drops below 3, sulphide minerals must create an optimum micro-environment for rapid oxidation and must continue to oxidise for a sufficiently long time to exhaust all of the neutralisation potential of the rock. The potential of sulphide rock to generate acid is strongly related to the amount of alkaline, often calcareous, material in the rock.

When reactive sulphide rock is initially exposed to flowing water and oxygen, sulphide oxidation and acid generation begins. Any calcium-based carbonate in the rock immediately neutralises this small amount of acidity and maintains neutral to

alkaline conditions in water passing over the rock (Broughton *et al*., 1992). As acid generation continues and the neutralising agent is consumed or is rendered ineffective in further neutralisation, the pH of the water decreases, which in turn enhances the conditions for further acid generation. As the rate of acid generation accelerates, the pH progressively decreases in a step-like manner. Each plateau of relatively steady pH represents the dissolution of a neutralising mineral that becomes soluble at that pH.

If the rate of acid generation remains high enough to remove all of the neutralisation potential in the rock, the pH-values will drop below 3 and AMD will become severe. These various stages can last for weeks, months, or centuries until the sulphide minerals completely oxidise and the rock becomes inert, or until special waste management and AMD control actions are taken (Durkin and Herrmann, 1996). The various stages are mineralogy dependent, and in South Africa often the observed quality is near neutral, high salt content, water due to carbonate buffering. Once this has been depleted, pH-values tend to fall relatively rapidly.

3.3 Acid-Base Accounting

Acid-Base Accounting (ABA) is a first-order classification procedure whereby the acid-neutralising potential and acid-generating potential of rock samples are determined and the difference (net neutralising potential) is calculated. The net neutralising potential and/or the ratio of neutralising potential to acid-generation potential is compared with a predetermined value, or set of values, to divide samples into categories that either require, or do not require, further determinative acid potential generation test work.

Different methods of conducting ABA test work will generate different sets of sample data for evaluation. Rules and guidelines have been developed by mine regulatory and permitting agencies (e.g. Price and Errington (1995), Steffen, Robertson and Kirsten (1991) and Brady *et al.* (1994)) for ABA procedures (Mills, 1998c). ABA indicates the overall balance of acidification potential (AP) and neutralisation potential (NP) (Schafer Laboratory, 1997).

In its most basic form, ABA is simply a screening process. It provides no information on the speed (or kinetic rate) with which acid generation or neutralisation will proceed and because of this limitation the test work procedures used in ABA are referred to as Static Procedures (Mills (1998c), Ziemkiewicz and Meek (1994)).

The potential for a given rock to generate and neutralise acid is determined by its mineralogical composition. This not only includes the quantitative mineralogical composition, but also individual mineral grain size, shape, texture and the spatial relationship with other mineral grains. The term "potential" is used because even the most detailed mineralogical analysis, when combined with ABA, can give only a "worst case" value for potential acid production and, depending upon the NP procedure used, a "worst case", "most likely case" or "best case" value for potential neutralisation capability. The field generation and neutralisation of AMD represent the degree to which these potential values are realised in practice (Mills, 1998c).

Neutralisation potential measures the sum total of carbonates, alkaline earths and bases available to neutralise acidity and represents the most favourable condition. Calculations of the maximum potential acidity and neutralisation potential are structured to equate the two measurements to a common basis for comparison. The resulting values, expressed as calcium carbonate equivalent, are compared to compute

a net acid-producing or neutralising potential. Material exhibiting a net acid production potential of 5 tons/1000 tons of overburden material or more as calcium carbonate equivalent is classed as toxic or potentially toxic (Hunter, 1997b and Sobek *et al.,* 1978).

Proposed new mines in British Columbia are required to evaluate potential AMD generation in considerable detail and to demonstrate comprehensive planning to prevent or suppress AMD generation at all phases of mine operation, from development to closure and post-closure. Such evaluation must include pit walls, overburden, waste rock, tailings and any other material produced by the mining process.

Application of this Acid-Base Accounting method to overburden handling and placement plans throughout the USA and Canada, has generally been effective in eliminating or reducing adverse water quality impacts. It becomes a more powerful tool when used in conjunction with hydrologic data, mining and reclamation plans, mineralogy data, etc. (Perry, 1997).

The primary **advantages** of the Acid-Base Accounting method are:

- Short turn-around time for sample processing.
- Low cost.
- Relatively simple analytical procedures.
- Relatively simple interpretation of results (Hunter, 1997b; Evangelou and Zhang, 1995).

Depending on the type of information required and the on-site conditions (complexity, disposal methods, available information, etc.), different portions of the methods need to be applied.

3.4 Basic Chemistry of AMD Generation and acid generating reactions

Acid mine drainage impacts stream and river ecosystems in several ways through acidity, ferric iron (Fe^{3+}) precipitation, oxygen depletion and release of heavy metals associated with coal and metal mining, such as aluminium, copper, gold, lead, manganese, silver, uranium and zinc (AMD Chemistry, 1997).

Pyrite (FeS_2) an iron disulphide (commonly known as fool's gold), is one of the most important sulphides found in the waste rock of mines. When exposed to water and oxygen, it can react to form sulphuric acid (H_2SO_4). The following oxidation and reduction reactions express the breakdown of pyrite that leads to acid mine drainage.

$FeS_2 + 7/2\ O_2 + H_2O \rightleftharpoons Fe^{2+} + 2SO_4^{2-} + 2H^+$ ……3.1

$Fe^{2+} + 1/4O_2 + H+ \rightleftharpoons Fe^{3+} + 1/2\ H_2O$ (rate limiting step) ……3.2

$Fe^{3+} + 3H_2O \rightleftharpoons Fe(OH)_3$ (yellow boy) $+ 3H^+$ ……3.3

$FeS_2 + 14Fe^{3+} + 8H_2O \rightleftharpoons 15Fe^{2+} + 2SO_4^{2-} + 16H^+$ ……3.4

(AMD Chemistry, 1997 and Evangelou, 1995)

Reaction 3.1 shows oxidation of the disulphide, thus releasing ferrous iron (Fe^{2+}) and two protons. In Reaction 3.2, the ferrous iron is oxidised to ferric (Fe^{3+}) which hydrolyses to form ferric hydroxide (an insoluble compound at pH greater than 3.5) and in the process, as shown in Reaction 3.3, three more protons are released. Thus for every mole of pyrite five protons are released. However, since one proton is consumed for the oxidation of ferrous to ferric, only four protons are actually produced (Evangelou, 1995). Upon initiation of pyrite oxidation, the ferric iron can be reduced by the pyrite itself, as shown in Reaction 3.4 (Stumm and Morgan (1970), Singer and Stumm (1970)).

Therefore, pyrite continues to oxidise as long as ferric iron (Fe^{3+}) is generated. The conversion of ferrous to ferric is also the rate-limiting step in the oxidation of pyrite. However, since oxidation of ferrous to ferric in the pH-range of 3 is extremely slow (half-life in the order of 100 days), it appears that pyrite oxidation in this pH-range would be extremely slow, unless oxidation of ferrous at low pH is catalysed by micro-organisms (Singer and Stumm, 1970). In the pH-range of 2.5 – 3.5 (Jaynes *et al.*, 1984), *Thiobacillus ferrooxidans* rapidly oxidise ferrous iron to ferric iron. Iron-oxidising bacteria can accelerate the rate of Fe^{2+} oxidation by a factor of 106 (Singer and Stumm (1970)).

Also, sulphur-oxidising bacteria such as *T. thiooxidans and T. ferrooxidans* can eliminate the need for ferric iron when in the presence of oxygen and some organic substrate (Evangelou, 1995). At low pH (<4.5) pyrite is oxidised by Fe^{3+} much more rapidly (Appelo and Postma, 1993) than by O_2, and more rapidly than dissolved Fe^{2+} is oxidised by O_2 to Fe^{3+} (Evangelou, 1995). This process rapidly consumes all Fe^{3+} and pyrite oxidation would cease unless Fe^{3+} is replenished by the process of oxidation of Fe^{2+} by oxygen (Appelo and Postma, 1993). For this reason, Reaction

3.2 is known to be the rate-limiting step in abiotic pyrite oxidation (Singer and Stumm, 1970).

T. ferrooxidans is an acidophilic chemolithotrophic organism that is ubiquitous in geologic environments containing pyrite (Nordstrom, 1982). Thus, in the presence of *T. ferrooxidans* and under low pH-conditions, pyrite oxidation can be described by Reactions 3.2 and 3.4. Reaction 3.3 taking place at pH-values as low as 3, is a readily reversible dissolution/precipitation reaction that serves as a source as well as a sink of solution Fe^{3+} and is a major step in the release of acid to the environment (Evangelou, 1995). The red colour often seen in streams receiving acid mine drainage is actually a stain on the rocks called "Yellow Boy" or Ferrous Hydroxide ($Fe(OH)_3$) formed during Reaction 3.3.

Acidity is caused by the liberation of hydrogen ions (H^+) in three of the four reaction steps.

The overall chemical reaction can be simplified to:

$$FeS_{2(s)} + 15/4O_2 + 7/2\ H_2O \rightleftharpoons Fe(OH)_3 + 2SO_4^{2-} + 4H^+ \qquad \text{……..……..3.5}$$

In the above reaction, every mole of pyrite yields four moles of acidity (Cohen (1996), Durkin and Herrmann (1996), Kempton *et al.* (1997) and Morin and Hutt (1994)). Observe the necessity for air and water (although the process can occur in a dry environment) (Cohen, 1996).

During the initial stage, pyrite oxidation is a relatively slow process (Ivanov, 1962). Most iron released during the initial stages of pyrite oxidation ends up as iron hydroxide, due to the relatively high pH on pyrite surfaces (Fornasiero *et al.,* 1992 and Ivanov, 1962). However, as acid production continues and the pH in the vicinity of the pyrite surface drops below 3.5, formation of ferric hydroxide is hindered and activity of Fe^{3+} in solution increases. Under these conditions, oxidation of pyrite by Fe3+ becomes the main mechanism for acid production in mining waste (Singer and Stumm, 1970 and Moses *et al.,* 1987). Singer and Stumm (1970) reported that Fe^{3+} can oxidise pyrite at a much higher rate than O_2. This can be seen in the oxidation of pyrite as described in the below reaction (Evangelou and Zhang, 1995):

$$FeS_2 + 14Fe^{3+} + 8H_2O \quad \rightleftharpoons \quad 15Fe^{2+} + 2SO_4^{2-} + 16H^+ \qquad \text{.....3.6}$$

------O_2-----

Iron-oxidising bacteria

It has been reported that pyrite in mining waste or coal overburden is initially oxidised by the atmospheric O_2, producing H^+, SO_4^{2-} and Fe^{2+}. The Fe^{2+} can be further oxidised by O_2 into Fe^{3+} that in turn hydrolyses and precipitates as amorphous iron hydroxide releasing additional amounts of acid (Nordstrom, 1982).

In addition to pyrite, the presence of both oxygen and water is required for process progression (Evangelou, 1995 and Mills, 1998a). The process is complex because it involves chemical, biological and electrochemical reactions and varies with environmental conditions. Factors such as pH, O_2, specific surface and morphology of pyrite, presence or absence of bacteria and/or clay minerals, as well as hydrological factors, determine the rate of oxidation. There is, therefore, no single rate law available to describe the overall kinetics of pyrite oxidation for all cases

(Evangelou, 1995). This has important ramifications in that removal of the oxygen source (e.g. by total submersion under water) or the water source (e.g. conditions of aridity) will halt AMD production. AMD production would also be considerably slowed or halted by the termination of *T. ferrooxidans* reproduction by a bactericidal agent.

The end products are sulphuric acid and ferric sulphate. Sulphuric acid is also an important intermediate product. From the onset of pyrite oxidation, pH falls (acidity increases) quickly and then stabilises, typically at values around pH 2.5 to 3.0. The pH of stabilisation is normally determined by the optimal habitat requirement of the site-specific strain of bacteria (Mills, 1998a).

If pyrite and/or pyrrhotite are the only sulphide minerals open to atmospheric oxidation, the products of the oxidation process are those described above. Depending upon the availability of water and oxygen, reactions may not always approach completion and in such cases intermediate phases of chemical compounds or minerals may remain at the oxidation site.

The reaction of sulphuric acid with pyrite is described by Levinson (1974):

$$FeS_2 + H_2SO_4 \rightleftharpoons FeSO_4 + H_2S + S \quad \ldots\ldots\ldots\ldots\ldots\ldots\ldots\ldots\ldots\ldots\ldots\ldots\ldots\ldots\ldots\ldots\ldots\ldots 3.7$$

This accounts for the presence of small amounts of native sulphur at outcrops. This could also explain why H_2S is a common gas around coal mines and mine dumps, other than the H_2S which is ascribed to bacterial sulphate reduction.

If metallic minerals (such as galena (lead sulphide, PbS), chalcopyrite (iron-copper sulphide, FeS. CuS), sphalerite (zinc sulphide, ZnS)) in addition to pyrite and pyrrhotite are present, there may be a secondary effect of the oxidation of the iron-sulphur minerals to sulphuric acid and ferric iron (Mills, 1998a).

The stable pH developed (2.5-3.0) and the products of sulphuric acid and ferric sulphate create conditions where the ferric iron ion itself can act as an oxidant. In the absence of ferric iron at pH 2.5-3.0, sulphuric acid will dissolve some heavy metal carbonate and oxide minerals, but has little reactive effect on heavy metal sulphides. However, ferric iron ion is capable of dissolving many heavy metal sulphide minerals, including those of lead, copper, zinc and cadmium, by the general reaction:

$$MS + nFe^{3+} \rightleftharpoons Mn^{+} + S + nFe^{2+} \qquad \ldots\ldots 3.8$$

Where: MS = solid heavy metal sulphide; Fe^{3+} = aqueous ferric iron ion; Mn^{+} = aqueous heavy metal ion; S = sulphur; Fe^{2+} = aqueous ferrous iron ion.

This process, together with the acidic environment, allows significant amounts of heavy metals to be solubilised by AMD. In addition, many metallic elements are often present at trace levels within the minerals pyrite and pyrrhotite. Oxidation of these minerals can therefore release and mobilise these trace elements.

Untreated (not neutralised) AMD creates two quite distinct environmental problems - the acidity from sulphuric acid (which is invariably a product by definition) and the heavy metal solubilisation caused by ferric iron (which may occur under the conditions described above). It is important that these two effects be recognised as separate, since their consequences to ecosystems are distinct, and because AMD generation and heavy metal transport are separate processes (Mills, 1998a).

3.5 Basic Chemistry of AMD Generation and Acid Generating Reactions

Acid mine drainage depletes the buffering ability of water by neutralising carbonate and bicarbonate ions to form carbonic acid (H_2CO_3) (AMD Chemistry, 1997).

$H^+ + CO_3^{2-} \rightleftharpoons HCO_3^-$ ……..3.9

$H^+ + HCO_3^- \rightleftharpoons H_2CO_3$ …….…….……3.10

Once exposed to acid mine drainage, the affected carbonate buffering system is not able to control changes in pH as effectively. The buffering system is completely destroyed below a pH of 4.2 where all carbonate and bicarbonate ions have been converted to carbonic acid. The carbonic acid readily breaks down into water and carbon dioxide (AMD Chemistry, 1997).

$H_2CO_3 \rightleftharpoons H_2O + CO_2$ ……..……3.11

(AMD Chemistry (1997), Todd and Reddick (1997))

If the pH of AMD is increased, as would happen with contact with basic minerals such as calcite ($CaCO_3$) or dolomite ($CaMg(CO_3)_2$) or entry into a water system of higher pH, then metallic ions such as Fe^{3+} and Cu^{2+}, Zn^{2+}, Pb^{2+} and metalloid ions As^{3+} will react to eventually form hydroxides as precipitates by the general reaction:

$Mn^+ + nOH^- \rightleftharpoons M(OH)_n$ 3.12

where: OH^- = hydroxyl ion; $M(OH)_n$ = metal hydroxide.

This over-simplification represents chemical neutralisation as it occurs by human intervention, rather than an accurate portrayal of natural occurrence, where the precipitation products are usually carbonates and sulphates and their hydrated and/or hydroxy-complex forms. In nature, acid-generating minerals such as pyrite often occur in close association with acid-neutralising minerals such as calcite ($CaCO_3$) and dolomite ($CaMg(CO_3)_2$) and acid produced from pyrite is neutralised *in situ* by these minerals. The sulphate most commonly formed is gypsum ($CaSO_4.2H_2O$), which is sparingly soluble in water and which therefore contributes to elevated sulphate levels in ground and surface waters (Shaw and Mills, 1998).

Factors that determine the neutralisation rate by carbonate and silicate minerals include: pH, pCO_2, equilibrium conditions, temperature and the presence of "foreign" ions. Comparison of rates shows that sulphides react the fastest, followed by carbonates and silicates (Sherlock *et al.*, 1995).

3.6 Sampling and analysis methodologies

3.6.1 Field methods

The sampling methods that should be considered when conducting detailed fieldwork should include the following, as suggested:

- Water sampling and ongoing monitoring.
- Representative sampling of spoil material, preferably through boreholes so that volumetric and depth determinations can be made.
- *In situ* profiling of water.
- Test pits in established spoils to determine areal and age variation.

The usefulness of field methods is that they:

- Are the most reliable measurements.
- Represent the best Kinetic reactor there is (As Morin and Hutt, 1997 state "Undoubtedly the most valuable and representative kinetic test that can be operated at a mine site is the full-scale operation of mine site components).
- Determine current situation.
- Provide understanding of controls on chemistry.
- Allow comparison to ABA.
- Serve as an early warning system.
- Provide information to make decisions on appropriate control measures.

3.6.2 Static tests

Several static methods have been extensively tested to determine differences and select methods to be used.

The following methods are recommended:

- Paste/initial pH and determination of solution products;
- Acid potential using hydrogen peroxide oxidation, analysis of oxidation products and
- Neutralising potential using sulphuric acid adaptation of the Sobek method

Based on previous studies conducted it can be concluded that:

- Acid-Base Accounting is an excellent first-order tool to determine whether mine waste has the potential to form acidic drainage.

- Well-established criteria exist for the classification of individual samples as potentially acid-generating or neutralising.
- When samples are obtained at specific locations, with depth, the use of depth normalisation and volumetric calculations provide an established methodology of evaluating ABA results for an entire spoil area.
- Where material is to be used for neutralisation, acid leachable metals should be determined, since these levels may be extremely high if acidification was to occur.
- The hydrogen peroxide acid potential method and the Total S determined, using a Leco analyser, should provide similar assessment of acid potential.
- The hydrogen peroxide method, however, provides additional information such as an indication of oxidised pH and the levels of different potential contaminants, which can be released. Furthermore uncertainties regarding the contribution of different types of sulphur are eliminated, since only reactive sulphur is measured.

3.6.3 Kinetic tests

- Humidity cells can provide reaction rates for different species. Reaction rates for all the cells tested could be obtained.
- Increasing the humidity causes an increase in the reaction rate, in agreement with international research.
- The rates of flushing were sufficiently high to prevent secondary mineral precipitation.
- Humidity cells may not provide an indication of acidity for samples that are uncertain, according to the static test results.

- Standardised tests should be used wherever possible, to build up a database of rates for South African coalfields.
- Where the influence of any particular aspect, e.g. the effect of a cover, is to be proved using a kinetic test, a standard test should be done as a base case for comparison.
- The degree and rate of Nuetralising potential (NP) depletion can be determined from cells.
- The theoretical depletion of NP correlated very well with the pH-development in the cells that acidified.
- A modified NAG/kinetic test showed that under highly oxidising conditions acidification of large boulders will occur due to reactions at the surface of the boulders. This acidification implies that the neutralising potential of the rock may be overestimated by any static NP determination.
- The $Ca^{2+}Mg/SO_4$ ratio appears to be an excellent early indicator of imminent acidification.
- Humidity cells should be able to provide "threshold" values for acid and neutralising potentials. This will greatly enhance the usefulness and likely success of the prediction of acidity.

3.6.4 Modelling

- Several input parameters which have been accurately determined are needed.
- Selection of appropriate model tool is vital.
- Provides long-term (+100 years) estimates of changes/trends in AMD quality.

- Enables a comparison between different options.
- Provides the basis for comparing the risk and costs associated with each option.
- It is often associated with large uncertainties.
- Field and laboratory validation can decrease uncertainty.
- Illustrations using simplified simulations showed how relatively minor variations (relative to the uncertainty of most of the data used in the models) can yield significantly different results.
- Despite limitations modeling is considered to be a very useful tool in prediction.

4. METHODOLOGY

4.1 Drilling

Five new boreholes were drilled into and around the rehabilitated areas. These were; one borehole at Block I extension A and extension B and three into Block I. The positions of the new boreholes are presented in Figure 1.1. The new boreholes were positioned in close proximity to exiting holes to enable monitoring of the existing boreholes during testing. No suitable boreholes existed in the southern part of Block I and two boreholes were drilled to accommodate the test work.

Table 4.1: Positions of newly drilled boreholes

Borehole ID	**Borehole Depth (m)**	**Collar elevation (mamsl)**	**Depth to floor (m)**	**Water level (mbgl)**	**Saturated thickness (m)**	**Geology Position**
KTL-28	21	1 583	21	13.99	~7	Spoil material Block I
KTL-29 Spoil material	18	1 580	18	11.02	~7	Block I
KTL-30	12	1 568	8	0.82	~7	Spoil material Block I
KTL-31	9	1 582	9	2.57	~6.5	Spoil material Block I ext B
KTL-32	30	1 604	N/A	9.73	N/A	Karoo sediments Block I ext A

4.2 Pump testing

Four pump tests, one test on each of the new holes in Block I extension A and extension B and two tests on the new holes in Block I, were run. The existing boreholes were used as observation points during the test work. The pump tests consisted of a set of step tests each of an hour duration followed by a recovery test. The information obtained from the step tests was used to select an optimum rate for a constant discharge test. Water level recovery was measured after the constant discharge test.

4.3 Sampling procedure

The water and soil samples were collected in July 2009. The water samples were collected in polypropylene plastic bottles which were originally soaked overnight in soapy water, acid washed with 1 M nitric acid and rinsed with deionised water (Mugo and Orians, 1993). Borehole water samples were collected from different boreholes in Block I of the operation and the surface water samples were collected from the streams in Block I and from a nearby farmer's dam (Fig. 1.1). The depth of the water in the boreholes was measured during each sampling session using a water level dip meter.

The soil samples were collected near each sampled borehole so as to get some insight into the quantity of leachates in the vicinity of boreholes. The soil samples collected were the topsoil, which was applied on the rehabilitated mining area at 400 mm thickness and the sub soil which was dug by an excavator at a depth of 1.5 m. Ground elevation at each sampling site was accurately surveyed. The soil samples

were stored in polypropylene plastic bags and polypropylene plastic bottles washed with 1 M nitric acid and rinsed with deionised water. Both the water and soil samples were stored in the refrigerator in the laboratory at 4°C before analyses.

4.4 Field measurements

Field measurements on water samples were recorded using a Universal Multiline field meter equipped with pH electrode, standard conductivity cell and oxidation reduction potential probe (WTW, Germany). The pH electrode was calibrated according to the International Union of Pure and Applied Chemistry (IUPAC) recommendations against two buffer solutions at pH 4 and 7. The Ag/AgCl redox potential electrode was checked with standard buffers. All the reported redox potentials were corrected relative to the standard hydrogen electrode (SHE). The temperature of the water samples was measured with a thermometer.

4.5 Sample preparation

4.5.1 Sampling procedure

The trace metal concentrations in the water samples were determined with a multi-element Genesis inductively coupled plasma optical emission spectrometer (ICP-OES) (Spectro, Kleve, Germany). The preparation of the water samples for trace metal analysis was performed as follows: Each water sample was filtered and the filtered sample divided into two aliquots whereby one aliquot was acidified with 1 M HNO3 and the other was non-acidified. The concentration of sulphates in the water was determined by analysing a filtered sample for sulphates with Metrohm 761 Compact Ion Chromatograph. The analysis of chlorides in the water samples was

conducted using Mohr's method of titration with a standardised solution of 0.01 M $AgNO_3$ and K_2CrO_4 as an indicator. The analysis for carbonates (HCO_3^- + CO_3^{2-}) was performed by titration with standardised solution of 0.01 M HCl, using methyl orange indicator as an endpoint detector (Clesceri *et al*., 1989).

4.5.2 Preparation of soil samples

Microwave digestion

Soil samples were weighed and dried in an oven overnight at a temperature of 100^oC. The dried samples were re-weighed and the moisture content of each sample was determined. Each sample was pulverised with a pestle and mortar to approximately < 2 mm. A mass of 0.1 g of each sample was weighed and dissolved with 6 ml of concentrated hydrochloric acid, 2 ml of concentrated nitric acid and 1 ml of concentrated hydrofluoric acid. The samples were digested using microwave digestion procedure at a time of 30 minutes. After each digestion procedure, 6 ml of boric acid was added to each sample. The samples were filled to the mark in a 100 ml volumetric flask and were analysed for total metal concentration with ICP-OES. The samples were analysed for chemical elements such as Al, As, Ca, Cd, Cu, Fe, K, Mn, Na, Ni, Pb, S and Zn.

Leaching tests

The samples were dried and pulverised as before and leaching tests were performed on them. The leaching test was done to measure the potential of the soil to release the metals. The leaching tests were performed with solutions of 0.1 M EDTA, 0.1 M Na_2CO_3, 0.01 M $CaCl_2$ and artificial rainwater. Solutions of EDTA, Na_2CO_3 and $CaCl_2$ were prepared with the artificial rainwater. The artificial rainwater was prepared by: adding a mixture of 11.6 mg NH_4NO_3; 7.85 mg K_2SO_4; 1.11 mg Na_2SO_4; 1.31 mg $MgSO_4.7H_20$ and 4.32 mg $CaCl_2$ in a 1 L volumetric flask. The

flask was filled to the mark with deionised water. The batch experiment was performed for the leaching test and the leaching was done by adding each of 0.1 M EDTA; 0.1 M Na_2CO_3; 0.01 M $CaCl_2$ and artificial rainwater to the sample at a sample to liquid ratio of 1:10. The samples were shaken for 16 hours at 100 rpm using a mechanical automated shaker. Samples were filtered with 0.45 µm filter paper and the filtrate was analysed for total metal concentration with ICP-OES.

Static acid base accounting studies

Static acid base accounting was performed on each pulverised sample. The following are the procedures used for the static acid base accounting studies:

Initial pH

A sample mass of 5 g was weighed and added 50 ml of deionised water and was left for 24 hours, after which the initial pH was measured (Usher *et al*, 2003).

Final pH

A volume of 80 ml of H_2O_2 (30% w/v) was added to a mass of 2 g of pulverised sample. The reaction was left to oxidise for 24 hours, after which the final pH was measured (Usher *et al*, 2003).

Acid potential

The acid potential (AP) was determined by reacting 2 g of the sample with 80 ml of 30% hydrogen peroxide and the sample was left for 24 hours to allow complete

oxidation. The supernatant was analysed for sulphate and acid potential was back-calculated by equation (3.14) (Usher *et al*., 2003).

$$AP = \frac{SO_4 \text{ (mg } l^{-1}\text{)/ sample weight (g) x Volume of } H_2O_2}{1000} \quad \text{…..……..3.13}$$

= kg SO4 t^{-1} of sample

$$AP\ (CaCO_3 \text{ kg } t^{-1}) = (SO_4 \text{ kg } t^{-1} \text{ x } 50) / 48 \quad \text{……..…..……..……..3.14}$$

Neutralising potential

Neutralising Potential (NP) was determined by adding 0.06 N H_2SO_4 to the pulverised sample and the pH of the slurry was measured after 24 hours to ensure that the pH was below 2.5. The sample was then back-titrated to pH 7 with standardised solution of 0.06 N NaOH. The samples which had a pH greater than 2.5 after 24 hours were added aliquots of H_2SO_4 until pH was less than 2.5 and were left for further 24 hours. The neutralising potential was calculated by equation (3.15) (Usher *et al*., 2003):

$$NP\ (CaCO_3 \text{ kg } t^{-1}) = \frac{(N\ H_2SO_4 \text{ x ml acid}) - (N \text{ NaOH x ml alkali}) \text{ x } 50}{\text{Weight (g)}} \quad \text{.....3.15}$$

Net neutralising potential (NNP)

NNP for the open system was calculated by equation (3.16) (Usher *et al*, 2003):

NNP (open) = NP – AP (open)……..…….....3.16

All solutions were prepared with purified water obtained by passing deionised water through a Milli-Q water purification system. All chemicals used were of analytical grade obtained from Sigma-Aldrich and Merck.

5. RESULTS AND DISCUSSION

5.1 Pump Testing Results

The results of the pump testing are detailed in Table 5.1 below.

Table 5.1: Pump testing results

Pumped borehole	Observation borehole [distance]	Test done	Comment
KTL-29	KTL-28 [90 m]	3 step tests and recovery	48 hour constant discharge with recovery Constant Discharge (CD) test yield 23 l s-1
KTL-30	30-Obs [350 m]	1 step tests and recovery	48 hour constant discharge with recovery CD test yield 0.5 l s-1 Low yield did not allow for additional steps.
KTL-31	31-Obs [200 m]	2 step tests and recovery	20 hour constant discharge with recovery CD test yield 4 l s-1 No drawdown was measured in observation borehole. Observation hole probably outside of rehabilitated area.
KTL-32	1564 [100 m]		1 step with recovery Test yield 0.25 l s-1. Short duration test as result of low yield. Borehole was drilled into in situ Karoo sediments.

The following observations were made during the field work:

Borehole KTL-29 was tested in the southern section of Block I. It was pumped at a rate of approximately 23 l s^{-1} for 48 hours during the constant discharge test. The drawdown in this hole was only 0.63 meters after 48 hours of pumping. The water level in observation borehole KTL-28 started responding after 8 hours and a maximum drawdown of 0.5 meters was recorded after 48 hours. The water level in borehole KTL-29 recovered to its original level within 5 minutes after the step tests. It did however not recover fully after the CD test, possibly due to dewatering of the soil material.

The newly drilled borehole KTL-30 was pump tested in the main part of Block I. This hole was pumped at a rate of 0.5 l s^{-1} during the constant yield test. No water level response was observed in the observation borehole (Obs-30). This may be due to the observation borehole (existing hole) not being drilled into the spoil area or that the distance between the holes exceeds the radius of influence of the pump test. The water level in borehole KTL-30 recovered to its original level within 60 minutes after the CD test was terminated.

Borehole KTL-31 was tested in Block I extension B. This hole was pumped at a rate of approximately 4 l s^{-1} during the constant discharge test. The saturated thickness of the spoil material was only approximately 6 meters in this area and the water level was drawn down to the pump intake after 16 hours of pumping. No response was measured in the existing observation borehole (Obs-31). Since no geological information for Obs-31 was available it could not be confirmed that it was drilled into the spoil material.

Borehole KTL-32 is situated on the edge of the rehabilitated area. The yield of this hole is very low and it could only be pumped at a rate of 0.25 l s^{-1} for 10 minutes

before the water level reached the pump inlet. This hole represents the in situ Karoo sediment's hydraulic properties.

The aim of the pump testing was to establish the yield (pump rate) of the boreholes in the spoil material as well as to estimate the specific yield (Sy – volume of water released from a volume of material) of the spoils. Specific yield, also known as the drainable porosity, is a ratio, less than or equal to the effective porosity, indicating the volumetric fraction of the bulk aquifer volume that the aquifer will yield when all the water is allowed to drain out of it under the forces of gravity

As a result of the variation in compaction and the presence of open voids in spoils the hydraulic properties are highly heterogeneous. This complicates the analyses of pump test data to the extent where traditional analytical methods may not accurately estimate the specific yield (Sy) of the spoils.

The data and pump test analyses are attached as Appendix 2 and discussed below.

A response in the observation borehole was only measured for the test run on KTL-29. It was therefore the only test that allowed for the estimation of the specific yield (Sy). Data obtained from the observation borehole (KTL-28) during the pump test on borehole KTL-29 was analysed in the FC method software, using the Neumann method for unconfined aquifers (Appendix 2). This analysis returned a Transmissivity value of approximately 5 700 $m^2 d^{-1}$ and a Specific Yield of 29 %.

Table 5.2 summarises the aquifer parameters and it can be seen that the spoil material has a highly variable transmissivity ranging from approximately 5 000 to approximately 100 m^2 d^{-1}. This confirms the heterogeneous nature of the material.

Table 5.2: Summary of pump test parameters (transmissivity)

Borehole Number	**Transmissivity (m^2 day^{-1})**
KTL-28	5 700
KTL-29	2 060
KTL-30	204
KTL-31	115
KTL32	N/A

5.2 Volume calculation

The volume of water that will be released from the rehabilitated areas can be estimated by multiplying the saturated volume of the spoil material with the specific yield (25 – 30%). From the borehole information it appears that the average saturated thickness in the rehabilitated areas is in the range of 7 meters. The average saturated thickness was multiplied with the pit areas to calculate the volumes of water in the spoils (Table 5.3).

Table 5.3: Summary of volumes of water in rehabilitated areas

Pit	**Surface area (m^2)**	**Saturated volume (m^3)**	**Volume of water (m^3)**	**Inflow into pit**		
				Recharge (m^3 a^{-1})	**Base flow (m^3 a^{-1})**	**Total (m^3 a^{-1})**
Block I ext A	271 311	1 899 179	550 762	26 453	2 858	29 311
Block I Ext B	169 100	1 183 699	343 273	16 487	1 883	18 370
Block I	955 821	6 690 747	1 940 317	93 193	6 923	100 116

The inflow into the rehabilitated areas (Table 5.3) was calculated by assuming that the effective recharge into the spoils will be in the range of 15% of MAP (650 mm a^{-1}). The following assumptions were made for the base flow calculation:

- Hydraulic conductivity of the surrounding Karoo aquifers is low (approximately 0.01 m d^{-1}).
- Groundwater gradient towards the spoil areas is in the range of 0.03.
- Inflow into the pits occurs along approximately 2/3 of the pit perimeter. Decant occurs along the remaining 1/3 of the perimeter.

5.3 Water Chemistry

The results in Table 8.1 (Appendix 1) show the various field measurements for pH, conductivity, redox potential and temperature as well as major anions and total metal concentrations of surface and borehole samples.

5.3.1 pH

The results of the pH measurements in Table 8.1 showed that the pH of the borehole and surface water in the area ranged from 5.9 to 9.0. Within the mining area, the surface water showed mostly neutral to alkaline pH while the borehole water showed moderately acidic to neutral pH. The pH variation showed that as the water flowed downward from the dam (Fig. 5.1) towards the decant point at KTL-7 (Fig. 5.1); there was a decrease in pH from alkaline to moderately acidic. The decrease in pH was possibly the result of the oxidation of pyrite as the ground water decanted from underground to the surface at borehole KTL-7. It was observed that some borehole waters within Block I had alkaline pH values of between 8.0 and 9.0. Examples are boreholes KTL-30 and BH 1563 (Table 8.1). This was attributed to the depth of the borehole water from the surface.

The lower the borehole water depth, the higher the pH because the borehole water was closer to the surface and its pH was increased by the presence of the lime that was applied on the top soil. The water depths of boreholes KTL-30 and 1563 were 0.8 m and 4.48 m respectively (Table 8.1). These depth values were contrasted to the values for boreholes KTL-28 and KTL-29 which had water depths of 14.5 m and 11.22 m and pH values of 6.7 and 5.9 respectively (Table 8.1). The dam that is located in the area also showed alkaline pH of 8.8 and this was possibly due to both the applied lime and the gypsum salt generated near the stream banks.

5.3.2 Electrical Conductivity

The results of the electrical conductivity (EC) of the borehole and surface water are as shown in Table 8.1. It was observed that the conductivity of the stream water

along Block I increased when comparing samples collected upstream to samples collected downstream (Block I upstream, midstream and downstream had conductivities 1.35; 1.37 and 1.61 mS cm^{-1} respectively) (Table 8.1). The highest conductivities obtained were 3.88 and 3.28 mS cm^{-1} corresponding to samples KTL-30 and the small stream at KTL-7 respectively (Table 8.1). A high conductivity from the small stream at KTL-7 reflected the high amount of dissolved solids and increased pollution. A high conductivity at the small stream near KTL-7 was probably due to the increased number of ions as a result of a higher pH of 9.0 (Table 8.1).

The plot in Fig. 5.1 shows the relationship between LogEC and pH of the borehole and surface waters. The plot clearly shows two distinct groups. The Group 1 samples showed a decrease in LogEC and the Group 2 samples showed an increase in LogEC. The Group 1 samples were mainly the borehole water samples and some surface water samples that are in close proximity to the impacted boreholes. This group had been polluted by the AMD containing water from the opencast workings. The Group 2 samples were the borehole water samples with a depth less than 1 m and some surface water samples as well. The borehole waters closer to the surface were buffered by the lime that was applied during the initial seeding of the rehabilitated area and annual vegetation management.

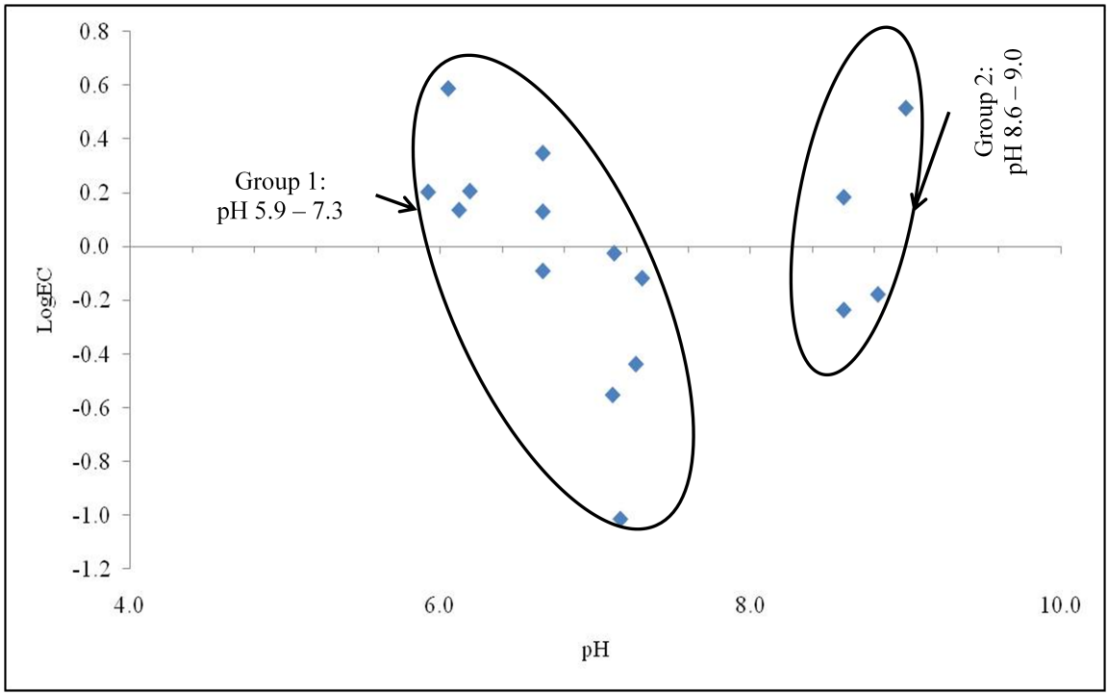

Figure 5.1: The log EC-pH relationship of the borehole and surface waters at the detailed site

5.3.3 Oxidation Reduction Potential (Eh)

The relationship between the redox potential and the pH of the water samples is shown by an Eh-pH plot in Fig.5.2. It was observed that there was a linear decrease of redox potential with increasing pH. The variation had two distinct groups; the water (both borehole and surface) located in close proximity to the lowest point of Block I and Extension B and water located above the lowest point of the Blocks. The analysis of the water closer to the lowest point showed a linear decrease of Eh with increasing pH at slope of -106 mV/pH units (R2 = 0.684) while the water above the discharge point (mostly surface water) showed a decrease with a slope -81.59 mv/pH units (R2 = 0.683). The slope of the line of the water on the lowest point corresponded closely with the predicted equilibrium between Fe(II) and pyrite according to equation 3.1 (Faure, 1998). This reflected the buffering capacity of the

soluble Fe(II) and the pyrite in the overburden material (Pourbaix, 1988). The surface water samples collected in the mining area were buffered by the Fe(II)-Fe(III) equilibrium. A decrease in Eh with an increase in pH reflected the precipitation of $Fe(OH)_3$ as shown by equation 3.3.

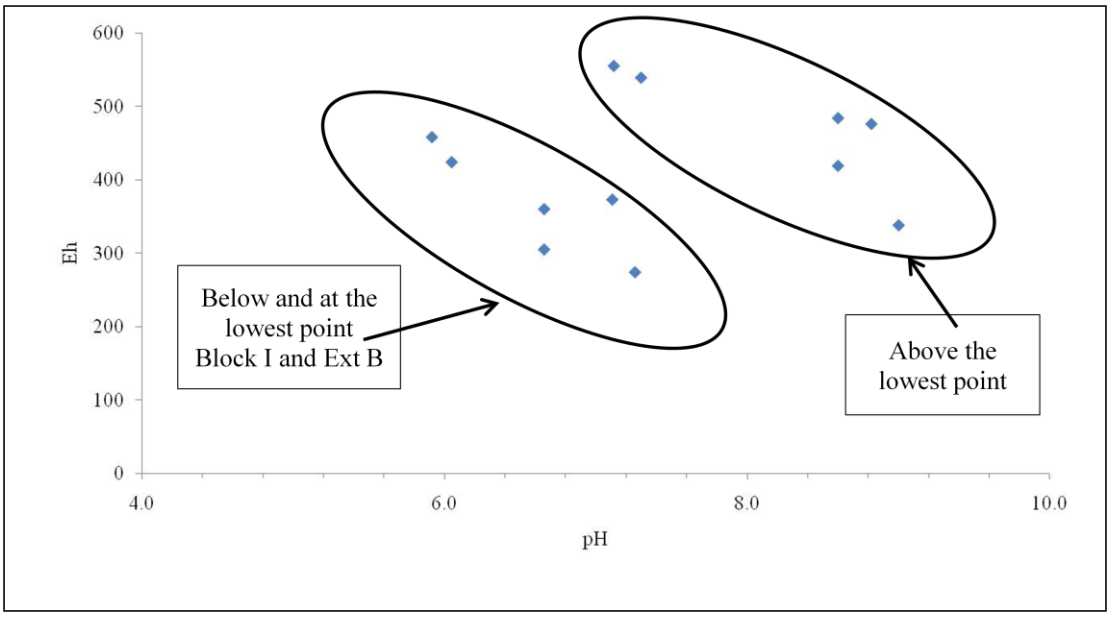

Figure 5.2: The Eh-pH relationship of the water in the lower discharge and above the discharge point.

5.3.4 Sulphates

The results of the sulphate concentrations are shown in Table 8.1. Some surface and borehole water samples in the mining area showed elevated concentrations of sulphates. A sample collected from small stream at KTL-7 had the highest concentration of sulphates at 3 522 mg l^{-1} (Table 8.1). The corresponding pH at this sampling point was 6.05, the second lowest pH recorded in the area. The elevated concentration of sulphates in a small stream at KTL-7 was possibly due to the oxidation of pyrite to form Fe^{3+}, H^+ and SO_4^{2-} according to equation 3.5. The

recorded concentrations of sulphates in Table 8.1 generally corresponded well with having increasing sulphates as pH decreases, as a result of pyrite oxidation. However, there were two borehole water samples which were the exception to the trend and they were KTL-30 and BH 1563 (Table 8.1). Their sulphate contents were 2 352 and 1 170 mg l^{-1} respectively. The recorded pH values of these two borehole water samples were 9.0 and 8.6 respectively. This deviation in the trend was the result of the addition of lime in the area as part of the rehabilitation plan. In the presence of carbonates, pyrite in the mining area was oxidised by dissolved oxygen to form Fe^{3+}, SO_4^{2-}, Ca^{2+} and CO_2 gas according to equation 3.7. This resulted in a more alkaline pH due to the neutralisation of H^+ by CO_3^{2-}, however the sulphate concentration could still be high.

5.3.5 Carbonates

The total carbonate concentrations of the borehole and surface water in the mining area are shown in Table 8.1. It was observed that generally, samples with lower pH had the lower concentrations of total carbonates as expected. However some samples that recorded the highest pH had a higher concentration of sulphates and lower carbonate content. An example was samples KTL-30 and BH 1563 with pH values of 9.0 and 8.6 but with the lower carbonate concentrations of 30 and 45 mg l^{-1} respectively (Table 8.1). The reason was probably due to the reaction of pyrite with the carbonate to yield high sulphate content and a higher pH as shown in equation 3.7.

The higher carbonate concentrations recorded were 186 mg l^{-1}, 114 mg l^{-1} and 123 mg l^{-1}. The carbonate concentrations of 114 mg l^{-1} and 123 mg l^{-1} corresponded to samples from a Dam and Block I upstream respectively (Table 8.1). The concentration of 186 mg l^{-1} corresponded with sample from surface water at KTL-6

(Table 8.1). The reason for the higher carbonates in these samples was attributed to the presence of gypsum salt crusts that were found in the banks of the stream. The capillary fringe above the water table impinges on the land surface on the stream banks and evaporation of the groundwater results in efflorescent crusts (Naicker *et al.*, 2003). This results in the formation of gypsum salt crusts along the stream banks and they can neutralise the water, where evaporation takes place forming efflorescent crusts of metal sulfates. The colour of these crusts is very variable and depends on the composition of the dissolved salt load in the groundwater. White crusts, dominated by gypsum (derived from partial neutralisation of AMD by lime), are the most common, but colours ranging from pale pink (Co, Mn) to various shades of green (Ni, Fe), and even yellow have been observed (Tutu, 2008).

The dissolution of carbonate minerals help with the neutralisation of AMD. The pH of the water is generally higher in the areas where the buffering of carbonate dissolution is significant. In the case where the mine drainage moves from underground to the surface to mix with the stream water at the surface, the oxidation of sulphide stops, whereas the dissolution of carbonates becomes more and more important, and the acidity previously produced by the oxidative dissolution of pyrite is buffered by carbonate minerals. This is accompanied by a rise in pH values. An example of this effect was observed on samples from small stream at KTL-7 and borehole KTL-7, whereby the total iron and sulphate concentrations were the highest (Table 8.1) but the pH of the water was only moderately acidic at pH 6.05 and 6.66 respectively. The pH of the water was not severely acidic because of the buffering effect of the carbonate minerals.

5.3.6 Trace Metal Concentration

The plots in Fig. 5.3 and complete data in Table 8.1 show the trace metal concentrations of the borehole and surface waters. These results showed that the dominant metal ions in the water were the alkali metals (Na and K) and the alkali earth metals (Ca and Mg) in all the samples. Heavy metals such as Fe, Mn, and Zn were dominant at the decant points (small stream at KTL-7 and borehole KTL-7) and at a sample from borehole KTL-29. The highest recorded concentration of Fe was 216 mg l^{-1} which was a sample collected from small stream at KTL-7 (Table 8.1). At borehole KTL-7 the ground water was decanting to the surface and as it was exposed to atmospheric oxygen, pyrite oxidised to form an insoluble Fe(III) which results in high iron content.

The highest recorded concentration of Mn was also from small stream at KTL-7 with 46.2 mg l^{-1} (Table 8.1). The highest concentrations of other heavy metals detected were Cu, Zn, Ni and Co at 0.033; 0.195; 0.635 and 0.31 mg l^{-1} respectively. Generally, heavy metals such as Cu, Zn, and Ni were detected at lower concentrations probably due to the effect of the added lime. The presence of carbonates from the lime precipitates metal ions, causing them to be bound to sediments at the bottom of the borehole or surface water.

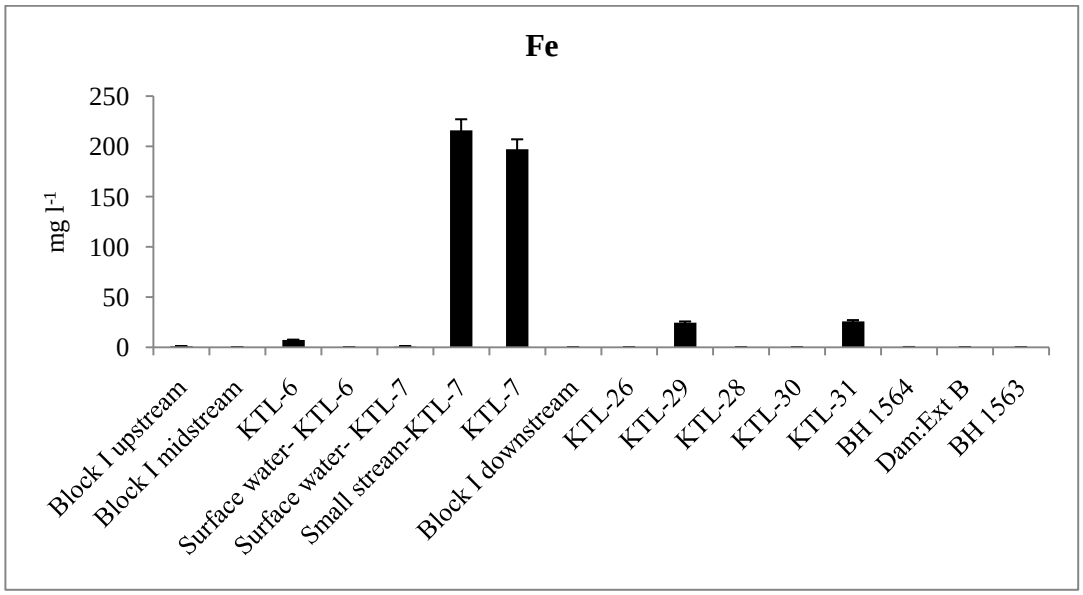
Fe
250
200
150
100
50
0
mg l-1
Block I upstream
Block I midstream
KTL-6
Surface water- KTL-6
Surface water- KTL-7
Small stream-KTL-7
KTL-7
Block I downstream
KTL-26
KTL-29
KTL-28
KTL-30
KTL-31
BH 1564
Dam:Ext B
BH 1563

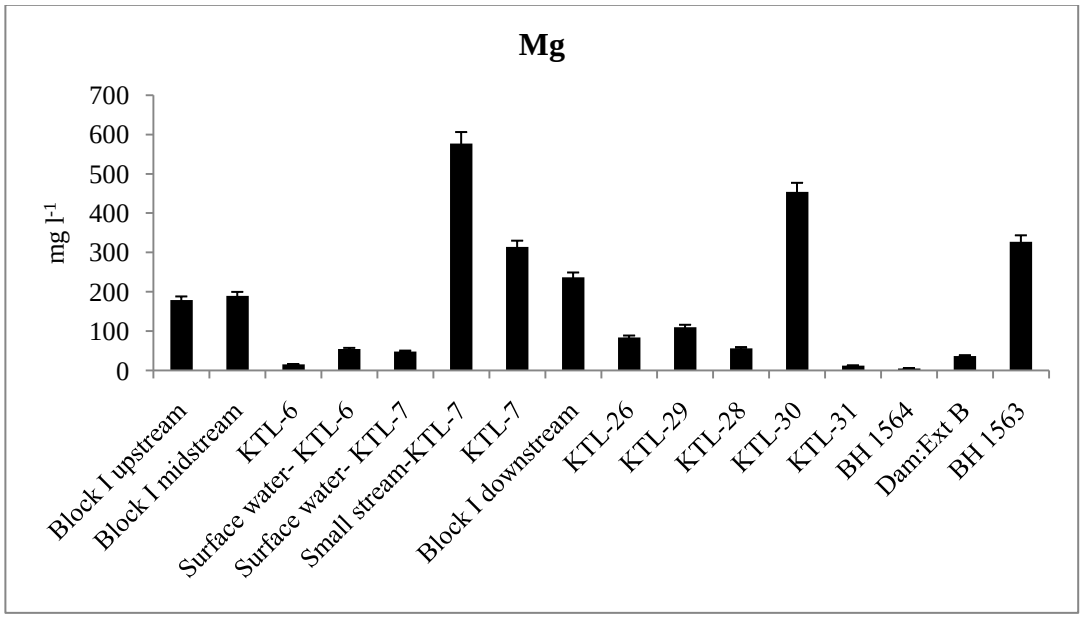
Mg
700
600
500
400
300
200
100
0
mg l-1
Block I upstream
Block I midstream
KTL-6
Surface water- KTL-6
Surface water- KTL-7
Small stream-KTL-7
KTL-7
Block I downstream
KTL-26
KTL-29
KTL-28
KTL-30
KTL-31
BH 1564
Dam:Ext B
BH 1563

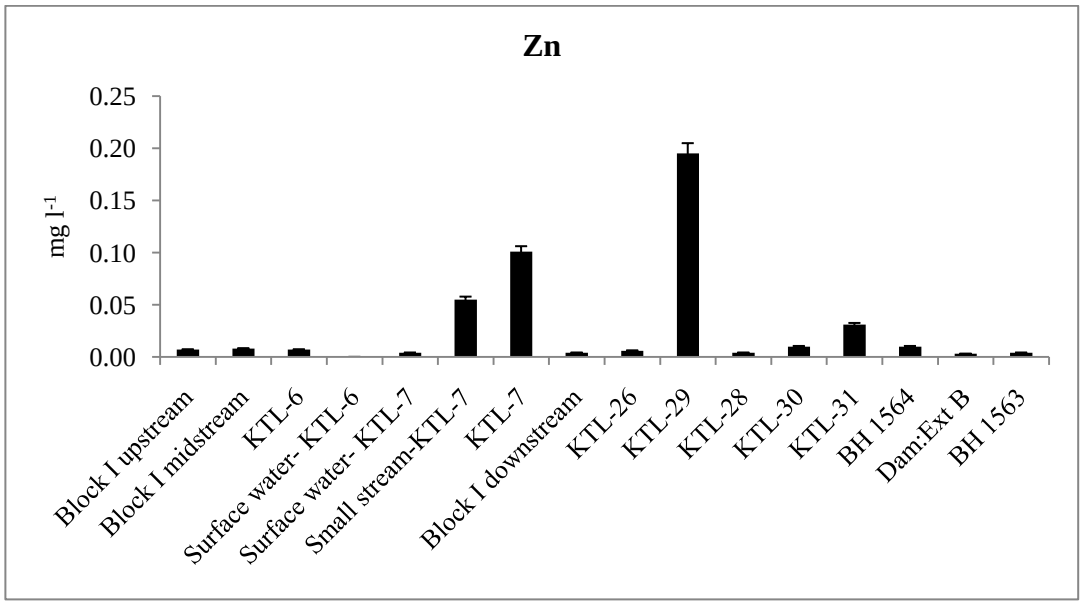
Zn
mg l-1
0.25
0.20
0.15
0.10
0.05
0.00
Block I upstream
Block I midstream
KTL-6
Surface water- KTL-6
Surface water- KTL-7
Small stream-KTL-7
KTL-7
Block I downstream
KTL-26
KTL-29
KTL-28
KTL-30
KTL-31
BH 1564
Dam:Ext B
BH 1563

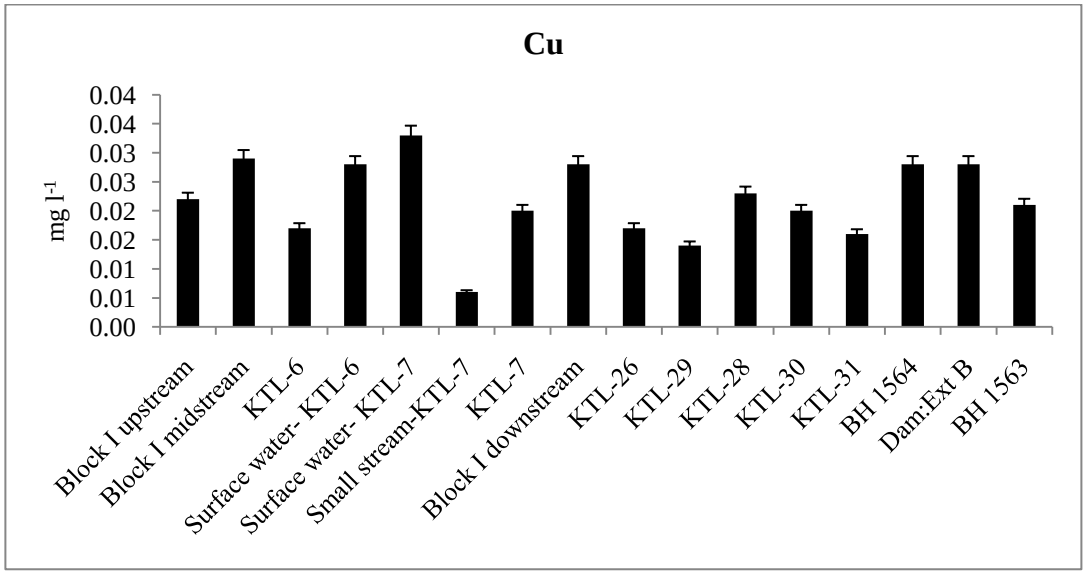
Cu
mg l-1
0.04
0.04
0.03
0.03
0.02
0.02
0.01
0.01
0.00
Block I upstream
Block I midstream
KTL-6
Surface water- KTL-6
Surface water- KTL-7
Small stream-KTL-7
KTL-7
Block I downstream
KTL-26
KTL-29
KTL-28
KTL-30
KTL-31
BH 1564
Dam:Ext B
BH 1563

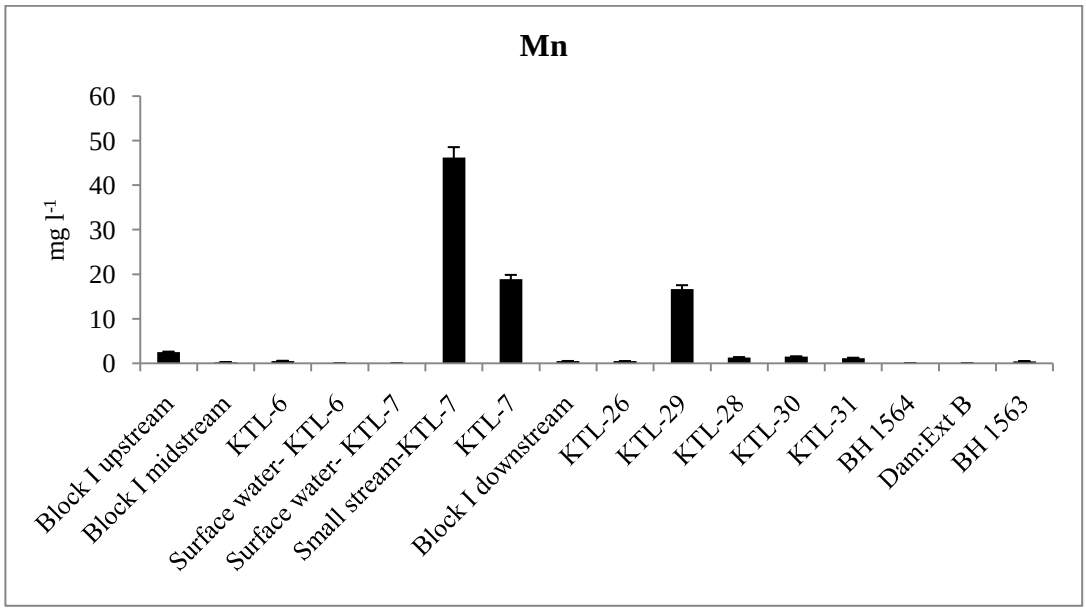

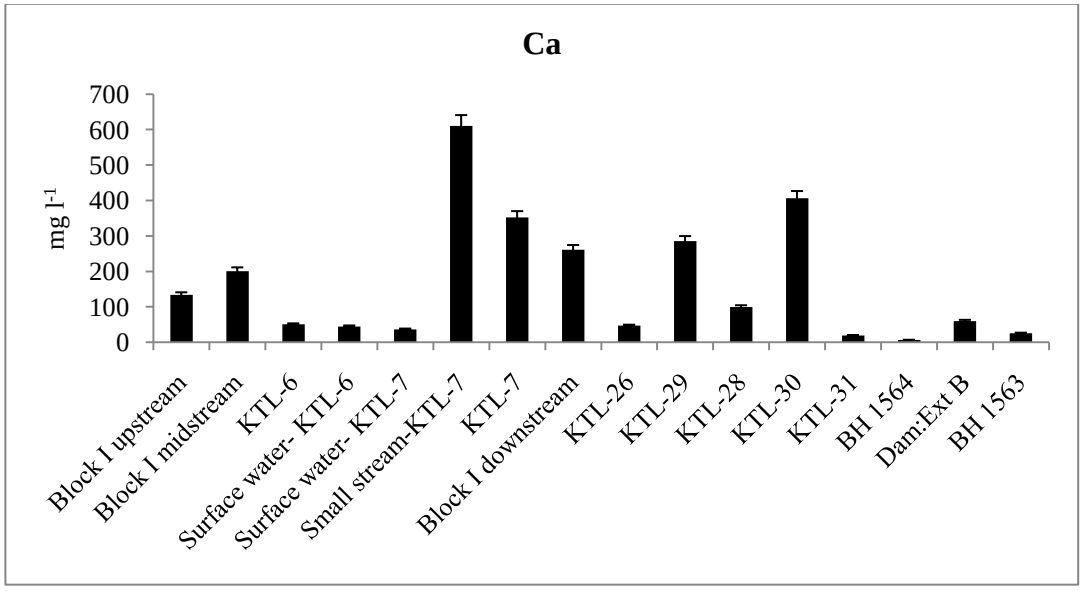

Figure 5.3: Trace metal concentrations of Cu, Mg, Fe Mn, Ca and Zn on the borehole and surface water at Block I

5.3.7 Water Classification

Trilinear plots (Piper diagrams) are used in hydrogeological studies as an effective graphical means of displaying data that contain three dominant components, each of which is typically expressed as a percentage of the total of the three. Analyses of ground water samples can be plotted on a trilinear plot to show relative percentages of cations (e.g., Na^+, K^+, Ca^{2+}, and Mg^{2+}), anions (e.g. Cl-, SO_4^{2-} and ($HCO_3^- + CO_3^{2-}$)). Multiple samples can be plotted on the same trilinear plot, and trends, groupings, and mixing patterns can easily be observed. Once plotted, multiple samples can then be classified or grouped together. A piper diagram in Fig. 5.4 shows the classification of the borehole and surface waters at the detailed site. As shown in Fig. 5.4, the cations Na^+, K^+, Ca^{2+} and Mg^{2+} were plotted on the left triangle and the anions Cl-, SO_4^{2-} and ($HCO_3^- + CO_3^{2-}$) were plotted on the right triangle. Points on the anion and cation diagrams were projected upward to where they intersect on the diamond.

The data plotted into two distinct groups: (1) the surface water samples plotted towards the increasing proportions of (bicarbonate + carbonate) anions and (2) the borehole samples plotted towards increasing proportions of the sulphate anion. Both surface and borehole waters had high proportions of calcium and magnesium as compared to sodium and potassium as a result of the lime applied in the area. The grouped data indicated that the borehole waters had increased sulphate content because of high concentration of oxidisable pyrite in the overburden material while the surface waters were more carbonate based due to the applied lime on the area, which tends to be transported easily from the surface into adjacent water bodies.

The water classification revealed the following facies: Ca-Mg sulphate type for the borehole water and Ca-Mg sulphate-bicarbonate for the surface waters.

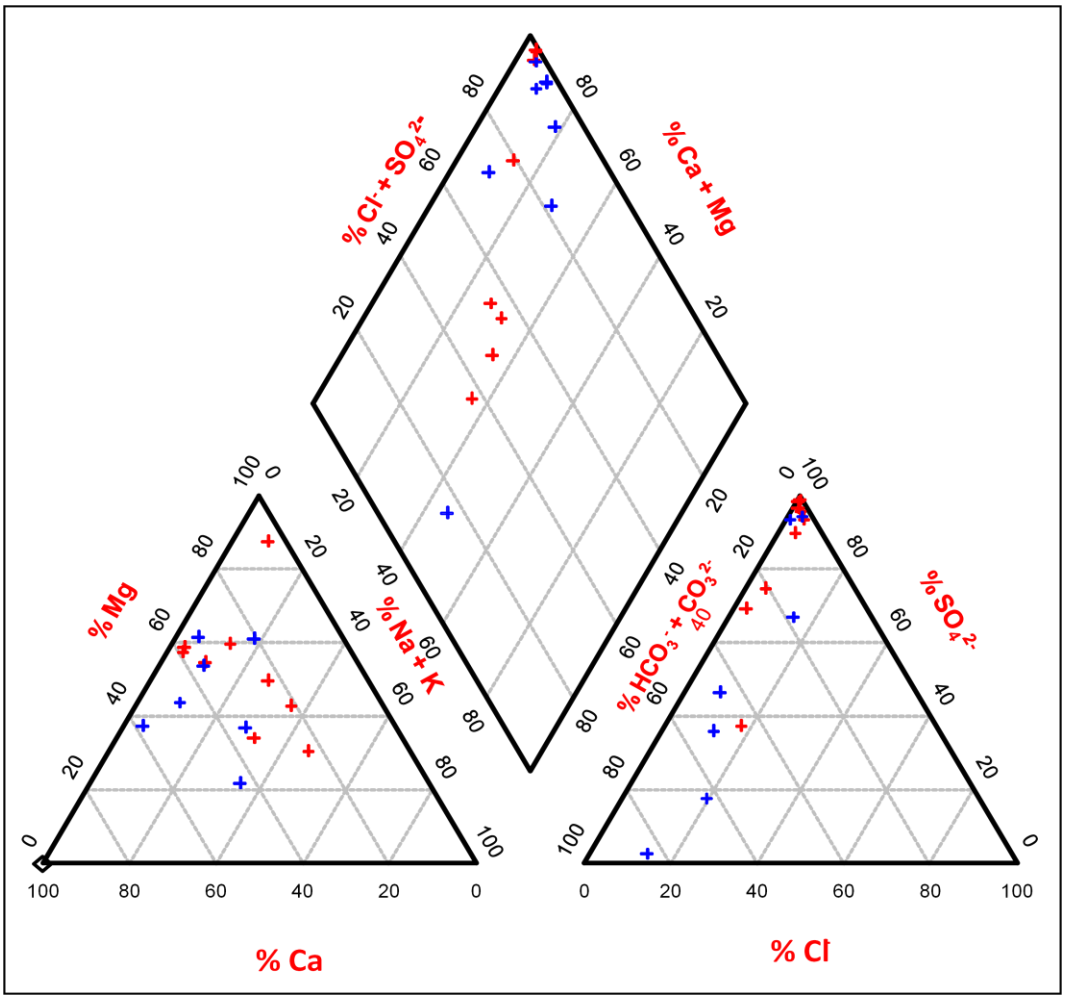

Figure 5.4: Distribution of % ($Na^+ + K^+$), % Mg^{2+}, and % Ca^{2+} and % Cl^-, % SO_4^{2-}, % ($HCO_3^- + CO_3^{2-}$) depicting the classification of borehole (+) and surface waters (+)at Block I

5.4 Soil Chemistry

5.4.1 Total metal analysis

The severity of AMD (low acidity and high amounts of sulphates and dissolved metals like Fe, Al, Mn, Cu, Zn, Cd, Pb and a metalloid As) is related with the coal mining mineralogy. Some of the AMD elements may be transported downstream as dissolved free ions, but others, especially Fe and Al, can be quickly removed from the

water by precipitation as solid phases depending on the physicochemical conditions along their migration path (Allen and Chen, 1993). The analytical results of the total metal concentration in the soil samples of the mining area are shown in Table 8.2 and plots of selected metals are shown in Fig.5.5. The results showed that the soil in the area was contaminated with heavy metals. The highest recorded concentrations of Fe, Mn, Cd and Cr were 78 252; 1 959; 165 and 2 402 mg kg^{-1} respectively (Table 8.2).

The mining area had the highest concentrations of Fe probably due to the abundance of pyrite in the overburden material. Other heavy metals found in the area were Pb and Cu with the highest recorded concentration of 8.57 and 80 mg kg^{-1} respectively (Table 8.2). Metals such as Zn, Co and metalloid AS were only detected at fewer sampling sites in the area and their highest concentrations were 15 109; 67 and 824 mg kg^{-1} respectively (Table 8.2). It was observed that elevated concentrations of Zn, Mn and As were specifically at sample no. 14 and 15 (Table 8.2). The ground elevation at those sampling site was lower compared to other site. Higher concentrations at the lower lying areas could be due to the accumulation of the metal ions in the sediments. High concentration of metal ions in the soil can be very toxic to plants growing in the area. Metal toxicity in plants leads to retarded growth.

A plot in Fig.5.6 showed the correlation of total concentration of various metal ions with total concentration of sulphur. It was observed that iron showed a stronger and linear correlation with sulphur as compared to metals such as Cu, Ni and Mn. The strong correlation of iron with sulphur was an indication of the presence of pyrite (FeS_2) in the overburden material. However, there are other forms of iron that could be bound to sulphur such as pyrrhotite (Fe_xS) and iron sulphate ($FeSO_4$).

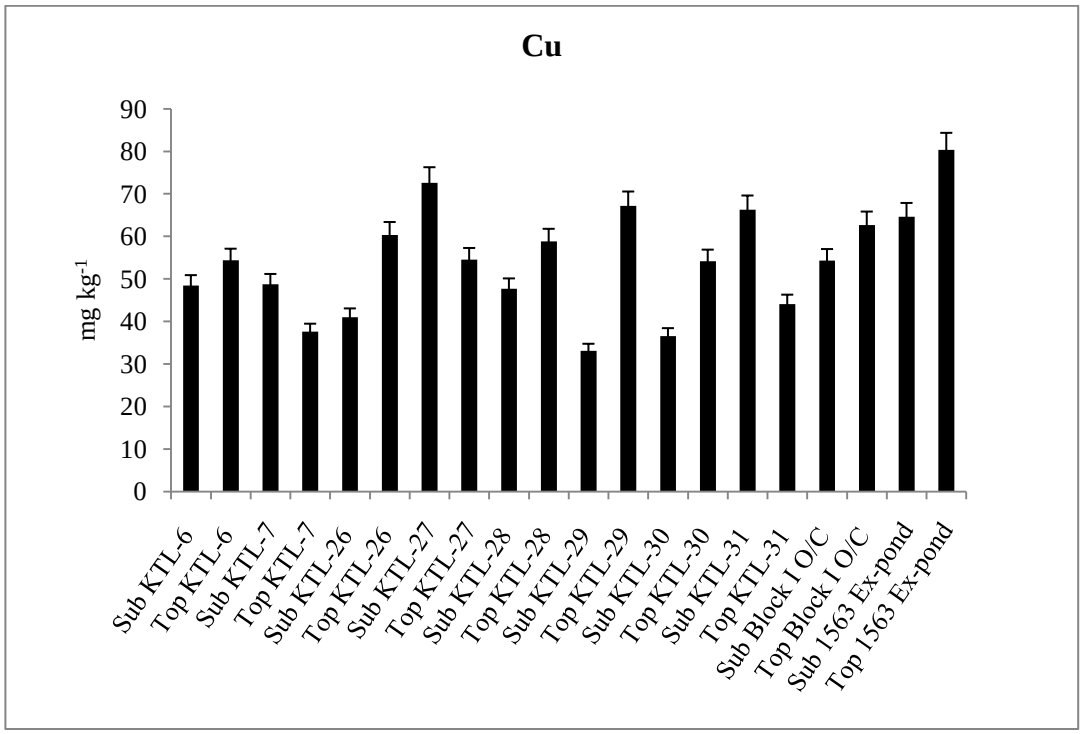
Cu
mg kg-1
90
80
70
60
50
40
30
20
10
0
Sub KTL-6
Top KTL-6
Sub KTL-7
Top KTL-7
Sub KTL-26
Top KTL-26
Sub KTL-27
Top KTL-27
Sub KTL-28
Top KTL-28
Sub KTL-29
Top KTL-29
Sub KTL-30
Top KTL-30
Sub KTL-31
Top KTL-31
Sub Block I O/C
Top Block I O/C
Sub 1563 Ex-pond
Top 1563 Ex-pond

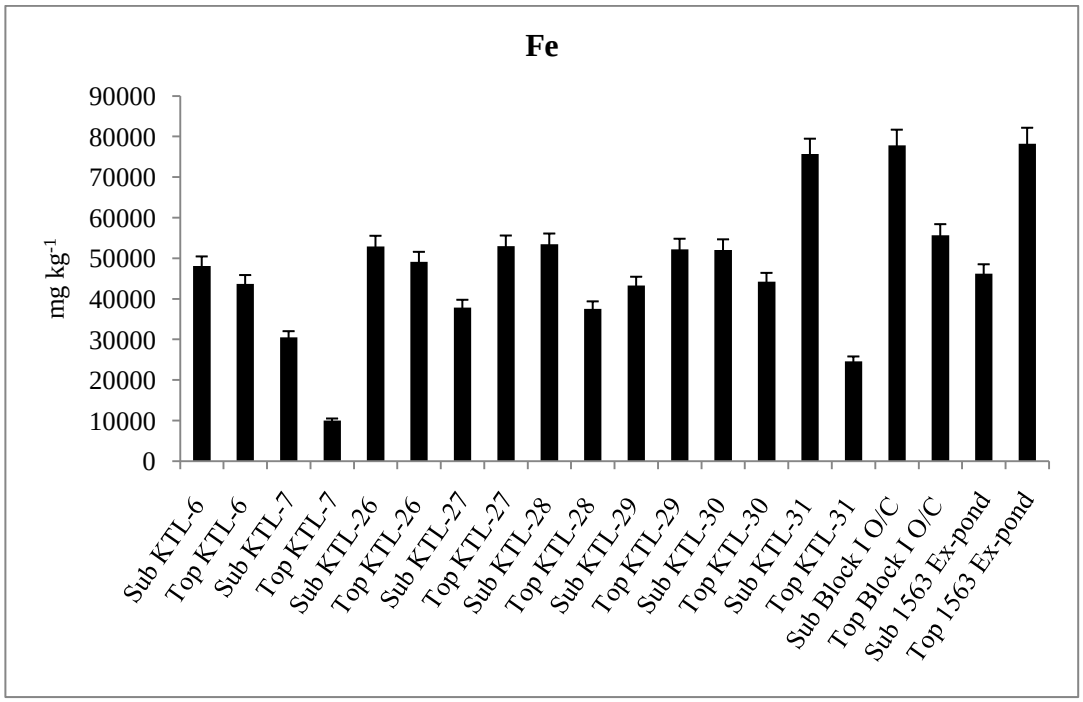
Fe
mg kg-1
90000
80000
70000
60000
50000
40000
30000
20000
10000
0
Sub KTL-6
Top KTL-6
Sub KTL-7
Top KTL-7
Sub KTL-26
Top KTL-26
Sub KTL-27
Top KTL-27
Sub KTL-28
Top KTL-28
Sub KTL-29
Top KTL-29
Sub KTL-30
Top KTL-30
Sub KTL-31
Top KTL-31
Sub Block I O/C
Top Block I O/C
Sub 1563 Ex-pond
Top 1563 Ex-pond

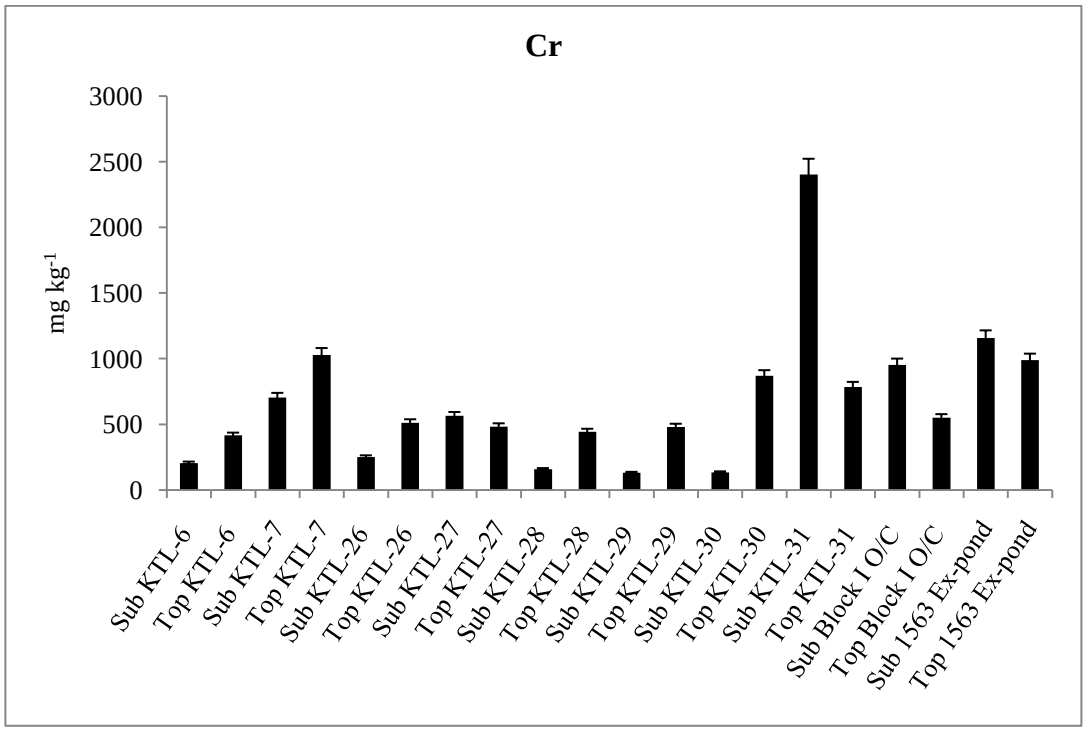
Cr
mg kg-1
3000
2500
2000
1500
1000
500
0
Sub KTL-6
Top KTL-6
Sub KTL-7
Top KTL-7
Sub KTL-26
Top KTL-26
Sub KTL-27
Top KTL-27
Sub KTL-28
Top KTL-28
Sub KTL-29
Top KTL-29
Sub KTL-30
Top KTL-30
Sub KTL-31
Top KTL-31
Sub Block I O/C
Top Block I O/C
Sub 1563 Ex-pond
Top 1563 Ex-pond

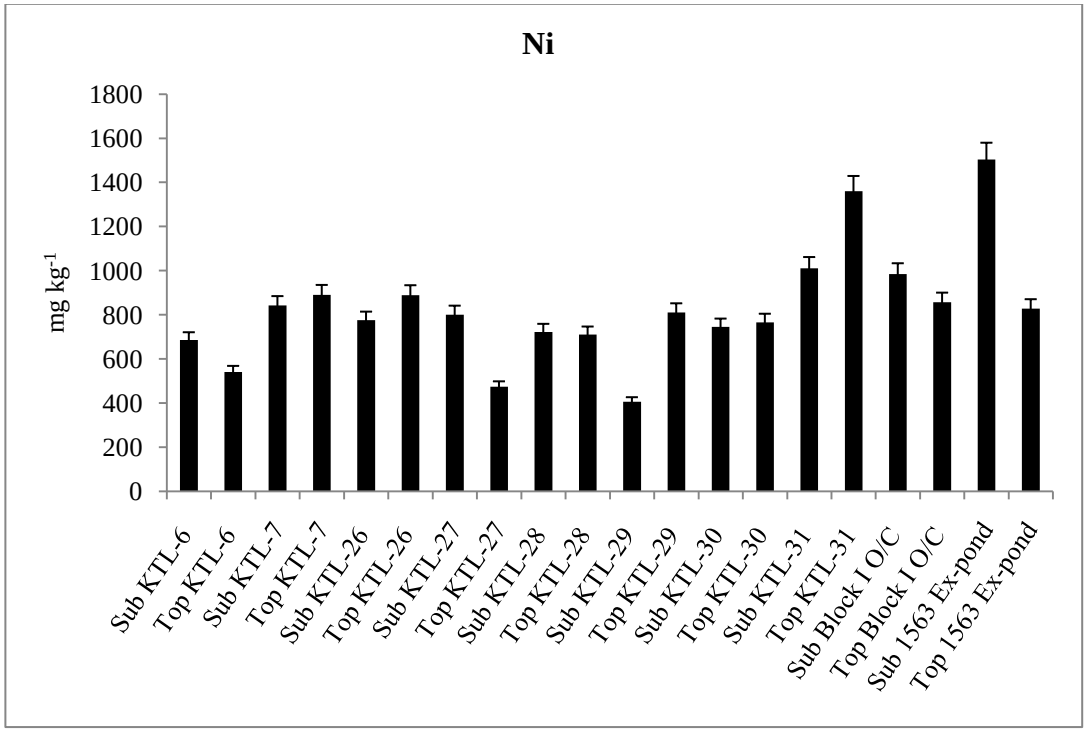
Ni
mg kg-1
1800
1600
1400
1200
1000
800
600
400
200
0
Sub KTL-6
Top KTL-6
Sub KTL-7
Top KTL-7
Sub KTL-26
Top KTL-26
Sub KTL-27
Top KTL-27
Sub KTL-28
Top KTL-28
Sub KTL-29
Top KTL-29
Sub KTL-30
Top KTL-30
Sub KTL-31
Top KTL-31
Sub Block I O/C
Top Block I O/C
Sub 1563 Ex-pond
Top 1563 Ex-pond

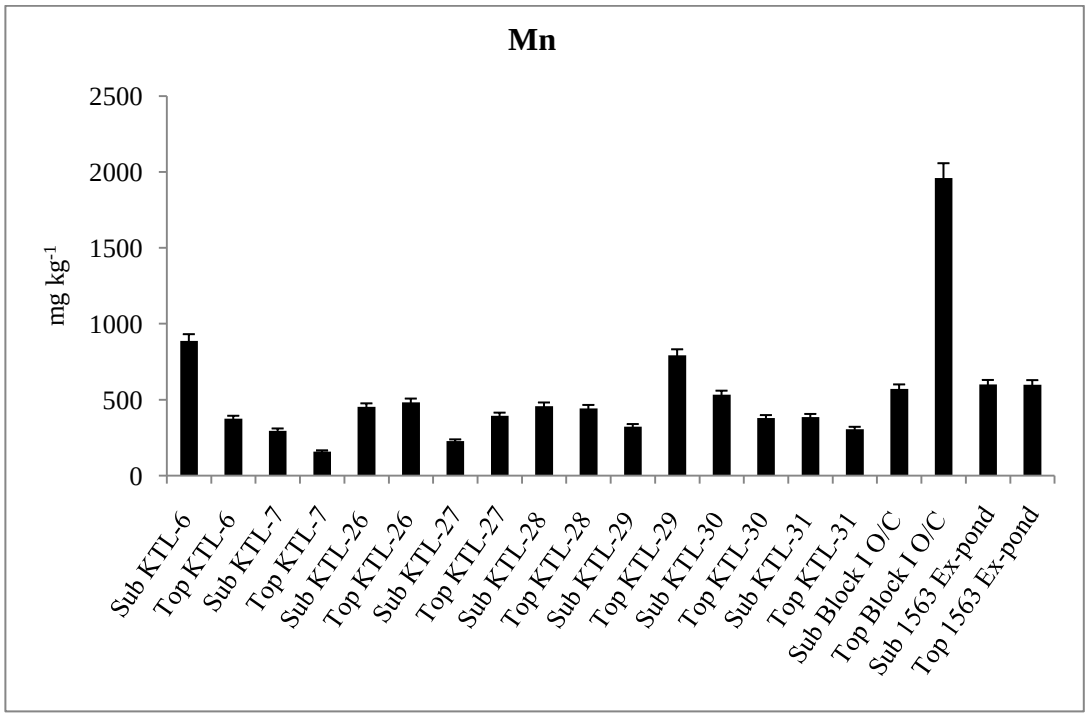

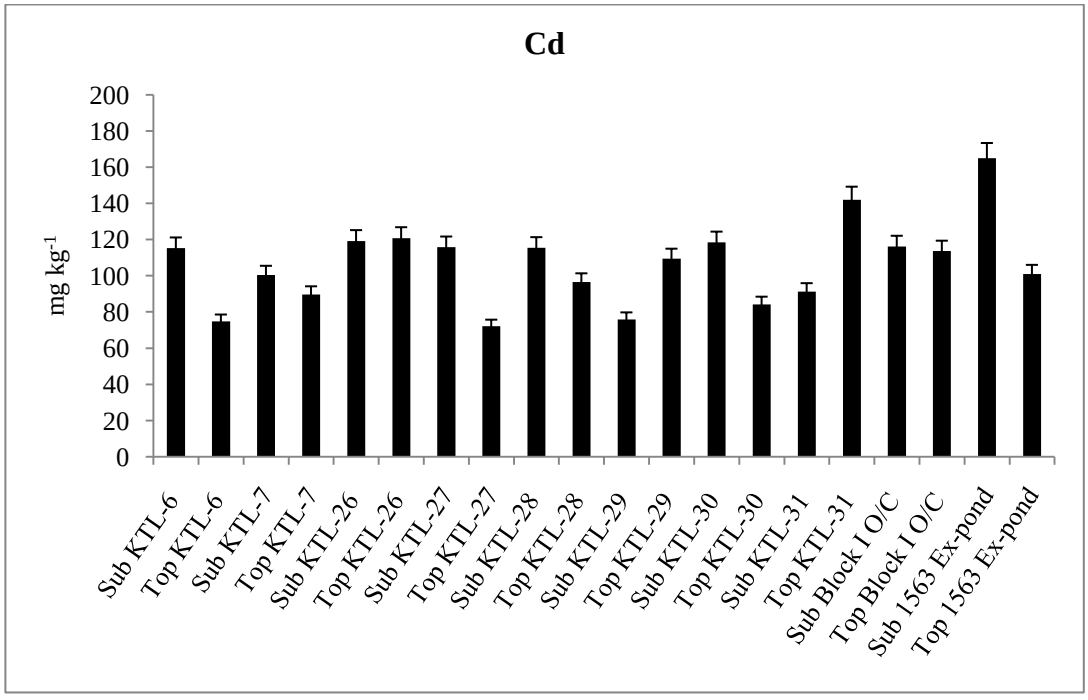

Figure 5.5: Plot of total concentrations of selected metal ions such as Cu, Fe, Cr, Ni, Mn and Cd

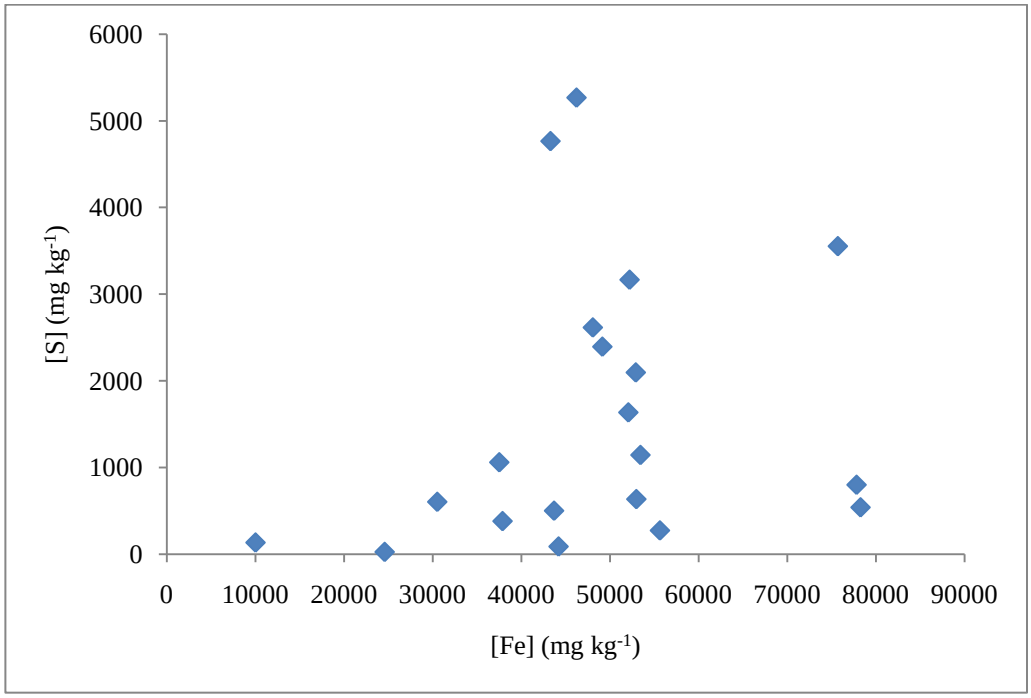
6000
5000
4000
3000
2000
1000
0
[S] (mg kg-1)
0
10000
20000
30000
40000
50000
60000
70000
80000
90000
[Fe] (mg kg-1)

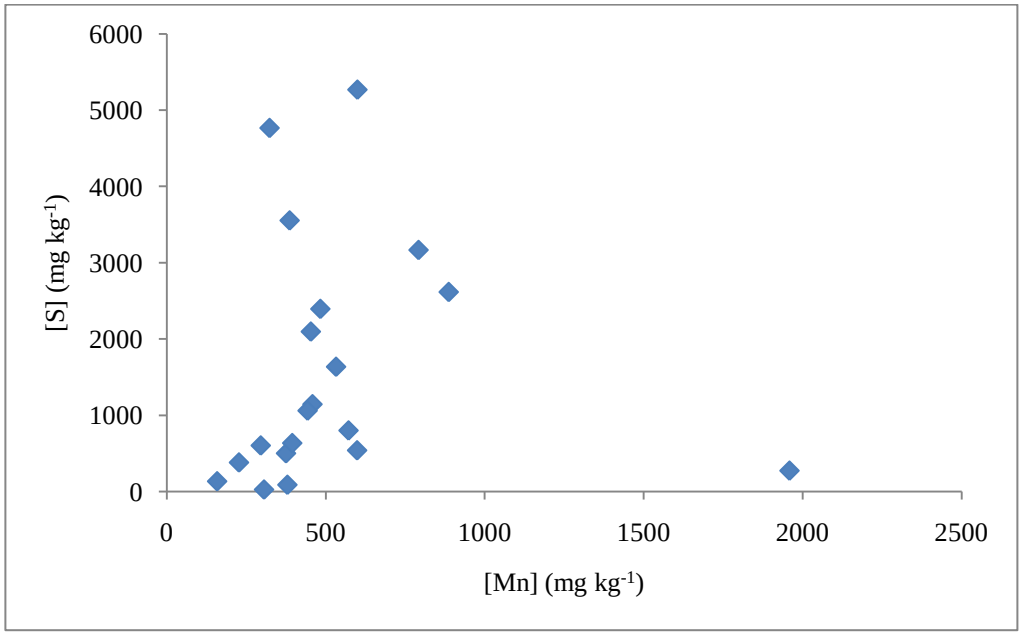
6000
5000
4000
3000
2000
1000
0
[S] (mg kg-1)
0
500
1000
1500
2000
2500
[Mn] (mg kg-1)

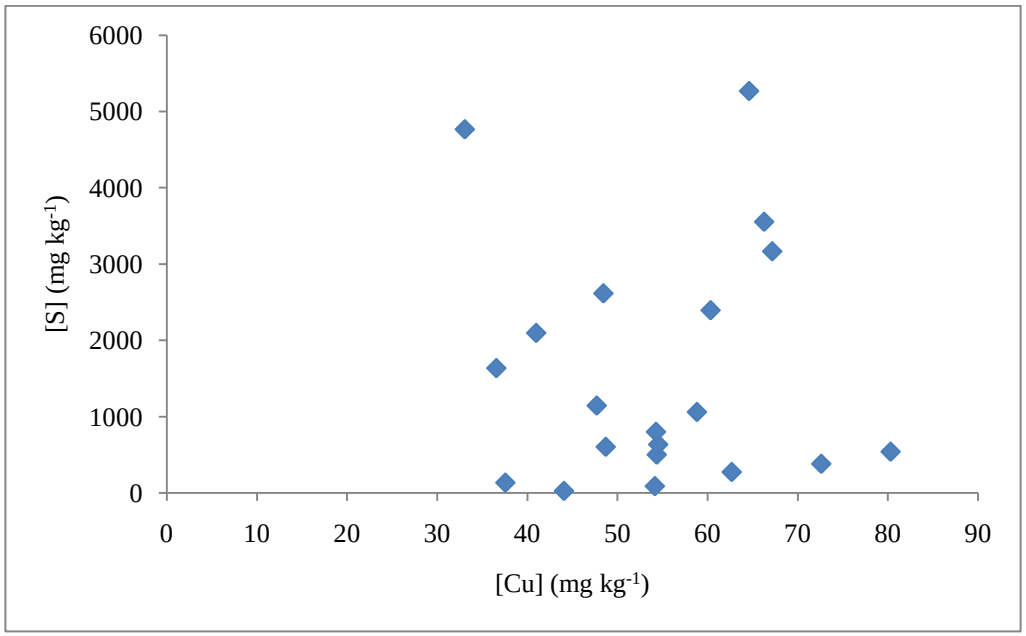

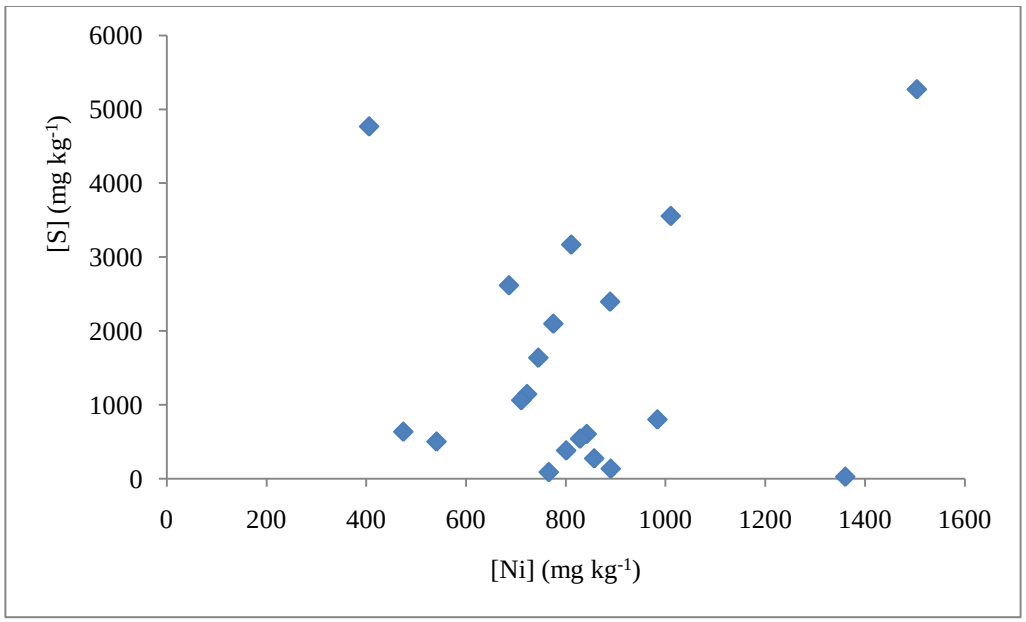

Figure 5.6: A correlation of concentration of sulphur with Fe, Mn, Cu and Ni.

5.4.2 Leaching tests

The leaching tests on soil samples are used to predict the mobile metals rather than the total metals in order to assess toxic effects and to study bio-geochemical pathways. In this study the evaluation of the bioavailability of trace elements in soils was performed by extraction of metals by various solutions of 0.1 M EDTA, 0.1 M Na_2CO_3, neutral salt of 0.01 M $CaCl_2$ and artificial rainwater.

Extraction of metals with 0.1 M EDTA

The stronger chelating ability of EDTA favours the greater extraction percentage of metal ions. The results of the extraction of various metal ions with 0.1 M EDTA are shown in Fig.5.8 and the complete data shown in Tables A3 and A4. The results suggested that when 0.1 EDTA was added to the soil samples, the order of extraction of metals was generally classified as follows: Fe > Cr > Ni > Cd. Other metals such as Cu and Mn were observed to have a higher concentration of the extractant than the total metal concentration (Table 8.3). This had led to obtaining an extraction percentage greater than 100% for all the analysed samples (Table 8.4), thus the extracted percentage was reported as 100%.

The extracted percentage of Cu and Mn greater than their total concentration was attributed to sample heterogeneity. In general, the percentages of metals extracted with EDTA were higher for all samples than those determined by solutions of Na_2CO_3, $CaCl_2$ or artificial rainwater. One possible explanation for the increased release using EDTA was that the chelating agent solution was aggressive enough to dissolve a large fraction of the solid phase mineral. The observed trend in the preference of EDTA for certain metal correlated well with the theoretical stability constants of the metal-EDTA complexes.

The theoretical stability constants of Fe(III), Cr(II), Ni(II) and Cd(II) with EDTA are 25.7; 23.0; 18.56 and 16.5 respectively (Allen and Chen, 1993) . Deviations in the expected trend of EDTA-metal complex stability constant could be the result of factors such as pH, soil type and texture, cation exchange capacity (CEC), natural organic matter, age of contamination, and the presence of other inorganic contaminants (Allen and Chen, 1993). The analysed samples from Block I consisted of mostly clay soil while other samples such as KTL-6 contained ash. The extraction with EDTA on contaminated clayey soils might have lower removal efficiency than sandy soils (Elliott and Brown, 1989; Yu and Klarup, 1994). This explained a lower extraction for sample sub KTL-26 (it consisted of clay soil) compared to sample sub KTL-6 (it consisted of ash).

Extraction of various metals ions with 0.01 M $CaCl_2$

In soil science, mild extractants such as $CaCl_2$ are frequently used as indicative of soil-to-plant transfer in a given soil and for certain plant conditions (Sahuguillo *et al*., 2002). Agriculturally, addition of $CaCl_2$ to soil helps with loosening the soil texture.

Theoretically, the $CaCl_2$ extractant works by exchanging Ca with metals on the exchange complex thus provides a measure of soil solution plus easily exchangeable metal, i.e., a measure of immediately bioavailable metal plus the buffering capacity of the soil (Gupta and Sinha, 2007). The analytical results of the extraction of Fe, Cu and Ni with 0.01 M $CaCl_2$ in Fig.5.7 showed higher extraction of Cu than Ni and Fe. This effect can be attributed to both the exchangeable capacity of calcium and the complex effect of chloride. In soils where Cu exists as $CuSO_4$, the exchange capacity can be higher with mild extractants such as $CaCl_2$. The results suggested that the order of extraction of metals from soil with 0.01 M $CaCl_2$ was Cu > Fe > Ni.

Extraction of various metal ions with 0.1 M Na_2CO_3

The presence of carbonate minerals in the soil immobilises heavy metals such as Fe, Pb and Zn by physical entrapment of metals by the carbonate minerals (Peters, 1999). Thus, pH of a solution used for extracting metals from soil can influence the soil's retention of metals by adsorption and complexity to different degrees depending on the pH of the soil (Peters, 1999). The analytical results of the extraction of various metal ions with 0.1 M Na_2CO_3 are shown in Table 8.4 and the plots in Fig.5.8. The results showed a higher extraction of Fe in most samples compared to Cr, Ni, Mn and Cd. Extraction of Cd showed a higher percentage on sample Top-KTL-6 (Fig.5.9).

The measured pHs of all the leachate samples prior to analysis were in the range 10 – 12. At this pH range Fe, Cr and Cd exist as $Fe(OH)_4^-$, $Cr(OH)_4^-$ and $Cd(OH)_{2(aq)}$ respectively (Fig.5.7) (Pourbaix, 1988). At this range the metal-hydroxide species are soluble due to the strong complexion ability of the hydroxide ligand. This explained the higher extraction of Fe, Cr and Cd with 0.1 M Na_2CO_3 in Fig.5.8. The Pourbaix diagram in Fig. 5.7a also showed that the $Mn(OH)_3$ complexes can be soluble at narrow pH range of 10.5 to 11.5, hence a weaker extraction of Mn in most samples (Table 8.4).

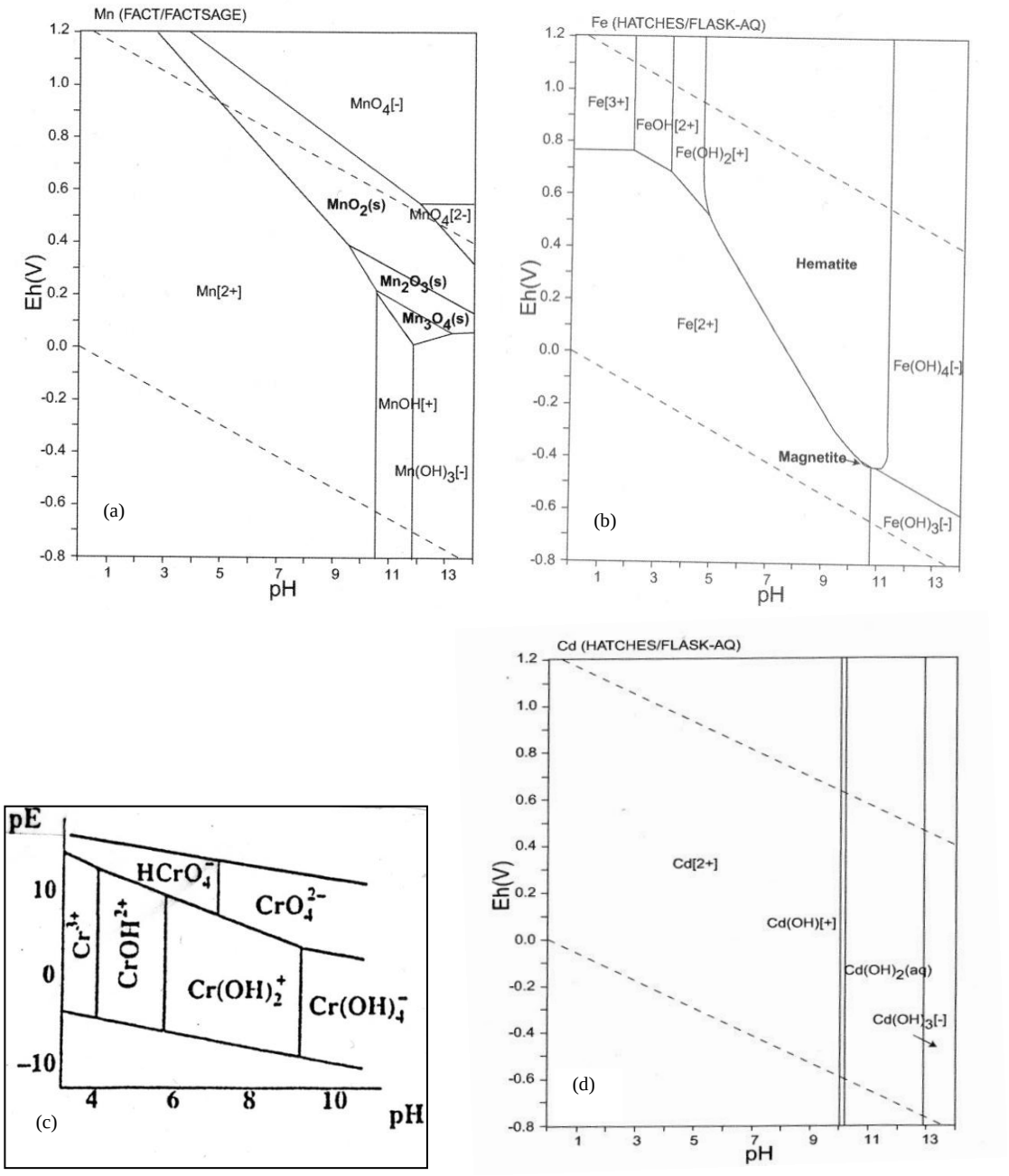

Figure 5.7: Pourbaix diagrams of (a) Mn, (b) Fe, (c) Cr and (d) Cd

Extraction of various metal ions with artificial rainwater

The extraction of the various metal ions with artificial rainwater was done as a reference to observe the relationships between the measured total metal concentrations and the extractable metal ions under natural conditions. The extraction of Cu was the most favoured in all the analysed samples (Fig.5.8) with the highest recorded extraction of 95.35% (sample Top KTL-6). This was probably due to Cu being readily leachable at pH of rainwater (pH 5.6). The extraction of metals with artificial rainwater had also shown that under natural conditions, the metals will not be mobile enough to be extracted. The leacheability of the metals depend on the number of factors. Some metals may be bound strongly to the soil than others due to the presence of organic matter, carbonates and oxides.

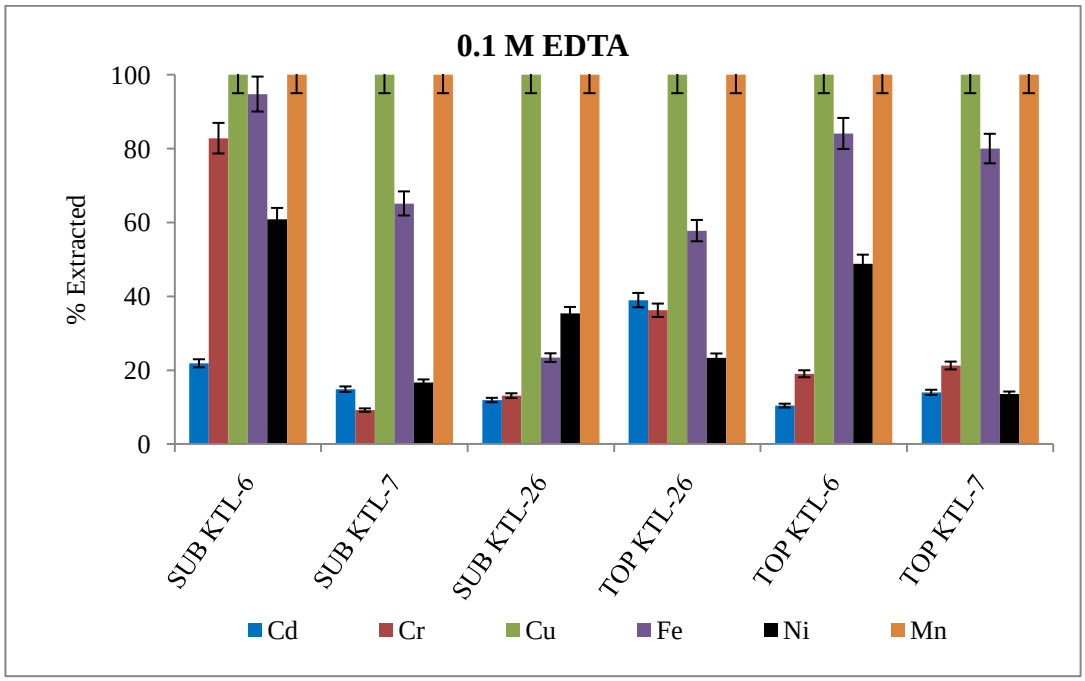
0.1 M EDTA
% Extracted
100
80
60
40
20
0
SUB KTL-6
SUB KTL-7
SUB KTL-26
TOP KTL-26
TOP KTL-6
TOP KTL-7
Cd
Cr
Cu
Fe
Ni
Mn

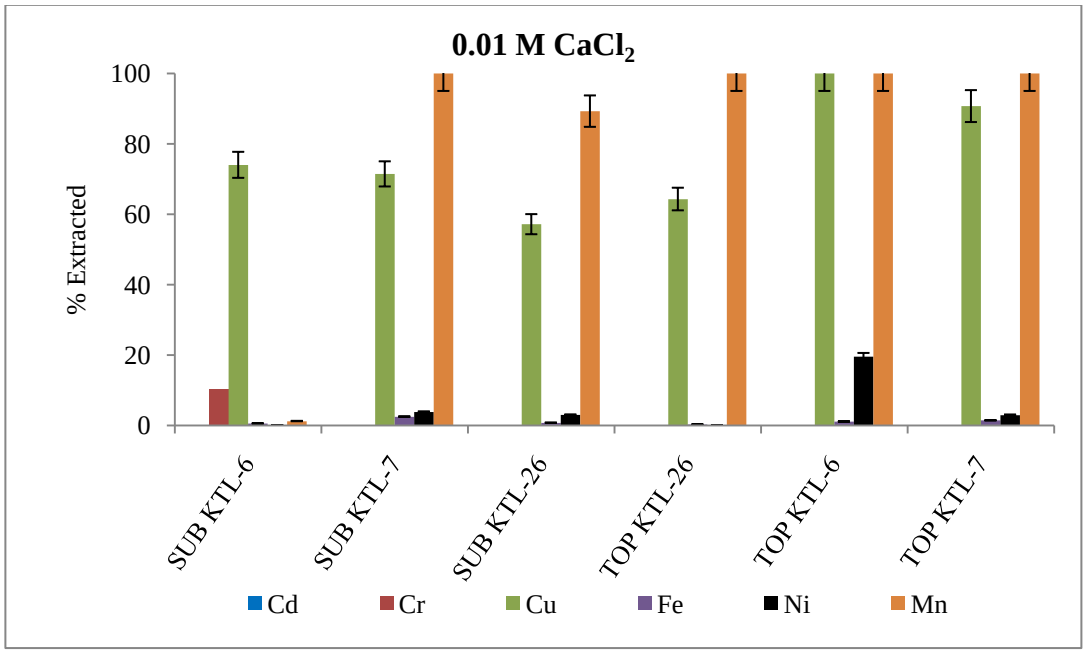
0.01 M CaCl2
% Extracted
100
80
60
40
20
0
SUB KTL-6
SUB KTL-7
SUB KTL-26
TOP KTL-26
TOP KTL-6
TOP KTL-7
Cd
Cr
Cu
Fe
Ni
Mn

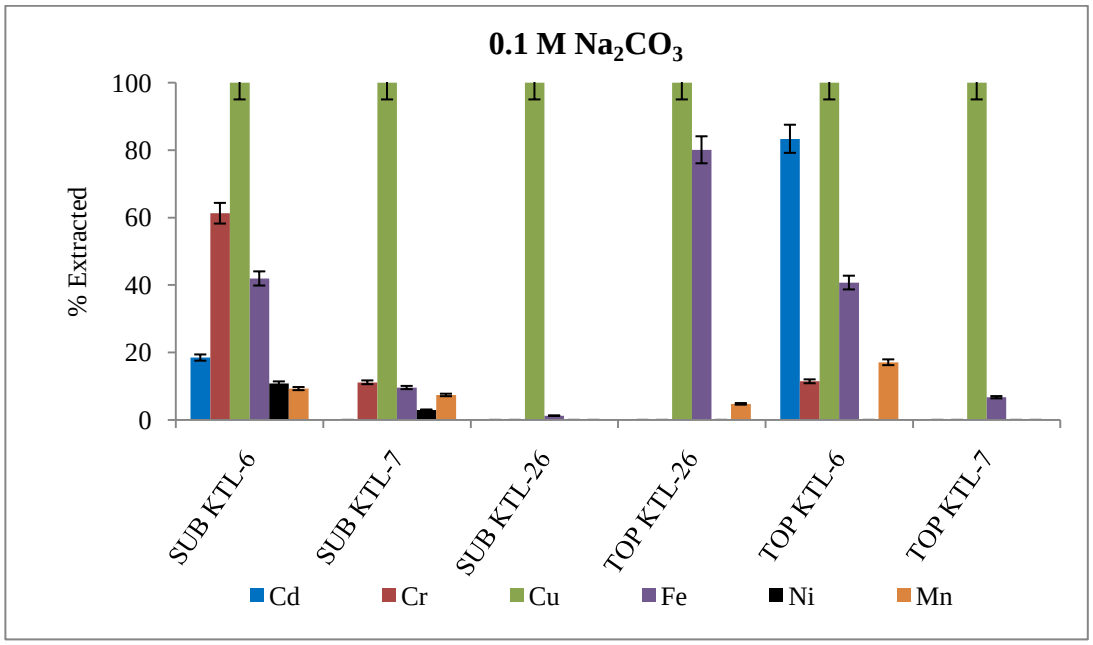

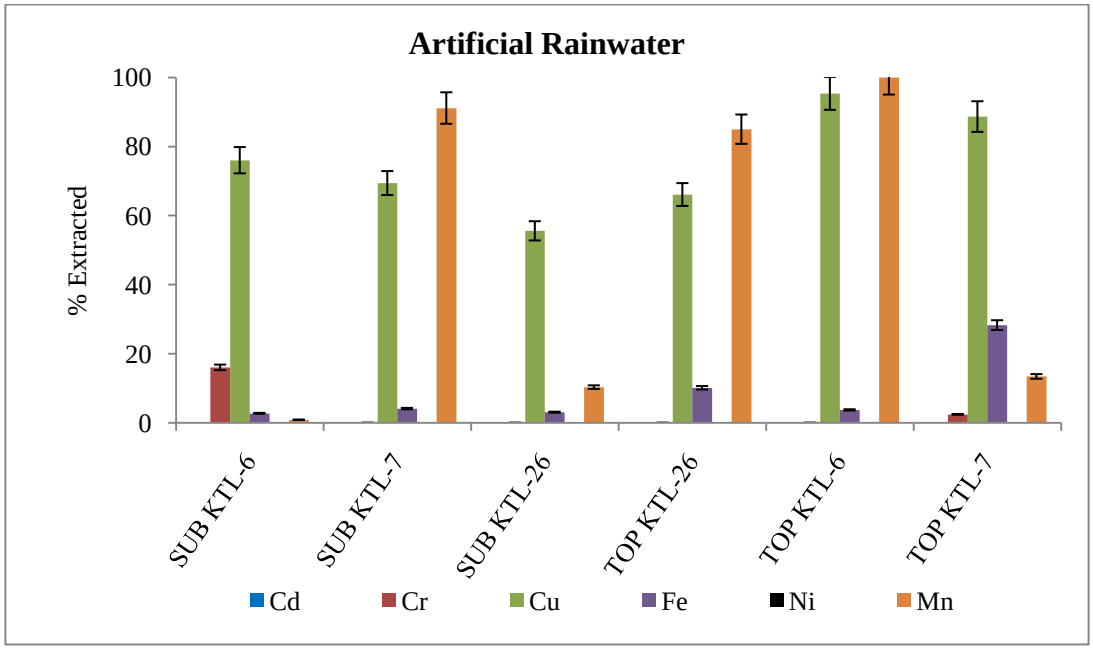

Figure 5.8: Extractions of various metal ions with solutions of 0.1 M EDTA, 0.01 M $CaCl_2$, 0.1 M Na_2CO_3 and artificial rainwater

5.4.3 Acid Base Accounting

The acid base accounting studies were used to predict the acid-generating potential and acid-consuming capacity of the soil samples and complete results are as shown in Table 8.5. A plot of the initial and final pH of the soil samples in Fig.5.9 showed that the initial pHs of the soil samples were in the range 4.54 to 6.29. The initial pH values indicate the immediate acidic or basic characteristic of the sample and it could also indicate if acid generation has already been generated (Usher *et al.*, 2003). Hence the pH values obtained in this study showed that the samples already had acid generation as a result of the abundance of oxidisable pyrite in the area. A higher initial pH of 7.66 was observed for sample SUB-KTL-6 (Table 8.5) and this was attributed to the soil type that was a mixture of clay soil and ash.

The final pH of the samples showed that after complete oxidation, the pH of the soil would be less than 2.5 in most samples and acidic conditions would dominate. Sample KTL-7 had a lower final pH of 1.94 (Table 8.5), and this suggested that the total available carbonates could already be leached out leaving a lesser source of alkalinity to buffer the acid. The other reason could be that there were more acid producing constituents than acid consuming constituents in the sample. It was also noted that sample KTL-7 was a soil sample collected next to the decant point (Fig. 2.1). This was the borehole where the groundwater was emerging at the surface and analytical results showed moderately acidic water (pH 6.66), elevated concentration of the sulphates (1 794 mg l^{-1}) and abundance of Fe (197 mg l^{-1}) at borehole KTL-7 (Table 8.1). This indicated that the KTL-7 borehole water contributed to the leaching of acid producing constituents from the soil.

Sample SUB-KTL-6 showed the lowest final pH due to the ash in the soil, which acted as a buffer and thus kept the pH higher. A plot of the acid potential and the

neutralising potential of the soil samples is as shown in Fig. 5.10. The plot showed that the samples had very negative neutralising potential and less positive acid potential. This indicated that there were insufficient carbonates in the overburden material to neutralise the acidity of the sample. The plot of the net neutralising potential (NNP) in Fig. 5.11 showed negative values for all the samples in the area, with the lowest recorded value of -9.8 kg t^{-1} $CaCO_3$. The more negative NNP implied that the soil did not have enough $CaCO_3$ to neutralise the acidity in the soil hence there was a potential of acid mine drainage in the area.

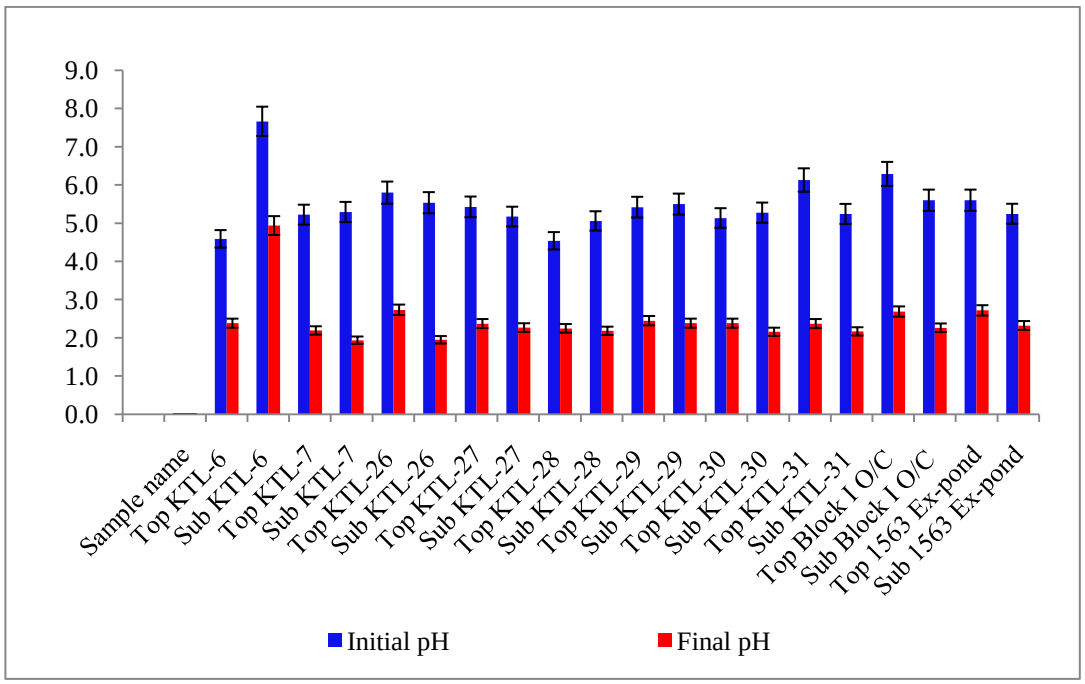

Figure 5.9: The initial and final pH of soil samples before and after complete pyrite oxidation

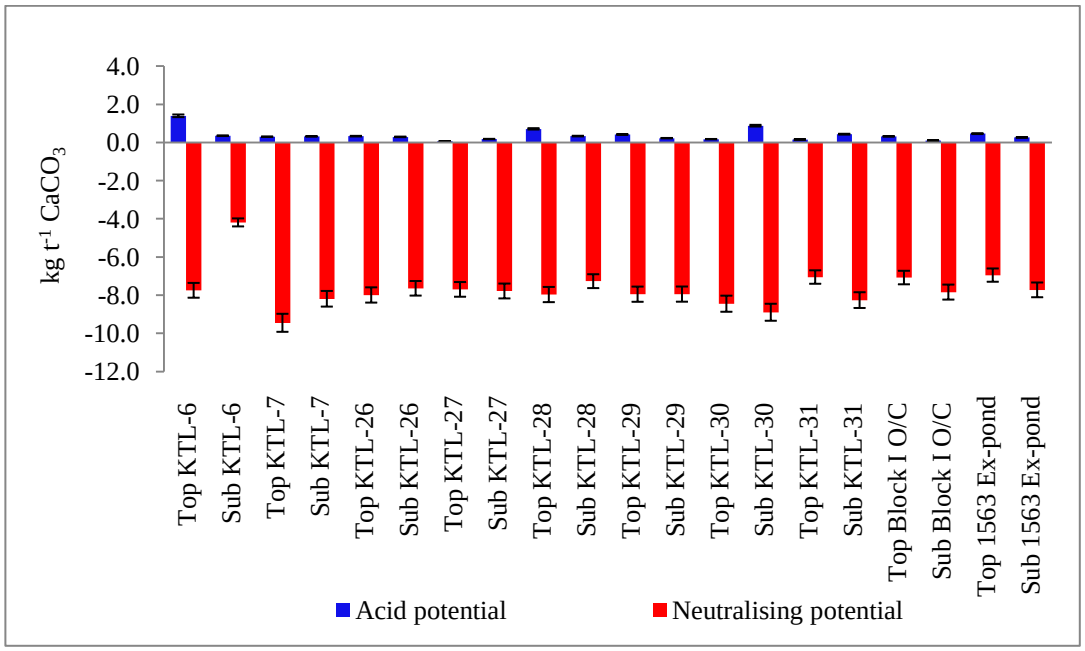

Figure 5.10: The acid potential and neutralising potential of soil samples from Block I.

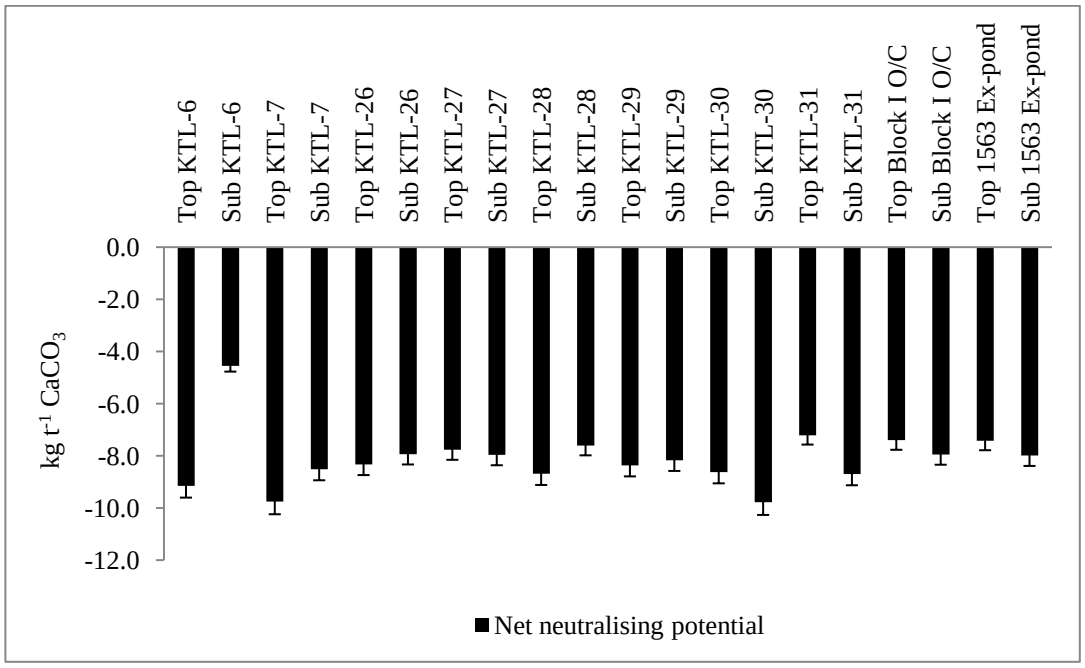

Figure 5.11: Variation in the net neutralising potential of soil samples at Block I

6. CONCLUSION AND FUTURE WORK

6.1 Conclusion

The following conclusions were made from the field and analytical data, the transmissivity of the boreholes in the spoil material was highly variable and ranges from 100 to 5 000 m^2 day^{-1}. As per the pump testing suggested that borehole yields of between 23 and 4 l s^{-1} can be expected in the spoil areas. Due to the observed high yields the monitoring borehole KTL 7 was noted to be overflowing. The specific yield of the spoil material was in the range of 25 to 30 %. The pump test in borehole KTL-32 indicated that the hydraulic conductivity of the surrounding Karoo sediments was low. This suggested that the inflow into the rehabilitated workings from the adjacent aquifers will be limited.

From previous experience the contribution of water in the spoil material was approximately 90% direct recharge and 10% groundwater inflow (base flow). Recharge was normally in the range of 15% of mean annual precipitation (MAP). The volumes of inflow into the rehabilitated areas were estimated to be 29 311 m^3 a^{-1} (approximately 1 l s^{-1}) for Block I Ext A, 18 370 m^3 a^{-1} (approximately 0.6 l s^{-1}) for Block I Ext B and 100 116 m^3 a^{-1} (approximately 3 l s^{-1}).

In order to dewater the pits the inflow as well as the storage will have to be removed. This means that if 15.5 l s^{-1} of water was removed from Block I it will take approximately 5 years to dewater the pit. Thereafter the pump rate will have to be reduced to the inflow rate of approximately 3 l s^{-1}. To dewater Block I Ext B at a rate of 2 l s^{-1} it will take approximately 5 years after which the pump rate will have to be reduced to approximately 0.5 l s^{-1}.

The total metal analyses on samples taken from Block I showed that there was an abundance of pyrite in both the top and the sub soil and hence it could be expected that acid mine drainage was likely to occur in the area. The acid base accounting studies of pH and net neutralising potential showed a final pH of less than 2.5 for most samples and the net neutralising potential of up to –9.8 kg t^{-1} $CaCO_3$. These results showed that should complete oxidation of pyrite occur, highly acidic waters will prevail and hence there was a potential for acid mine drainage in the area.

Although the area was neutralised by the addition of lime, it is evident that there was insufficient carbonates to provide long-term neutralisation. The addition of lime was only a short term neutralizing strategy to alkaline pH in the surface water, thus enhancing the precipitation and immobilisation of the metals in the soil. This strategy was only considered temporary because the metals still remain in the soil and the pH of the water will vary depending on the season and the available carbonates in the area.

The water classification in Block I was found to be Ca-Mg sulphate type for the borehole water and Ca-Mg sulphate-bicarbonate type for the surface waters. The classification was however likely to change as the amount of added carbonates in the area changes depending on the season and the rate of infiltration taking place during the rainy periods. The previous results of the pH of the borehole waters (Table 8.1) showed that towards the end of the year, the pH of the boreholes decreased as the added carbonates get exhausted. It was found that the decanting boreholes discharge water into the nearby stream. As a result, elevated concentrations of Fe, Mn and Zn were found on the samples taken from these boreholes. This poses a threat to the downstream water as those heavy metals can be carried downstream.

The study of the extraction of metal ions with various solutions showed that EDTA was a stronger extractant compared to the other solutions. High extractions of Cu and Fe were obtained as compared to Cr, Cd and Ni in most samples. The extraction with 0.1 M Na_2CO_3 showed that the pH played a role in the extraction of the metals from soil. At more alkaline pH there could be a formation of soluble metal-hydroxide species which are mobile for extraction. As a result extraction of Fe, Cr and Cd was higher in some samples. The extraction of metals with 0.01 M $CaCl_2$ and artificial rainwater had proven favourable for mobilisation of metal such as Cu, which was extracted with a higher efficiency due to exchange reactions. Higher extraction efficiencies of metal ions such as Fe and Cu with EDTA had proven to be useful for phytoremediation strategies.

6.2 Future Studies and Recommendations

6.2.1 Future studies

Developing new technologies for measuring and monitoring sulfide-containing materials from coal pyrites to improve the understanding of the effectiveness of controls applied by coal mining operations and reduce the risk associated with the sulfide-containing materials.

To determine the rate at which the oxidation of pyrite and other iron sulfides material in a coal mining environment could take place. The abundance of pyrite in the mine was obviously a likely factor in determining acid generation. The crystallinity and impurity content of the pyrite may affect oxidation rate. .Further studies need to be conducted to assess and determine the rate at which the oxidation of pyrite and other iron sulfides material in a coal mining environment.

An investigation of the extraction efficiencies of metal ions from the soil with chelating agents such as can be improved by varying parameters such as pH, contact time during leaching process and the concentration of the extractant. This will assist in obtaining optimum values at which higher extraction efficiencies are achieved. Extraction procedures such as column experiment can also be performed instead of the batch experiment.

Kinetic tests need to be performed on the samples to access the rate of oxidation of pyrite in the area. This test is usually done on samples with the net neutralising potential value between -20 and 20 kg t^{-1} $CaCO_3$. This is the grey range of uncertainty whereby the sample may or may not generate acidity. The test is done with humidity cells to simulate the weathering process in weekly cycles for a period of 20 weeks (Usher *et al*., 2003). At the end of each week, the pH of the sample is measured and the weathered products are collected in the rinse/leach process (Usher *et al*., 2003).

6.2.2 Recommendations

This study has shown that the former mining area of Block I, Block I Extension A and B have increased quantity of water in the pits, elevated concentrations of pyrite and heavy metal ions such as Fe, Cd, Cu, Zn, Ni and Mn. Due to the contact of infiltration water and pyrite bearing materials, these metals are further immobilised by the presence of the added lime in the area. Although this strategy assists in prevention of the leaching of the metals to the water systems, it is not a permanent solution. The metals are still retained in the soil and this will have an impact on the vegetation in the area. It is recommended that:

- The mine affected water from the pits must be pumped to control and immediately prevent the discharge into the environment into a containment facility. This water may also be pumped into an underground storage facility in case whereby there is no surface storage facility available, but to do this neutralization of the water is recommended.
- A small package reverse osmosis plant is also an option that the mine might need to look at and also consider the management of the additional waste that is a combination of brine and sludge that will be generated due to high metal content of the water.
- The use of both reactive barriers and phytoremediation may also be utilize to extract metals by using a combination these methods as detailed below:

Use of reactive barriers

A permeable reactive barrier (PRB) is a wall built below ground to clean up polluted groundwater (US EPA, 1998). The wall is permeable, which means it has tiny holes that allow groundwater to flow through it. Reactive materials in the wall trap toxic metal ions by adsorption and clean groundwater flows out the other side of the wall (US EPA, 1998). This barrier can be placed downstream where the water from the former mining area accumulates and subsequently discharges into natural streams.

Phytoremediation by using metal hyperaccumulators

An emerging remediation technique that is used for removal of metals from contaminated soils is phytoremediation. Phytoremediation is a technique that involves use of metal hyperaccumulator plants to remove metals from contaminated soils (Lasat, 2000) It is an environment friendly, green technology that is cost effective and energetically inexpensive (Lasat, 2000). This technique makes use of the intrinsic capacity of plants to accumulate

metal and transport them to shoots, ability to form phytochelatins in roots and sequester the metal ions (Shah and Nongkynrih, 2007).

Hyperaccumulators are conventionally defined as species capable of accumulating metals at levels 100-fold greater than those typically measured in common nonaccumulator plants (Lasat, 2000). Thus, a hyperaccumulator will concentrate more than: 10 mg kg^{-1} Hg; 100 mg kg^{-1} Cd; 1 000 mg kg^{-1} Co, Cr, Cu, and Pb; 10 000 mg kg^{-1} Ni and Zn (Lasat, 2000). To date, approximately 400 plant species from at least 45 plant families have been reported to hyperaccumulate metals (Lasat, 2000). The table below shows some of the known hyperaccumulator plants.

Plant species	**Metal**	**Leaf content (mg kg^{-1})**	**Reference**
Thlaspi caerulescens	Zn:Cd	39 600:1 800	(Baker and Walker, 1990)
Haumaniastrum robertii	Co	10 200	(Brooks 1977)
Ipomea alpina	Cu	12 300	(Baker and Walker, 1990)
Berkheya coddii	Ni	more than 1 000 µg Ni per g dry matter	(Katarzyna *et al*., 2003)

Advantages of phytoremediation

- Plants offer a permanent, non-intrusive, self sustaining method of removal of soil contaminant. The plants used in bioremediation do not disturb the topsoil thus conserving its utility (Sykes *et al*., 1999).

- Planting vegetation on a contaminated site acts a cover to reduce erosion by wind and water.

- Metal hyperaccumulators can also be beneficial for phytomining. Phytomining is a process whereby phytominers grow a crop of a metal-hyperaccumulating plant species, harvest the biomass and burn it to produce a bio-ore (Brooks *et al*., 1999). The Ni-hyperaccumulators Alyssum bertolonii from Italy and Berkheya coddii from South Africa have even greater potential to extract Ni, because of their high biomass and high Ni content. On many soils, Berkheya coddii can yield over 20 tonnes per hectare with a Ni concentration of 1% in the dry matter (Brooks *et al*., 1999).

7. REFERENCES

Allen, H.E., Chen, P.H. (1993), Remediation of metal contaminated soil by EDTA incorporating electrochemical recovery of metal. Environmental Progress, pp. 12, 284.

Appelo, C.A.J. and Postma, D. (1993). Geochemistry, Groundwater and Pollution. A.A Balkema Publishers, Rotterdam, Netherlands.

Brady, K.B.C., Perry, E.F., Beam, R.L., Bisko, D.C., Gardner, M.D. and Tarantino, J.M. (1994). Evaluation of Acid-Base Accounting to predict the quality of drainage at surface coal mines in Pennsylvania, U.S.A. In: Proceedings of the International Land Reclamation and Mine Drainage Conference. Vol. 1, April 24 – 29, Pittsburgh, PA, pp. 138 – 147.

Bredell, J.H. (1987), South African coal resources explained and analysed, Geological Survey of South Africa, pp. 1987 – 0154.

Baker, A.J.M., Walker, P.L., 1990. Ecophysiology of metal uptake by tolerant plants. Heavy Metal Tolerance in Plants: Evolutionary Aspects, ed AJ Shaw, CRC Press, Boca Raton, pp. 155 – 177.

Brooks, R.R., 1977. Copper and cobalt uptake be Haumaniastrum species. Plant Soil 48, pp.541 – 544.

Brooks, R.R., Anderson, C., Steward, R.B., Robinson, B.H., 1999. Phytomining, growing a crop of a metal, Biologist 46 (5), pp.201 – 205.

Clesceri, S., Greenberg, E., Rhodes, R., 1989. Standard Methods for the Examination of Water and Waste Water, 17th ed. American Public Health Association, Washington, DC. pp. 22 – 45.

Cohen, R.R.H. (1996). The Technology and Operation of Passive Mine Drainage Treatment Systems. EPA Seminar Publication/625/R-95/007 on Managing Environmental Problems at Inactive and Abandoned Metals Mine Sites.

De Jager, F.S.J. (1992), Mineral Resources of the Republic of South Africa, Handbook 7, Government Printer, Pretoria, pp. 289 – 330.

Department of Water Affairs and Forestry, (2000), Blesbokspruit Catchment-Geohydrological Report for Acid Mine Drainage Collection and Conveyance System for Abandoned Mines, WQM/01/00.

Domvile, S.J., Li, M.G., Sollner, L.D. and Nesbitt, W. (1994). Weathering behaviour of mine tailings and waste rock: A surface investigation. In: Proceedings of the International Land Reclamation and Mine Drainage Conference. Vol. 1, April 24 – 29, Pittsburgh, PA, pp 167–176.

Durkin, T.V. (1996). Acid Mine Drainage: Reclamation at the Richmond Hill and Gilt Edge Mines, South Dakota. EPA Seminar Publication/625/R-95/007 on Managing Environmental Problems at Inactive and Abandoned Metals Mine Sites.

Durkin, T.V. and Herrmann, J.G. (1996). Introduction: Focusing on the Problem of Mining Wastes. EPA Seminar Publication/625/R-95/007 on Managing Environmental Problems at Inactive and Abandoned Metals Mine Sites.

Elliott, H. A., Brown, G. A., 1989. Water, Air, and Soil Pollution, pp. 45, 361.

Evangelou, V.P. (1995), Pyrite oxidation and its control. CRC Press, Boca Raton, Florida.

Evangelou, V.P. and Zhang, Y.L. (1995). A Review: Pyrite Oxidation Mechanisms and Acid Mine Drainage Prevention. Critical Reviews in Environmental Science and Technology, 25(2), pp. 141 – 191.

Faure, G., 1998. Principles and Applications of Inorganic Geochemistry, second ed. Macmillan Publishing Company, NY, USA.

Fornasiero, D., Eijt, V. and Ralston, J. (19962), An electrokinetic study of pyrite oxidation, Colloids Surf, pp. 62, 63.

Gupta, A.K., Sinha, S., 2007. Journal of Hazardous Materials 149, pp. 144 – 150

Hadley, R. and Snow, D. (1974). Water Resources and Problems Related to Mining. American Water Resource Assodiation, MN., 1974.

Hodgson, F.D.I. (1992), A first report on: The preliminary evaluation of the impact of coal strip mining on ground-water resources at Optimum Colliery.

Ivanov, V.I. (1962), Effect of some factors on iron oxidation by cultures of Thiobacillus ferrooxidans, Microbiology, (Engl. Transl.), pp. 31, 645.

Jaynes, D.B., Rogowski, A.S. and Pionke, H.B. (1984). Acid Mine Drainage from reclaimed coal strip mines. I. Model description, Water Research Resources, pp. 20, 233.

Jeffrey, L.S. (2005), The Journal of The South African Institute of Mining and Metallurgy: Characterisation of the coal resources of South Africa, pp. 95 – 96.

Katarzyna, T., Jolanta, M., 2003. Mycorrhiza 13, pp.185 –190.

Kempton, J.H., Swanson, D., Bennett, M., MacDonald, R. and Locke, W. (1997). Application of probabilistic Acid/Base Accounting to minimize waste-rock handling

in semi-arid climates. In: Proceedings of the Fourth International Conference on Acid Rock Drainage. Vol. 1, May 31 – June 6, Vancouver, BC, pp. 871-887

Lasat, M.M., 2000. Journal of Hazardous Substance Research, pp. 703, 603.

Lawrence, R.W. and Day, S. (1997a). Chemical prediction techniques for ARD. Short Course 2. Fourth International Conference on Acid Rock Drainage. May 31 – June 6, Vancouver, BC.

Lawrence, R.W. and Wang, Y. (1997b). Determination of neutralisation potential in the prediction of acid rock drainage. In: Proceedings of the Fourth International Conference on Acid Rock Drainage. Vol. 1, May 31 – June 6, Vancouver, BC., pp. 449-464.

Levinson, A.A. (1974). Introduction to Exploration Geochemistry. Applied Publishing Ltd., Illinois, USA.

Miller, S. (1998). Prediction - Predicting Acid Drainage Groundwork, No.1 Vol. 2, Australian Minerals & Energy Environment Foundation.

Morin, K.A. and Hutt, N.M. (1994). Observed preferential depletion of Neutralisation potential over sulphide minerals in kinetic tests: site-specific criteria for safe NP/AP ratios. In: Proceedings of the International Land Reclamation and Mine Drainage Conference. Vol. 1, April 24 – 29, Pittsburgh, PA., pp. 148 – 156.

Morin, K.A. and Hutt, N.M. (1997). Environmental Geochemistry of Minesite Drainage: Practical Theory and Case studies, Minesite Drainage Assessment Group, MDAG Publishing, Vancouver, Canada.

Moses, C.O., Nordstrom, D.K., Herman, J.S. and Mills, A. (1987). Aqueous pyrite oxidation by dissolved oxygen and by ferric iron. Geochim. Cosmochim. Acta., pp.54, 395.

Mugo, R.K., Orians, K.J., 1993. Seagoing methods for the determination of chromium (III) and total chromium in sea water by electron-capture detection gas chromatography. Anal. Chim. Acta 271, pp. 1 – 9.

Naicker, K, Cukrowska, E and Mc Carthy, T.S. 2003. Acid mine drainage from gold mining activities in Johannesburg, South Africa and environs. Environmental Pollution, 122: pp. 29 – 40.

Nordstrom, D.K. (1982), Aqueous pyrite oxidation and the consequent formation of secondary iron minerals, in Acid Sulfate Weathering, Pedogeochemistry and Relationship to Manipulation of Soil Minerals, Hossner, L.R., Kittrick, J.A. and Fanning, D.F. (Eds.), Soil Science Society of America Press, Madison, WI, pp. 46.

Nordstrom D.K., Alpers, C.N., Ptacek, C.J. and Blowes, D.W. (1999) Negative pH and Extremely Acidic Mine Waters from Iron Mountain, California Environmental Science & Technology ACS.

Price, W.A. and Errington, J.C. (1995). ARD Guidelines for Mine Sites in British Columbia, BC Ministry of Energy, Mines and Petroleum Resources, Victoria, pp. 29.

Plumstead, E. (1957). Coal in South Africa. Witwatersrand University Press, Johannesburg.

Pourbaix, M., 1988. Atlas of Electrochemical Equilibria in Aqueous Solutions. Cebelcor, Brussels.

Prevost, X.M. (2004), South African reserves and the Minerals Act. Coaltrans South Africa, Cape Town, 1 – 2 March, pp. 6.

Robertson, A.M. (1996). The Importance of site Characterization for Remediation of Abandoned Mine Lands. EPA Seminar Publication/625/R-95/007 on Managing Environmental Problems at Inactive and Abandoned Metals Mine Sites.

Schafer Laboratory Testing (1997). "Acid Rock Drainage: A historical perspective".

Schafer, W. (2000), Use of Net Acid Generation pH Test for Assessing Risk of Acid Generation, In: Proceedings of the Fifth International Conference on Acid Rock Drainage, Vol. 1. Denver, Colorado.

Scharer, J.M., Garga, V., Smith, R. and Halbert, B.E. (1991), Use of steady state models for assessing acid generation in pyritic mine tailings. The Second International Conference on the Abatement of Acidic Drainage, Vol. 2, Sept 16 – 18, Montreal, Canada.

Shah, K., Nongkynrih, J.M., 2007. Biologia Plantarum 51 (4), pp. 618 – 634.

Sherlock, E.J., Lawrence, R.W. and Poulin, R. (1995). On the neutralisation of acid rock drainage by carbonate and silicate minerals. Environmental Geology 25, pp. 43 – 54.

Singer, P.C. and Stumm, W. (1970), Acidic mine drainage: the rate-determining step. Science, pp. 167, 1121.

Sobek, A.A., Schuller, W.A., Freeman, J.R. and Smith, R.M. (1978). Field and Laboratory methods Applicable to Overburdens and Minesoil, WVU, EPA Report No. EPA-600/2-78-054, pp. 47 – 50.

Steffen, Robertson and Kirsten (BC) Inc. (1991). Sulphate Reduction as a Water Treatment Alternative at the Faro Mine. Report for Curragh Resources Inc.

Stumm, W. and Morgan, J.J. (1970). Aquatic Chemistry, 2nd Ed. John Wiley & Sons, Inc., New York, NY.

Sahuguillo, A., Rigol, A., Rauret, G., 2002. Comparison of leaching tests for the study of trace metals remobilisation in soils and sediments, J. Environ. Monit. 4, pp. 1003 – 1009.

Tutu H., (2008). The chemical characteristic of acid mine drainage with particular reference to sources, distribution and remediation. The Witwatersrand basin South Africa, a case study. 2008 Elsevier ltd.

U.S. EPA, 1998. Permeable Reactive Barrier Technology for Contaminant Remediation, EPA/600/R-98/125 September, Washington DC.

Usher, B.H., Cruywagen, L.M., de Necker, E. and F.D.I. Hodgson, F.D.I. (2003), On-site and Laboratory Investigations of Spoil in Opencast Collieries and the Development of Acid-Base Accounting Procedures, Water Research Commission, WRC Report No. 1055/1/03, ISBN 1-77005-053-1, Vol.1., pp. 3, 9, 11, 13, 25

Usher, B.H., Cruywagen, L.M., de Necker, E. and F.D.I. Hodgson, F.D.I. (2003), On-site and Laboratory Investigations of Spoil in Opencast Collieries and the Development of Acid-Base Accounting Procedures, Water Research Commission, WRC Report No. 1055/2/03, ISBN 1-77005-053-1, Vol.2.

Yu, J., Klarup, D., 1994. Extraction kinetics of copper, zinc, iron and manganese from contaminated sediment using disodium ethylene-diaminetetraacetate. Water Air Soil Pollution, pp. 75, 205.

Ziemkiewicz, P.F. and Meek, F.A. (1994). Long term behaviour of acid forming rock: Results of 11-year field studies. In: Proceedings of the International Land Reclamation and Mine Drainage Conference. Vol. 3, April 24 – 29, Pittsburgh, PA., pp. 49 – 56.

Websites References

Acid Mine Drainage Chemistry (1997).

http://www.chem.uky.edu/research/atwood/matlock/AMD/AMD%20Chem/AMD%20Chemistry.htm

BC Mining Watch (1998). "Acid Mine Drainage".

http://www.cpaws-sask.org/common/pdfs/mine_impacts_kit.pdf

Hunter, D. (1997b). "Overburden sampling and analytical techniques – Acid-Base Accounting and Leaching Tests".

http://www.osmre.gov/obabact.html

Mills, C. (1998a). "An Introduction to Acid Rock Drainage"

http://technology.infomine.com/enviromine/ard/Introduction/ARD.HTM

Mills, C. (1998c). "Acid-Base Accounting (ABA)"

http://technology.infomine.com/enviromine/ard/acid-base%20accounting/ABAdiscussion.htm

Perry, E. (1997). “More on Acid-Base Accounting”.

http://www.info-mine.com/List_archives/enviromine_technical/0908.htmL

Shaw, S. and Mills, C. (1998). “Petrology and Mineralogy in ARD Prediction”.

http://www.enviromine.com/ard/Mineralogy/Petrology%20and%20Mineralogy.htm

Stevenson, P. (1997). Heavy Metals: What are they? And why are they dangerous?

http://www.avon.net.au/globe/features/heavymet.html

Todd, J. and Reddick, K. (1997). “Acid Mine Drainage”.
http://www.cee.vt.edu/ewr/environmental/teach/gwprimer/acidmine/acidmine.html

8. APPENDIX

8.1 Appendix 1: Test Results

Table 8.1: Field measurements of surface and borehole samples

Analytical results for ground and surface waters collected at Block I. Note: Samples that were obtained 2 days after sampling were only analysed for pH and conductivity, since that analysis have less variation.

'nd' means: not detected and 'na' means not analysed

				Field parameters			Major anions			Major cations				Trace elements						
No.	**Sample name**	**Description**	**Water depth**	**pH**	**Eh**	**EC**	**SO_4^{2-}**	**CO_3^{2-}**	**Cl^-**	**Na**	**K**	**Ca**	**Mg**	**Fe**	**Mn**	**Ni**	**Zn**	**Cu**	**Al**	**Co**
			m		**mV**	**mS cm^{-1}**	**mg l^{-1}**			**mg l^{-1}**				**mg l^{-1}**						
1	**KTL-31**	Borehole	2.3	7.3	60	0.37	107.7	18.0	17.73	13	8.9	19	12.1	25.8	1.2	nd	0.03	0.02	nd	0.02
2	**BH 1564**	Borehole	0.0	7.2	na	0.10	2.0	37.5	7.09	13	3.2	6.5	5.1	0.34	0.05	nd	0.01	0.03	0.18	nd
3	**Dam @ Ext B**	Dam	0.0	8.8	262	0.67	187.8	114.0	24.82	60	8.2	60	36.9	0.05	0.02	nd	0	0.03	0.22	nd
4	**Block I upstream**	Stream	0.0	6.7	na	1.35	708.0	123.0	31.91	69	13	134	179	1.07	2.5	0.02	0.01	0.02	0.01	nd
5	**Block I midstream**	Stream	0.0	6.1	na	1.37	987.0	18.0	31.91	57	18	201	190	0.17	0.24	nd	0.01	0.03	nd	nd
6	**Downstream KTL-7**	Stream	0.0	7.3	325	0.76	130.2	99.0	46.09	44	11	37	47.9	0.87	0.05	nd	0	0.03	0.59	nd
7	**Small upstream-KTL-7**	Stream	0.0	6.1	210	3.88	3522.0	9.0	17.73	34	59	610	577	216	46.2	0.64	0.06	0.01	nd	0.31
8	**KTL-7**	Borehole	0.0	6.7	91	2.23	1794.0	10.5	7.09	24	22	352	314	197	18.9	0.2	0.1	0.02	nd	0.09
9	**Block I downstream**	Stream	0.0	6.2	na	1.61	1188.0	19.5	28.36	69	29	261	237	0.08	0.5	nd	0	0.03	0.04	nd
10	**KTL-30**	Borehole	0.8	9.0	124	3.28	2352.0	30.0	28.36	54	34	406	454	0.05	1.5	nd	0.01	0.02	0.02	nd
11	**BH 1563**	Borehole	4.5	8.6	205	1.53	1170.0	45.0	7.09	37	41	26	327	0.1	0.45	nd	0	0.02	0.02	nd
12	**KTL-29**	Borehole	11.2	5.9	244	1.60	1146.0	16.5	17.73	18	13	285	110	24.5	16.7	0.15	0.2	0.01	0.34	0.27
13	**KTL-26**	Borehole	5.1	7.1	341	0.95	435.0	19.5	14.18	37	20	47	84.4	0.04	0.5	nd	0.01	0.02	0.01	nd
14	**KTL-28**	Borehole	14.5	6.7	146	0.81	326.7	82.5	10.64	19	7.7	99	56.5	0.17	1.3	nd	0	0.02	nd	nd
15	**KTL-6**	Borehole	0.0	7.1	159	0.28	72.9	66.0	17.73	38	15	51	15.3	7.3	0.55	nd	0.01	0.02	0.02	nd
16	**Surface water- KTL-6**	Stream	0.0	8.6	270	0.58	84.3	186.0	67.36	80	11	45	54.5	0.12	0.04	nd	nd	0.03	0.11	nd

Table 8.2: Results of the total metal concentration in the soil samples of the mining area

The total metal concentrations and metalloid (AS) of soil samples collected next to boreholes of Block I. nd means: not detected.

					Total Metal concentration													
No.	**Sample name**	**Description**	**Elevation**	**% Moisture**	**Fe**	**Mn**	**Ni**	**Zn**	**Cu**	**Al**	**Cd**	**Cr**	**As**	**Co**	**Ca**	**Mg**	**S**	**Pb**
			m		**mg kg^{-1}**													
1	**Sub KTL-28**	Sub soil	1589	12.6	53435	458	722	nd	48	24427	115	158	141	nd	21851	13645	1145	4.77
2	**Top KTL-28**	Top soil		6.6	37512	443	711	5689	59	26615	96	444	nd	nd	22951	12825	1061	0.96
3	**Sub KTL-29**	Sub soil	1584	24.4	43288	323	406	nd	33	28988	76	131	nd	30	936	1362	4767	0.00
4	**Top KTL-29**	Top soil		8.6	52207	792	811	48	67	23417	109	480	nd	nd	32438	18810	3167	1.92
5	**Sub KTL-26**	Sub soil	1575	15.8	52908	453	775	nd	41	39085	119	251	214	nd	7054	2097	2097	6.67
6	**Top KTL-26**	Top soil		13.4	49138	483	889	7950	60	25096	121	512	nd	nd	28927	17050	2395	4.79
7	**Sub KTL-27**	Sub soil	1586	13.7	37880	227	801	nd	73	44063	116	565	nd	nd	499	1668	382	2.94
8	**Top KTL-27**	Top soil		14.8	52970	394	474	nd	55	36417	72	483	77	55	2142	1266	636	1.95
9	**Sub KTL-30**	Sub soil	1573	13.7	52069	532	745	nd	37	22137	118	135	143	nd	28874	21655	1636	4.81
10	**Top KTL-30**	Top soil		17.1	44197	379	766	nd	54	44004	84	868	nd	30	314	907	89	0.97
11	**Sub KTL-7**	Sub soil	1571	14.4	30517	295	842	nd	49	26839	100	704	114	nd	14016	9543	604	1.99
12	**Top KTL-7**	Top soil		16.3	10019	158	890	nd	38	30058	90	1029	nd	nd	297	582	135	0.96
13	**Sub Block I O/C**	Sub soil	1577	17.3	77810	571	984	nd	54	13905	116	952	204	nd	7143	2952	801	8.57
14	**Top Block I O/C**	Top soil		8.5	55632	1959	857	16	63	9794	114	549	824	nd	26053	1567	274	3.92
15	**Sub 1563 Ex-pond**	Sub soil	1572	14.7	46223	599	1504	15109	65	20676	165	1157	nd	nd	55268	32505	5268	6.96
16	**Top 1563 Ex-pond**	Top soil		6.5	78257	598	829	nd	80	23898	101	988	117	67	4212	486	541	5.88
17	**Sub KTL-31**	Sub soil	1593	26.9	75696	386	1011	nd	66	21422	91	2402	nd	41	648	1021	3554	0.96
18	**Top KTL-31**	Top soil		10.1	24584	306	1360	nd	44	26836	142	784	nd	nd	572	790	26	3.92
19	**Sub KTL-6**	Sub soil	1576	26.6	48062	887	686	nd	48	21318	115	205	110	nd	26841	18023	2616	2.91
20	**Top KTL-6**	Top soil		20.4	43689	375	541	nd	54	23689	75	416	nd	36	540	1262	502	0.00

Table 8.3: The concentrations of metal ions extracted by solutions of 0.1 M sodium carbonate, 0.1 M EDTA, 0.01 M calcium chloride and artificial rainwater.

Extraction of metals with 0.1 M sodium carbonate								
Sample name	**Cd**	**Co**	**Cr**	**Cu**	**Fe**	**Mn**	**Ni**	**Zn**
	mg l^{-1}							
SUB KTL-6	0.022	0.044	0.346	0.397	20.8	0.085	0.077	0.098
SUB KTL-7	0.00	0.021	0.079	0.122	2.95	0.022	0.025	0.035
SUB KTL-26	0.00	0.00	0.00	0.370	0.65	0.00	0.00	0.00
TOP KTL-26	0.00	0.00	0.00	0.490	56.2	0.024	0.00	0.008
TOP KTL-6	0.15	0.14	0.049	0.760	22.6	0.066	0.00	0.038
TOP KTL-7	0.00	0.00	0.00	0.430	0.7	0.00	0.00	0.00

Extraction of metals with 0.1 M EDTA								
Sample name	**Cd**	**Co**	**Cr**	**Cu**	**Fe**	**Mn**	**Ni**	**Zn**
	mg l^{-1}							
SUB KTL-6	0.026	1.84	0.256	1.187	47	42	1.163	0.126
SUB KTL-7	0.015	1.01	0.065	0.302	20	11	0.141	0.154
SUB KTL-26	0.015	1.093	0.05	0.632	12	22	0.328	0.392
TOP KTL-26	0.03	1.74	0.07	0.707	26	34	0.13	0.17
TOP KTL-6	0.013	1.031	0.155	2.900	66	7	0.397	0.992
TOP KTL-7	0.013	0.063	0.227	0.822	13	0.545	0.125	0.11

Extraction of metals with 0.01 M calcium chloride								
Sample name	**Cd**	**Co**	**Cr**	**Cu**	**Fe**	**Mn**	**Ni**	**Zn**
	mg l^{-1}							
SUB KTL-6	< -0.001	< 0.002	0.022	0.037	0.251	0.011	nd	0.006
SUB KTL-7	< 0.006	0.041	< 0.003	0.035	0.759	1.0	0.032	0.027
SUB KTL-26	< 0.006	< 0.010	nd	0.036	0.375	0.424	0.024	0.044
TOP KTL-26	< 0.005	0.025	< 0.000	0.036	0.099	1.5	nd	0.01
TOP KTL-6	< 0.007	0.285	< 0.001	0.043	0.594	4.79	0.109	0.301
TOP KTL-7	< 0.000	0.019	< 0.004	0.043	0.146	0.346	0.027	0.04

Extraction of metals with artificial rainwater								
Sample name	**Cd**	**Co**	**Cr**	**Cu**	**Fe**	**Mn**	**Ni**	**Zn**
	mg l^{-1}							
SUB KTL-6	< 0.005	< 0.004	0.034	0.038	1.36	0.008	nd	0.004
SUB KTL-7	< 0.004	< 0.013	< 0.002	0.034	1.26	0.326	nd	0.008
SUB KTL-26	< 0.003	< 0.006	< 0.005	0.035	1.57	0.052	nd	0.009
TOP KTL-26	< 0.005	< 0.009	< 0.008	0.037	4.56	0.328	nd	0.011
TOP KTL-6	< 0.004	0.051	< 0.008	0.041	2.07	1.18	< 0.009	0.049
TOP KTL-7	< 0.006	< 0.005	0.026	0.044	2.94	0.022	nd	0.013

Table 8.4: The extracted metal ions expressed as a percentage of the total metal ion concentration. Extraction was done with various solutions of 0.1 M Na_2CO_3, 0.1 M EDTA, 0.01 M $CaCl_2$ and artificial rainwater.

Sample No.	Sample	% Extracted by 0.1 M EDTA					
		Cd	Cr	Cu	Fe	Ni	Mn
1	SUB KTL-6	21.85	82.81	100	94.76	60.88	100
2	SUB KTL-7	14.85	9.18	100	65.15	16.65	100
3	SUB KTL-26	11.90	13.08	100	23.39	35.34	100
4	TOP KTL-26	38.96	36.21	100	57.78	23.34	100
5	TOP KTL-6	10.40	19.01	100	84.09	48.83	100
6	TOP KTL-7	13.98	21.25	100	80.00	13.53	100

Sample No.	Sample	% Extracted by 0.01 M calcium chloride					
		Cd	Cr	Cu	Fe	Ni	Mn
1	SUB KTL-6	0.00	10.38	74.00	0.51	0.00	1.20
2	SUB KTL-7	0.00	0.00	71.43	2.47	3.78	100
3	SUB KTL-26	0.00	0.00	57.14	0.73	2.95	89.26
4	TOP KTL-26	0.00	0.00	64.29	0.22	0.00	100
5	TOP KTL-6	0.00	0.00	100.00	1.07	19.57	100
6	TOP KTL-7	0.00	0.00	90.70	1.40	2.92	100

Sample No.	Sample	% Extracted by 0.1 M sodium carbonate					
		Cd	Cr	Cu	Fe	Ni	Mn
1	SUB KTL-6	18.49	61.27	100	41.94	10.88	9.29
2	SUB KTL-7	0.00	11.16	100	9.61	2.95	7.41
3	SUB KTL-26	0.00	0.00	100	1.27	0.00	0.00
4	TOP KTL-26	0.00	0.00	100	80.07	0.00	4.76
5	TOP KTL-6	83.33	11.45	100	40.72	0.00	17.10
6	TOP KTL-7	0.00	0.00	100	6.73	0.00	0.00

Sample No.	Sample	% Extracted by artificial rainwater					
		Cd	Cr	Cu	Fe	Ni	Mn
1	SUB KTL-6	0.00	16.04	76.00	2.74	0.00	0.87
2	SUB KTL-7	0.00	0.00	69.39	4.10	0.00	91.10
3	SUB KTL-26	0.00	0.00	55.56	3.06	0.00	10.32
4	TOP KTL-26	0.00	0.00	66.07	10.13	0.00	84.97
5	TOP KTL-6	0.00	0.00	95.35	3.73	0.00	100
6	TOP KTL-7	0.00	2.43	88.64	28.27	0.00	13.41

Table 8.5: Analytical results of acid base accounting analysis on soil samples collected near boreholes at Block I.

Sample name	Initial pH	Final pH	Acid potential	Neutralising potential	Net neutralising potential
			kg t^{-1} $CaCO_3$	kg t^{-1} $CaCO_3$	kg t^{-1} $CaCO_3$
Sub KTL-30	5.3	2.2	0.88	-8.90	-9.78
Sub KTL-29	5.5	2.4	0.22	-7.95	-8.17
Sub KTL-28	5.1	2.2	0.33	-7.27	-7.60
Sub KTL-6	7.7	4.9	0.35	-4.19	-4.54
Sub KTL-26	5.5	1.9	0.29	-7.64	-7.93
Sub KTL-27	5.2	2.3	0.18	-7.78	-7.96
Sub Block I O/C	5.6	2.3	0.10	-7.84	-7.94
Sub 1563 Ex-pond	5.2	2.3	0.26	-7.73	-7.99
Sub KTL-7	5.3	1.9	0.32	-8.19	-8.51
Sub KTL-31	5.2	2.2	0.43	-8.26	-8.69
Top Block I O/C	6.3	2.7	0.32	-7.08	-7.40
Top 1563 Ex-pond	5.6	2.7	0.46	-6.95	-7.41
Top KTL-31	6.1	2.4	0.15	-7.05	-7.21
Top KTL-7	5.2	2.2	0.30	-9.45	-9.75
Top KTL-30	5.1	2.4	0.17	-8.45	-8.62
Top KTL-27	5.4	2.4	0.06	-7.70	-7.76
Top KTL-26	5.8	2.7	0.33	-7.99	-8.32
Top KTL-29	5.4	2.4	0.42	-7.95	-8.37
Top KTL-28	4.5	2.2	0.71	-7.97	-8.68
Top KTL-6	4.6	2.4	1.39	-7.75	-9.14

8.2 Appendix 2: Borehole logs

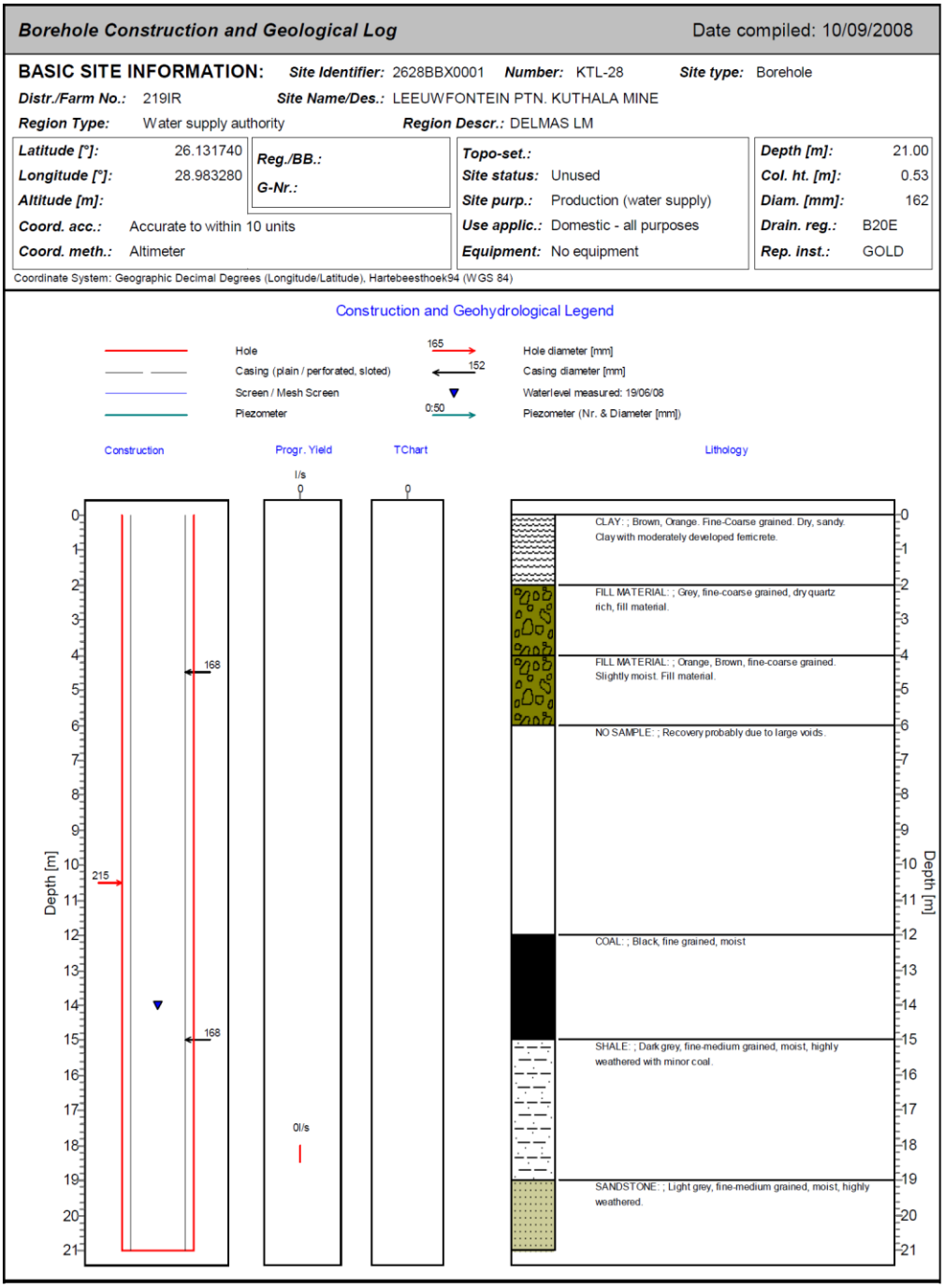

Borehole Construction and Geological Log

Date compiled: 10/09/2008

BASIC SITE INFORMATION: ***Site Identifier:*** 2628BBX0002 ***Number:*** KTL-29 ***Site type:*** Borehole

Distr./Farm No.: 219IR ***Site Name/Des.:*** LEEUWFONTEIN PTN. KUTHALA MINE

Region Type: Water supply authority ***Region Descr.:*** DELMAS LM

Latitude [°]:	26.131760	***Reg./BB.:***	***Topo-set.:***	***Depth [m]:***	18.00
Longitude [°]:	28.982360	***G-Nr.:***	***Site status:*** Unused	***Col. ht. [m]:***	0.53
Altitude [m]:			***Site purp.:*** Production (water supply)	***Diam. [mm]:***	162
Coord. acc.:	Accurate to within 10 units		***Use applic.:*** Domestic - all purposes	***Drain. reg.:***	B20E
Coord. meth.:	Altimeter		***Equipment:*** No equipment	***Rep. inst.:***	GOLD

Coordinate System: Geographic Decimal Degrees (Longitude/Latitude), Hartebeesthoek94 (WGS 84)

Construction and Geohydrological Legend

Hole — Hole diameter [mm] (165)

Casing (plain / perforated, sloted) — Casing diameter [mm] (152)

Screen / Mesh Screen — Waterlevel measured: 19/06/08

Piezometer — Piezometer (Nr. & Diameter [mm]) (0:50)

Construction | TChart | Lithology

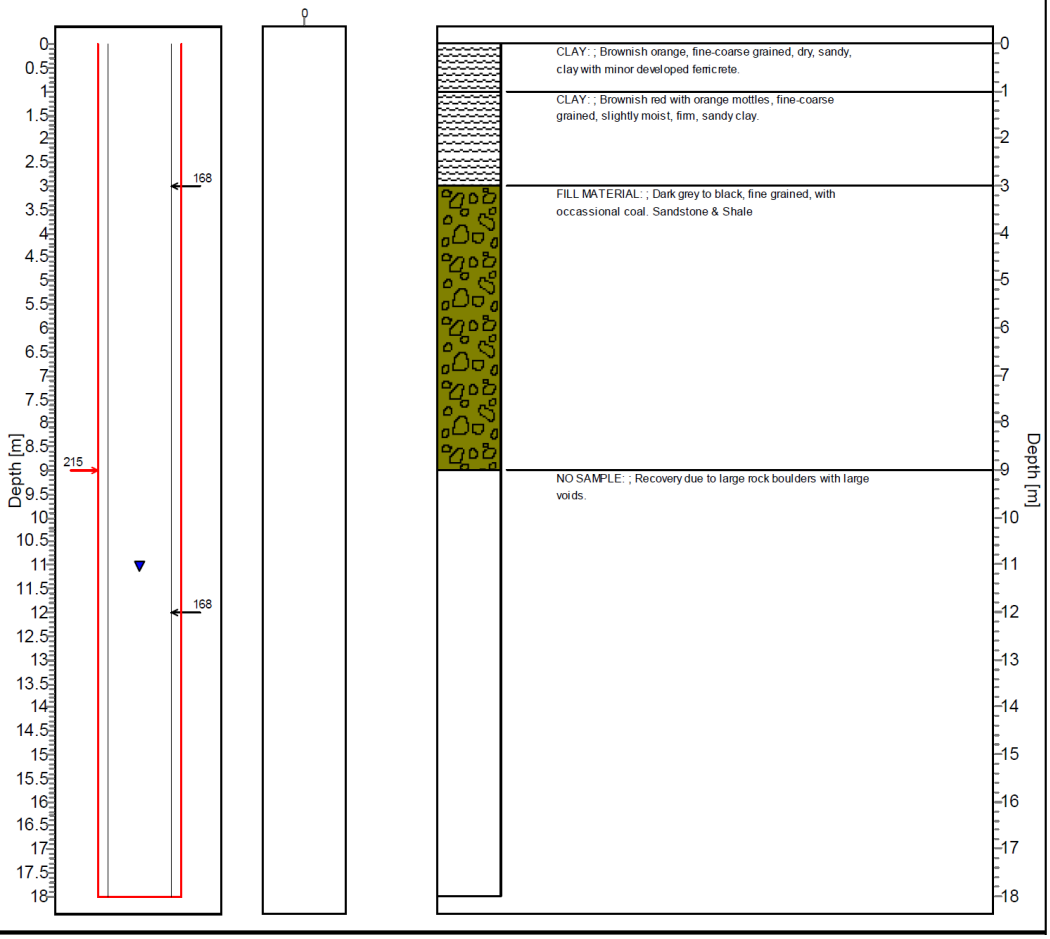

Borehole Construction and Geological Log

Date compiled: 10/09/2008

BASIC SITE INFORMATION: ***Site Identifier:*** 2628BBX0003 ***Number:*** KTL-30 ***Site type:*** Borehole

Distr./Farm No.: 219IR ***Site Name/Des.:*** LEEUWFONTEIN PTN. KUTHALA MINE

Region Type: Water supply authority ***Region Descr.:*** DELMAS LM

Latitude [°]:	26.128280	***Reg./BB.:***	***Topo-set.:***	***Depth [m]:***	12.00
Longitude [°]:	28.976740	***G-Nr.:***	***Site status:*** Unused	***Col. ht. [m]:***	0.55
Altitude [m]:			***Site purp.:*** Production (water supply)	***Diam. [mm]:***	162
Coord. acc.:	Accurate to within 10 units		***Use applic.:*** Domestic - all purposes	***Drain. reg.:***	B20E
Coord. meth.:	Altimeter		***Equipment:*** No equipment	***Rep. inst.:***	GOLD

Coordinate System: Geographic Decimal Degrees (Longitude/Latitude), Hartebeesthoek94 (WGS 84)

Construction and Geohydrological Legend

Hole — Hole diameter [mm] (165)

Casing (plain / perforated, sloted) — Casing diameter [mm] (152)

Screen / Mesh Screen — Waterlevel measured: 20/06/08

Piezometer — Piezometer (Nr. & Diameter [mm]) (0:50)

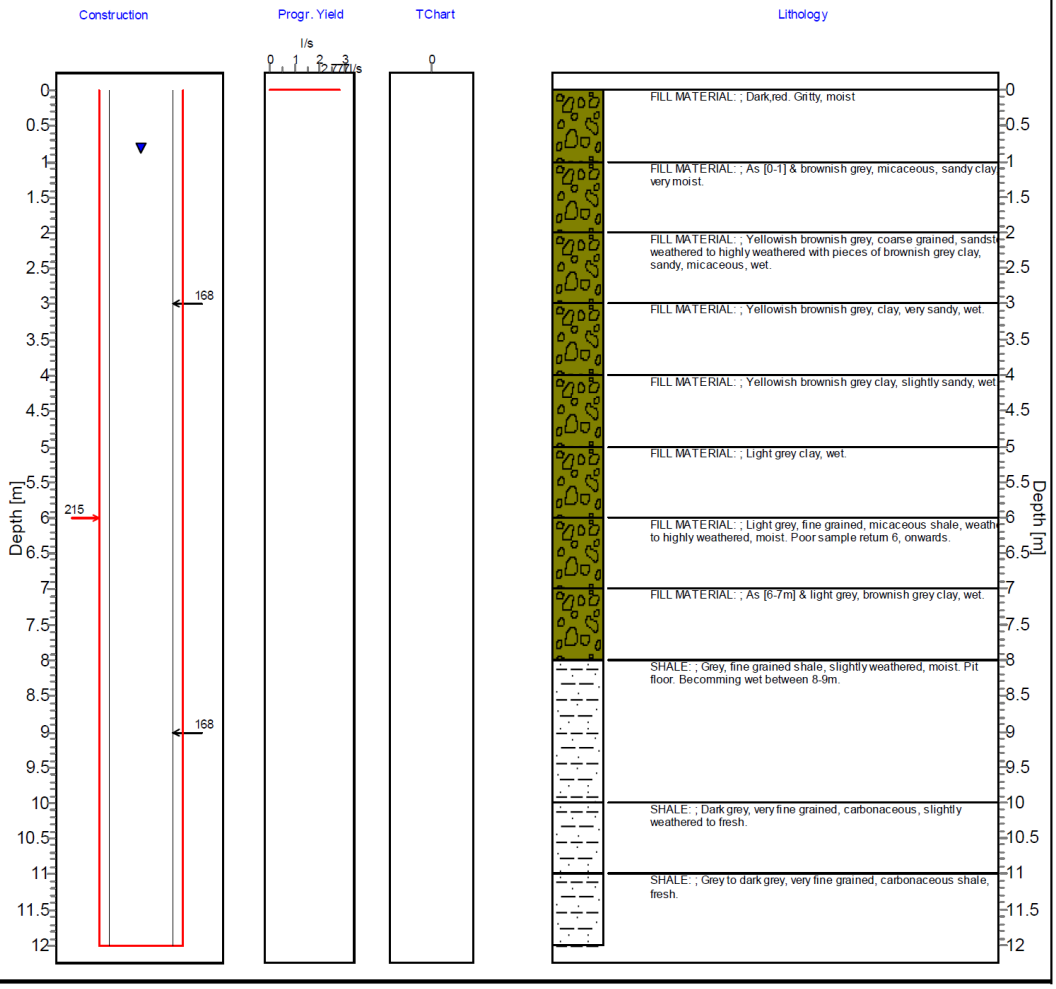

Borehole Construction and Geological Log

Date compiled: 10/09/2008

BASIC SITE INFORMATION: ***Site Identifier:*** 2628BBX0004 ***Number:*** KTL-31 ***Site type:*** Borehole

Distr./Farm No.: 219IR ***Site Name/Des.:*** LEEUWFONTEIN PTN. KUTHALA MINE

Region Type: Water supply authority ***Region Descr.:*** DELMAS LM

Latitude [°]:	26.119001	***Reg./BB.:***	***Topo-set.:***	***Depth [m]:***	9.00
Longitude [°]:	28.981100	***G-Nr.:***	***Site status:*** Unused	***Col. ht. [m]:***	0.55
Altitude [m]:			***Site purp.:*** Production (water supply)	***Diam. [mm]:***	162
Coord. acc.:	Accurate to within 10 units		***Use applic.:*** Domestic - all purposes	***Drain. reg.:***	B20E
Coord. meth.:	Altimeter		***Equipment:*** No equipment	***Rep. inst.:***	GOLD

Coordinate System: Geographic Decimal Degrees (Longitude/Latitude), Hartebeesthoek94 (WGS 84)

Construction and Geohydrological Legend

Hole — Hole diameter [mm] (165)
Casing (plain / perforated, sloted) — Casing diameter [mm] (152)
Screen / Mesh Screen — Waterlevel measured: 20/06/08
Piezometer — Piezometer (Nr. & Diameter [mm]) (0:50)

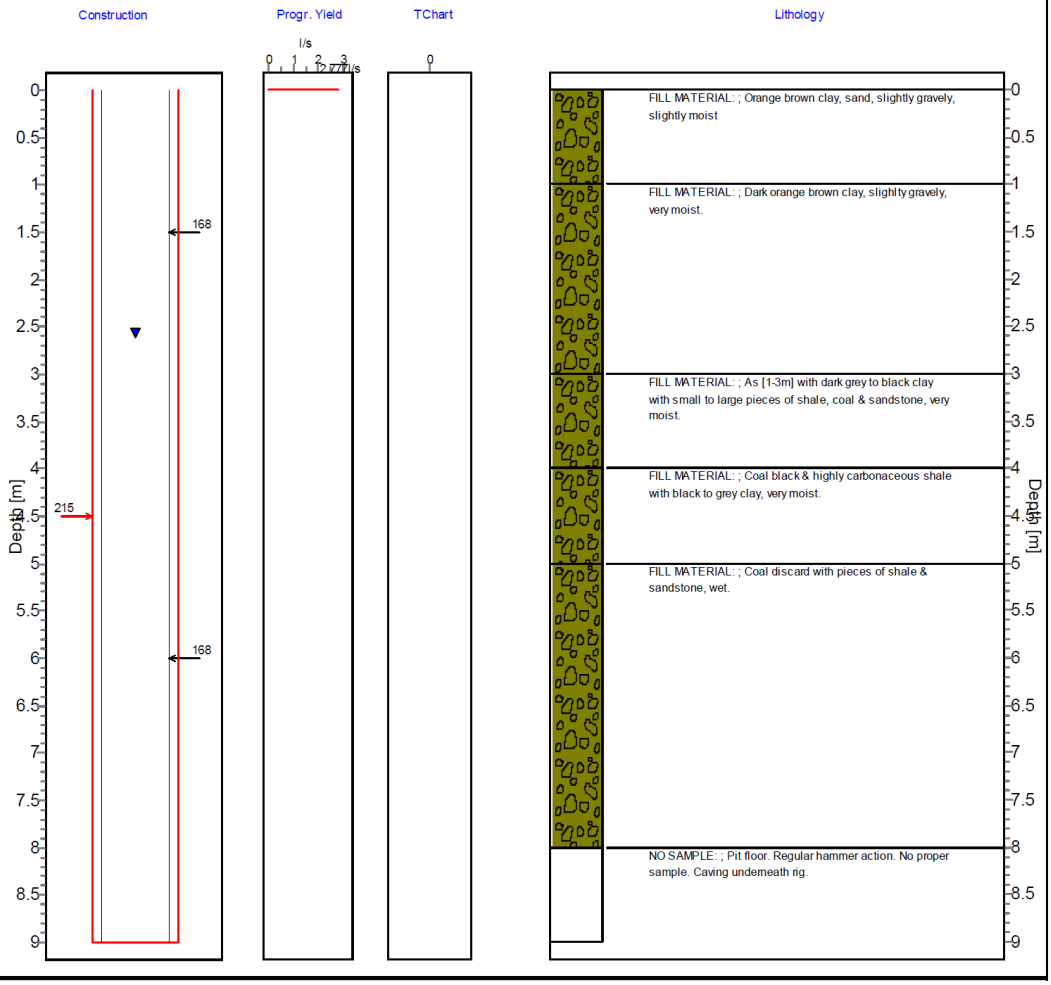

Borehole Construction and Geological Log

Date compiled: 10/09/2008

BASIC SITE INFORMATION: ***Site Identifier:*** 2628BBX0005 ***Number:*** KTL-32 ***Site type:*** Borehole

Distr./Farm No.: 218IR ***Site Name/Des.:*** SCHOONGEZICHT PTN. KUTHALA MINE

Region Type: Water supply authority ***Region Descr.:*** EMALAHLENI LM

Latitude [°]:	26.112901	***Reg./BB.:***	***Topo-set.:***	***Depth [m]:***	30.00
Longitude [°]:	28.982880	***G-Nr.:***	***Site status:*** Unused	***Col. ht. [m]:***	0.59
Altitude [m]:			***Site purp.:*** Production (water supply)	***Diam. [mm]:***	138
Coord. acc.:	Accurate to within 10 units		***Use applic.:*** Domestic - all purposes	***Drain. reg.:***	B20E
Coord. meth.:	Altimeter		***Equipment:*** No equipment	***Rep. inst.:***	GOLD

Coordinate System: Geographic Decimal Degrees (Longitude/Latitude), Hartebeesthoek94 (WGS 84)

Construction and Geohydrological Legend

Hole — Hole diameter [mm] (165)
Casing (plain / perforated, sloted) — Casing diameter [mm] (152)
Screen / Mesh Screen — Waterlevel measured: 20/06/08
Piezometer — Piezometer (Nr. & Diameter [mm]) (0:50)

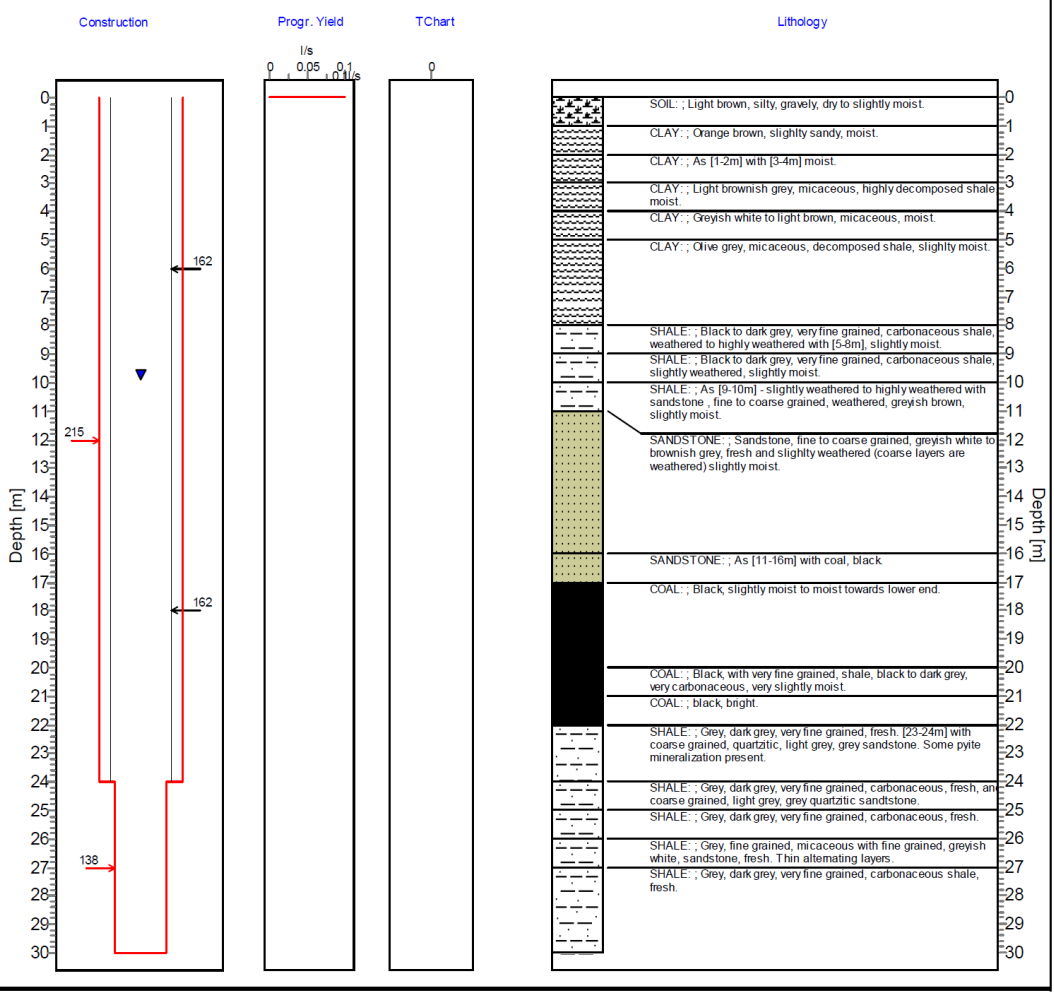

8.3 Appendix 3: Pump Testing Results

Location:	Pumping test: KTL-29 CD	Pumping well: KTL-
Test performed by: Test date: 2008/08/0	Evaluated by: Evaluation date: 2008/09/16	
Analysis method: COOPER & JACOB Time-Drawdown	Aquifer thickness: 18 [m] Discharge rate: 23.923696 [l/s]	

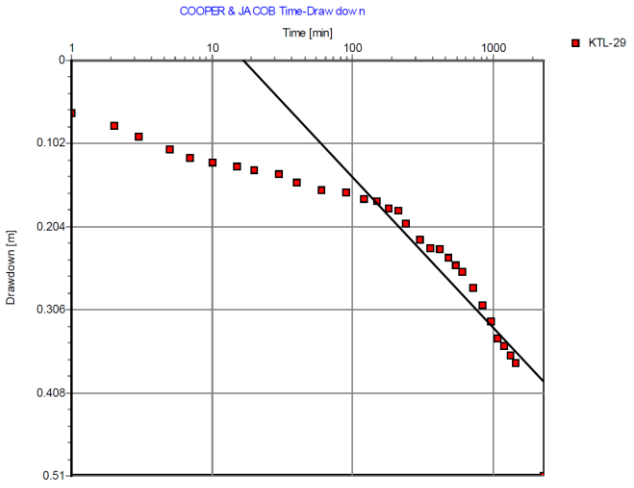

Transmissivity: 2.06×10^+3 [m²/d]

Conductivity: 1.14×10^+2 [m/d]

Location:	Pumping test: KTL-30CD	Pumping well: KTL-
Test performed by: Test date: 2008/09/1	Evaluated by: Evaluation date: 2008/09/16	
Analysis method: COOPER & JACOB Time-Drawdown	Aquifer thickness: 12 [m] Discharge rate: 0.53 [l/s]	

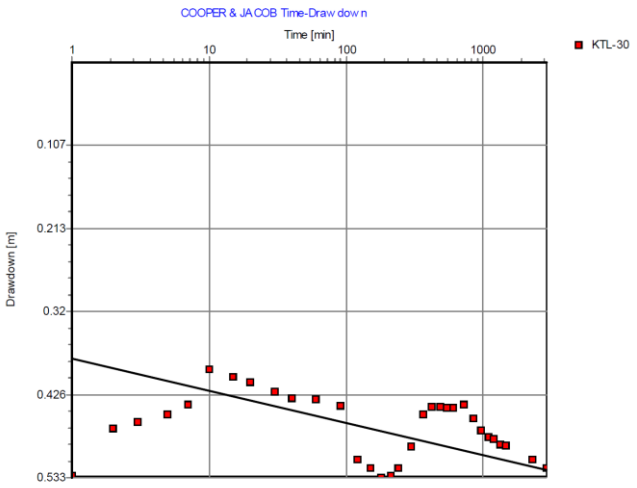

Transmissivity: 2.02×10^+2 [m²/d]

Conductivity: 1.69×10^+1 [m/d]

Location:	Pumping test: KTL-31CD	Pumping well: KTL-
Test performed by: Test date: 2008/09/1	Evaluated by: Evaluation date: 2008/09/16	
Analysis method: COOPER & JACOB Time-Drawdown	Aquifer thickness: 7 [m] Discharge rate: 4 [l/s]	

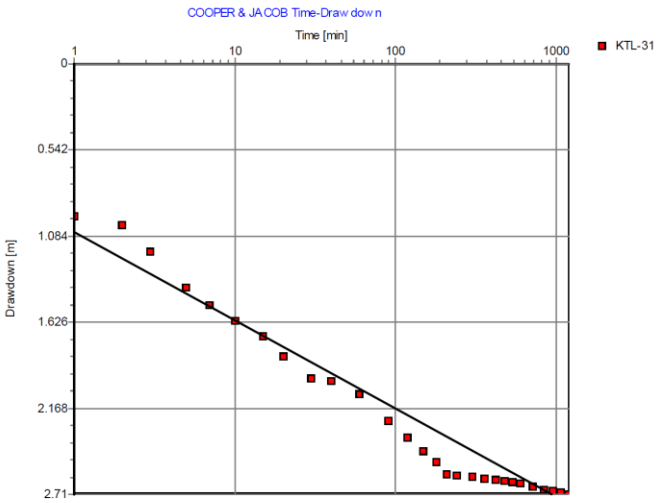

Transmissivity: 1.14×10^+2 [m²/d]

Conductivity: 1.62×10^+1 [m/d]